Republic of Iraq

Ministry of Higher Education

and Scientific Research

University of Misan

College of Science

Department of Biology

Production and Partial Purification of Biopolymer and Biosynthesis of Gold Nanoparticles from Actinomycetes and Detect of Their Biological Activity

A Thesis Submitted to
The college of Science / University of Misan as Partial Fulfillment of the Requirements for the Master's Degree of Science in Biology

By
Ruqaya Talib Hassan
B.Sc. Biology (2021)

Supervised
Prof . Dr. Rashid Rahim Hateet

2026 A.D **1447 A.H**

بِسْمِ اللَّهِ الرَّحْمَنِ الرَّحِيمِ

(قَالُوا سُبْحَانَكَ لَا عِلْمَ لَنَا إِلَّا مَا عَلَّمْتَنَا إِنَّكَ أَنْتَ الْعَلِيمُ الْحَكِيمُ)

صدق الله العلي العظيم

سورة البقرة الآية 32

Dedication

To my beloved family my father and mother, the source of love, generosity, and the foundation of my earliest successes; to my husband and life partner; to my sister and brothers, who have always been a source of support, encouragement, and strength; and to my little princesses, who have granted me the strength and hope to persevere.
I dedicate to you the fruit of this work in appreciation of your patience, encouragement, and prayers.

Acknowledgments

All praise and thanks are due to Allah, Lord of the Worlds, who taught by the pen, perfected all blessings upon us, and bestowed His mercy upon us through Muhammad (peace and blessings be upon him), the teacher of humanity, and upon his pure and righteous family, who illuminated the paths of knowledge and spread guidance and goodness among people. Furthermore, I acknowledge that those who offered me assistance and support in completing this work have a debt upon me that transcends mere thanks and appreciation. I extend my sincere gratitude and profound thanks to my supervisor, Professor Dr. Rashid Rahim Hateet, for his patience, sound guidance, and invaluable scientific advice throughout the research process. I pray that Allah Almighty grants him abundant health and well-being, and continued success in serving science and knowledge. I also express my deepest gratitude to the Dean of the College of Science, the Head of the Department of Life Sciences, Professor Dr. Saleh Hassan Jaza', and the esteemed faculty members for their cooperation and support. May Allah reward them abundantly for their assistance and support. I also express my sincere gratitude and appreciation to the esteemed professors Dr. Hassan Ghali, Dr. Alaa Hussein, and Dr. Hawraa Qais for their continuous support in completing the research requirements. I pray that God grants them continued health and success. Finally, I extend my deepest thanks and gratitude to my family and my husband's family, who have been my true support and primary source of strength throughout my academic journey. Their moral support, constant encouragement, patience, and perseverance played a major role in overcoming difficulties and completing this work. I ask God to reward them abundantly, bless them, and protect them from all harm and evil.

Ruqaya

Abstract

The current study will take ten soil samples at sites along the banks of the Tigris River in Maysan province between November 1, 2024, and June 1, 2025, since they are not adequately studied biologically. The use of anaerobic isolation allowed bacteria to be isolated and identified by morphology under a light microscope, after which they were further identified through molecular identification through the use of the 16S rRNA gene sequence. The molecular analyses showed that the identified isolated bacteria are a novel bacterial strain that was registered in the NCBI database with the accession ID of PV945972 and was designated as *Schaalia natura* strain RFAT2.

The capacity of this strain to produce a biopolymer and biosynthesize gold nanoparticles was examined in terms of cell-free bacterial supernatant . A variety of analytical methods were used to characterize the biopolymer, such as UV-Vis, FTIR, XRD, FESEM, AFM, zeta potential analysis, and thermogravimetric analysis (TGA), as well as to determine the solubility and carbohydrate content. On the other hand, the formation of gold nanoparticles was verified and described by means of UV-Vis, FTIR, XRD, FESEM, TEM, AFM, and zeta potential analysis. The efficacy of the biopolymer and gold nanoparticles against the *Candida albicans* and *Candida krusei* isolates was tested at various concentrations (500, 250, 125, and 62.5 µg/ml). The findings indicated that a 62.5 µg/ml concentration did not have an inhibitory effect on the growth of the fungus, whereas the higher the concentration, the more evident the inhibitory effect, with the highest growth in diameter of the inhibition zones. Dissimilar concentrations of the biopolymer and the gold nanoparticles (25, 50, 100, 200, and 400 µg/ml) were tested to determine the cytotoxicity of the biopolymer and gold nanoparticles against the thyroid cancer cells (FTC-133) and normal human

dermal fibroblasts (HdFn). The findings indicated that the cytotoxic effect was concentration dependent, as the gold nanoparticles had the best inhibitory capacity against cancer cells (60.46) at 400 µg/ml concentration, with less effect on normal cells. Significant differences ($p \leq 0.05$) were confirmed by statistical analysis of the results using GraphPad Prism software. These findings indicate the possibility of the strain of the bacteria being used as a promising biosource, in the manufacture of biopolymers and gold nanoparticles, which could be applied in the medical sector in the antifungal and anticancer treatment.

Lists of Contents

Lists of Figures

Lists of Tables

Chapter One

Introduction

1.1 Introduction:

Applied microbiology is working tirelessly to come up with new remedies to all world challenges, especially in the medical sector, including drug resistance, and the dwindling effectiveness of the traditional treatment of life-threatening diseases. This field is based on the exploitation of the biological potential of microorganisms and their combination with the latest methods of biotechnology, thus helping to create better and safer treatment approaches (Kumar et al., 2017; Abd-Elsalam, 2024).

Antimicrobial resistance is one of the most important issues among them. Multidrug resistance in Candida species has become an increasing worldwide health issue because it directly relates to the unsuccessful achievement of the standard therapeutic treatment and results in higher morbidity and mortality rates (de Moraes & Ferreira-Pereira, 2024). there is a tangible risk of reverting to a scenario reminiscent of the "pre-antibiotic era," (Makary et al., 2018). In a related context, the limited effectiveness of current cancer therapies , including surgery, chemotherapy, and radiotherapy constitutes an equally serious medical challenge. The World Health Organization reports that cancer remains one of the leading causes of death worldwide, with a continuous rise in both incidence and mortality rates.

Thyroid cancer is among the most prevalent endocrine system malignancies that have experienced a remarkable rise in the rates of occurrence in most parts of the world, especially in women; it is three to four times more prevalent in women than in men (Tran and Davies, 2023 :Xin et al., 2024).

Currently , in vitro tissue culture methods have been widely employed to determine the effects of experimental treatments and to evaluate the cytotoxicity

by using cancerous and normal cells (Koch et al., 2021). Riverbank zones represent transitional environments between terrestrial and aquatic ecosystems and are among the least studied habitats in terms of bacterial diversity (Ding et al., 2021). With advances in molecular techniques, universal ribosomal RNA gene (16S rRNA) sequencing has become a powerful tool for the accurate identification and classification of microbial diversity within such environments, (Liu et al., 2019 : Gomes et al., 2023).

Actinomycetes are a significant group of Gram-positive bacteria, well known for their ability to produce a wide variety of secondary metabolites with diverse chemical structures and biological functions. (Rui et al., 2025).

Hermann Staudinger was the first to define the modern understanding of polymers at the beginning of the twentieth century. Through the development of biochemistry and microbiology, the notion of biopolymers was born, which are macromolecules occurring in nature that are synthesized by living organisms (Saharan et al., 2024).

The microbial-based biopolymers have attracted great attention in the world over recent years following the vast biotechnology applications (Bhatia, 2023). Microbiologically obtained biopolymers are said to be superior in terms of chemical purity, biological activity, functional significance, and production efficiency as compared to plant and algae biopolymers because bacteria are highly efficient cellular factories. (Mohamed et al., 2018 : Ghosh et al., 2021).

Biopolymers are believed to be the alternatives to the common antifungal drugs that could help eliminate the pathogenic fungi in situations when they are resistant to traditional antibiotics (Muangsawat et al., 2024). Besides being antifungal, biopolymers also have significant anticancer properties. They are

defined by a high capacity of preventing the proliferation of cancer cells and low toxicity to normal cells (Wadhwa et al., 2019; Al-Zuwaini et al., 2025).

Nanotechnology, along with biopolymers, is one of the new branches of science that crosses the frontiers of applied microbiology. Nanoparticles have a special set of characteristics, such as small size, surface structure, charge, and solubility, and are therefore ideal models to study the interactions between nanoparticles and living cells (Asha and Narain, 2020; Hammami et al., 2021).

The biological synthesis of nanoparticles has been the subject of more and more research, especially the bacterial-mediated synthesis, as it is environmentally friendly, bacteria can be cultured and isolated easily, controllable experimental conditions, including pH and temperatures, can be used, the generation time is short, and economically cheap (Jang et al., 2015.)

Gold nanoparticles have received increasing attention relative to other metallic nanoparticles and have been regarded as a pillar of numerous technologies in the twenty-first century. It is explained by high stability, outstanding chemical inertness, and high biocompatibility (Ahmed & Ikram, 2016)

Au NPs serve as mechanical and biochemical agents on the cell wall of Candida species (Penman et al., 2024) . also very effective anticancer agents with few side effects and a variety of mechanisms of action (Patil et al., 2019).

Although the studies on the microbial synthesis of biopolymers and gold nanoparticles are on the rise, there is a significant gap in the research on the production capacity of anaerobically isolated bacteria of riverbanks. In line with this, there is a need to study the capacity of bacterial isolates in such settings to biosynthesize biopolymers and gold nanoparticles and to determine their biological functions.

1.2 Aim of the Study

1. To isolate Actinomycetes bacteria in riverbank soils and determine them using molecular approache .
2. To determine the capacity of the bacterial strain to produce biopolymers and gold nanoparticles.
3. To define the produced biopolymer through ultraviolet-visible (UV-Vis) spectrophotometry, Fourier transform infrared (FTIR) spectroscopy, X-ray diffraction (XRD), scanning electron microscopy (SEM), thermogravimetric analysis (TGA), zeta potential, solubility, and polymer content of total carbohydrate.
4. To describe the synthesized gold nanoparticles based on the ultraviolet-visible (UV-Vis) , Fourier transform infrared (FTIR) spectroscopy, X-ray diffraction (XRD), scanning electron microscopy (SEM), transmission electron microscopy (TEM), atomic force microscopy (AFM), and zeta potential.
5. To compare the antifungal effect of the bacterial products against Candida spp., the anticancer effect on the human thyroid carcinoma cell line FTC-133, and the human dermal fibroblast normal cells (HdFn).

Chapter Two

Literature Review

2.1 Actinomycetes

The term "actinomycetes" originates from ancient Greek, combining the words ἀκτίς (aktís)meaning "ray" and μύκης (múkēs) meanin "fungus" . (Patel et al .,2021)

Actinomycetes are gram-positive, aerobic, and spore-forming bacteria that have a high guanine-cytosine (GC) content of between 57 and 75 in the genome. They belong to the order *Actinomycetales*, which is characterized by the presence of both substrate and aerial mycelium (filamentous structures). When cultured on the surface of agar, actinomycetes develop branched structures that form a network of hyphae growing both above and beneath the agar surface. The hyphae that grow above the surface are known as **aerial hyphae**, while those that grow beneath are referred to as **substrate hyphae**. (Bhatti et al.,2017)

Actinomycetes are prokaryotic organisms belong into the taxonomic group of bacteria to the phylum Actinobacteria, one of the biggest taxonomic units within the 18 significant phylogenetic group recognized inside the Domain of Bacteria ،belonging to order Actinomycetales, and family Actinomycetaceae .

Playing a fundament role within the microbiota of ever environments These bacteria adapt under harsh conditions, such as alkaline or saline habitats, dehydrated stress, and high temperatures. The characteristics of cell and metabolic adaptability allow these bacteria to be existent and presist in a broad range of environments (Ventura et al., 2007: Farda et al .,2022).

Among the predominant categories of bacteria in the soil ecosystem, actinomycetes account for over 30% of the whole microbial biomass, and their abundance is between 10^6 and 10^9 cells per gram of soil (Silva et al., 2022).

Actinomycetes play a vital role in the soil via biodegradation and humus formation , they recycle the nutrients associated to intractable polymers, like keratin,chitin, and lignocelluloses,this produces various aerosolizable compounds such as geosmin especially by Streptomyces in terrestrial and aquatic environments , Geosmin is produced by enzyme geosmin synthase encoded in geoA , is responsible for the characteristic "wet earth odor.

Free-living actinomycetes are widely distributed in soil environments as well as in freshwater and marine ecosystems. they play an important ecological role in the turnover of organic matter. Many actinomycetes have developed symbiotic relationships with plants, fungi, insects, and animals. These interactions are often beneficial, as actinomycetes produce natural compounds that help their hosts protect antipathogenic or pests. (Van der meij et al.,2017)

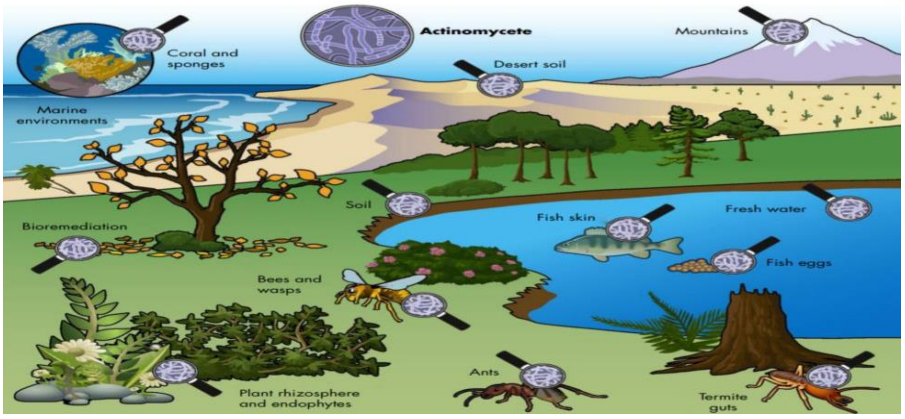

Figure (2-1) Distribution of actinomycetes bacteria in different habitats **(Van der Meij et al., 2017).**

Actinomycetes are among the most prominent microorganisms of high commercial value due to their saprophytic nature and remarkable ability to secrete a wide spectrum of secondary metabolites and extracellular enzymes. The number of bioactive secondary metabolites produced by microorganisms is

estimated to be around 23,000, of which approximately 10,000 are produced by actinomycetes, representing about 45% of all discovered microbial bioactive metabolites. **(Sharma et al ., 2014)**

2.2 Genus : Schaalia

Schaalia gen. nov. a new Latin feminine name designated in honor of the German medical microbiologist Klaus P. Schaal, in recognition of his significant contributions to the study and taxonomy of the genus Actinomyces (Nouioui et al., 2018).

The results of Nouioui et al .,2018 study revealed the presence of six clades within the genus Actinomyces, occupying isolated positions in the phylogenetic tree constructed from whole-genome analysis, and not belonging to the main cluster of the other species within the genus. These clades exhibited significant protein-level differences, both in total protein content and gene sequences, exceeding those observed between some officially recognized separate genera. Based on these genomic and physiological differences, a new classification was proposed, resulting in the establishment of the genus Schaalia gen. nov. to regroup these species, which were previously classified under Actinomyces, as their genetic and genomic relationships demonstrated sufficient independence to warrant a separate genus.

According to Nouioui et al. (2018), the genus Schaalia was distinguished (established) from Actinomyces based on a set of shared characteristics among the species transferred to this new genus. Reclassification was carried out based on the branching patterns revealed by whole-genome phylogenetic analysis, which were inconsistent with the traditional classification that relied primarily on morphological and chemical characteristics.

Whole-genome analysis provides the highest level of accuracy for distinguishing microorganisms, as it can reveal very subtle differences that may be overlooked by conventional methods. Although techniques such as 16S rRNA gene sequencing, housekeeping genes, and core genome SNPs have been widely used, these methods may lack the resolution to distinguish closely related strains or species. Therefore, there is a pressing need for whole-genome phylogenetic analysis to obtain the most accurate and comprehensive evolutionary relationships and to provide robust evidence for species classification and identification. It is also important to note that biochemical tests using the API system offer only preliminary species identification, whereas whole-genome sequencing can deliver more precise taxonomic resolution through comprehensive genomic profiling (Tian et al., 2024).

2.2.1 Characteristics of Schaalia

Schaalia are aerobic or facultatively anaerobic gram-positive bacteria with cell morphologies classified as straight or slightly curved rods, and some are even branched (Tian et al., 2023). These bacteria are mostly slow-moving and comprise the commensal group in the oral cavity, pharynx, gastrointestinal tract, and female genitourinary tract (Cronin et al., 2023).

Members of Schaalia are exclusively human and animal mouth microbiota and have been implicated in some human diseases. They are crucial to oral health by their capacity to form biofilm, their interaction with other microorganisms, and their manner of promoting host immune responses (Tian et al., 2023).

The cell wall of the Schaalia species has a chemical and physiological structure of L-lysine as its main diamino acid, peptidoglycan of the A5alpha or A5beta type, and the residues of muramic acid in the peptidoglycan are N-acetylated.

The cell-wall sugars are mainly mannose and rhamnose, the major respiratory quinone being MK-9(H4) in small traces of MK-10(H4) and MK-8(H4). DPG and PG are the main polar lipids, and the fatty acid composition contains a lot of saturated and unsaturated fatty acids, iso- and anteiso-branched fatty acids (Nouioui et al., 2018).

Schaalia species have been recovered in cultures taken in deep infections after a variety of shoulder operations, such as rotator cuff repair, joint arthroplasty, and shoulder instability (Cronin et al., 2023).

2.2.2 Classification of *schaalia naturae*

According to **BacDive (2018),** the **taxonomic classification of** schaalia *naturae*:

Domain: Bacteria

Phylum: Actinomycetota

Class: Actinomycetes

Order: Actinomycetales

Family: Actinomycetaceae

Genus: *Schaalia*

Species: *Schaalia naturae*

Phylogenetic analyses based on 16S rRNA gene sequences of the bacterial isolates examined in the study by Rao et al. (2012) revealed that they represent a distinct evolutionary lineage within the genus Actinomyces, showing low similarity to previously described species. These isolates occupy a unique position within the phylogenetic diversity of the genus, forming a cluster that includes eleven species out of the thirty-eight known Actinomyces species. *Actinomyces naturae* was identified as the first species of this genus to be isolated from a non-human and non-animal environmental source. It was therefore proposed as a novel species, designated *Actinomyces naturae* sp. nov.,

highlighting the importance of natural environments as unexplored reservoirs that may harbor novel strains with distinct physiological characteristics.

Following the taxonomic reclassification conducted by Nouioui et al. (2018) , *Actinomyces naturae* was transferred to the newly established genus Schaalia and is currently recognized under the name *Schaalia naturae.*

S. naturae (from the Latin naturae, meaning "of nature," intended to indicate that it is derived from the environment (Nouioui et al., 2018).

was first isolated from groundwater contaminated with chlorinated solvents by Rao et al. (2012). The isolation was part of a study aimed at characterizing the microbial community structure of contaminated groundwater at the Petro-Processors of Louisiana, Inc. (PPI) Superfund Site, located near Baton Rouge, Louisiana, USA.

This bacterium was described as a facultatively anaerobic, Gram-positive, rod-shaped, non–spore-forming, and motile organism. Physiological tests indicated that the strain was oxidase- and catalase-negative, yet capable of nitrate reduction. Growth occurred within a temperature range of 20–43°C (optimum, 30–37°C) and a pH range of 4.5–9.0 (optimum, pH 6.5). The organism was able to utilize several mono-, di-, and trisaccharides as carbon sources.

These metabolic capabilities form the basis for their production of a diverse range of biopolymers. They also highlight the ability of bacteria, as microbial cells, to synthesize various functional biological materials, including nanomaterials.

2.3 Historical overview of polymer

Polymers have been present throughout the history of life, forming the essential building blocks of all living beings, from plants to animals. It was not until the mid-20th century that scientists gained a deeper understanding of their true characteristics. This knowledge concurred with the invention of plastics, fully synthetic materials that exhibit human creativity and innovation.

The term polymer is derived from classical Greek words poly ,meaning "many" and meres ,meaning "parts." Thus a polymer is a large molecule (macromolecule) built up by the repetition of small chemical units. (Ebewele,2000) .

The term "polymer" was originally introduced by the Swedish chemist J. J. Berzelius, who, for example, considered benzene (C_6H_6) to be a polymer of ethyne (C_2H_2). (Feldman .,2008)

The concept of polymers is considered one of the most significant scientific ideas of the 20 th century. In 1920, the chemist Hermann Staudinger sparked considerable debate within the international chemical community when he proposed that certain materials, such as natural rubber, possess extremely high molecular weights. In his research paper entitled "Über Polymerisation," Staudinger presented a series of reactions demonstrating how large molecules could be formed by linking numerous small molecules together. He coined this process "polymerization," in which the repeating units, called monomers, are joined through strong covalent bonds to form long chains. According to Staudinger, these compounds consist of macromolecules comprising more than 10,000 monomers.

Polymers are play essential role in daily life, with applications ranging from advanced biomaterials, such as prosthetic hip and knee joints, to aerospace materials. Their popularity stems from their ease of processing and the ability to tailor their properties. By modifying the atomic composition of repeating units or the molecular weight, polymers can be customized to meet specific needs (Puoci et al .,2008) .

2.3.1 Biopolymer

Since the dawn of humanity, nature and natural systems have served as a rich source of both raw materials and inspiration for the majority of processes and applications developed by humans. Biopolymers, which play an indispensable role in natural ecosystems, are a clear example of this. (Kalina et al.,2015)

Biopolymers are polymers synthesized by living organisms through enzymatic processes that link basic building blocks such as sugars, hydroxyl fatty acids, and amino acids to form high-molecular-weight molecules. Living organisms can produce a wide range of biopolymers, including polyamides (amino acids joined by peptide bonds), polysaccharides (sugars or sugar acids linked by glycosidic bonds), polyphosphates (inorganic phosphates connected by anhydride bonds), and polyesters (hydroxyl fatty acids linked by ester bonds).

Biopolymers, according to Baranwal et al. (2022), are organic compounds found in natural sources. They are large macromolecules composed of many repeating units. According to the IUPAC, these units are defined as biopolymers. Biopolymers are both biocompatible and biodegradable, which makes them suitable for a variety of applications. These include edible films, emulsions, food packaging materials, as well as drug delivery systems, medical implants, wound healing, tissue scaffolds, and dressing materials in the pharmaceutical industry.

The most common macromolecules in biopolymers are nucleic acids, proteins, carbohydrates, and lipids.

Biopolymers produced by bacteria exhibit superiority over those extracted from plants and algae in terms of chemical purity, biological activity, functional significance, and production efficiency (Mohamed et al., 2018).

Bacteria act as highly efficient cellular factories, converting carbon and nitrogen sources into various intracellular and extracellular biopolymers. When bacteria are pathogenic, the polymers they produce often serve as key virulence factors. In contrast, when non-pathogenic bacteria produce them, the biopolymers can be used as food ingredients or biomaterials. (Ghosh et al., 2021)

Bacteria support the production of biopolymers, despite the fact that this process consumes both nutrients and chemical energy, because it represents an adaptive strategy that enables them to grow and survive under a wide range of unfavorable environmental conditions, including overcoming immune responses within host cells.

Biopolymers serve multiple biological roles, including protection, energy storage, and adhesion. They act as protective capsules that safeguard cells and their storage components, and they also contribute to forming the structural matrix involved in biofilm development. It is well established that bacteria produce extracellular polymeric substances (EPS), which interlace to form a network surrounding bacterial cells, acting as a supportive scaffold. EPS production is essential for biofilm formation, which consists of organized cellular communities considered among the most resilient forms of life on Earth.

2.3.2 Classification of Biopolymers

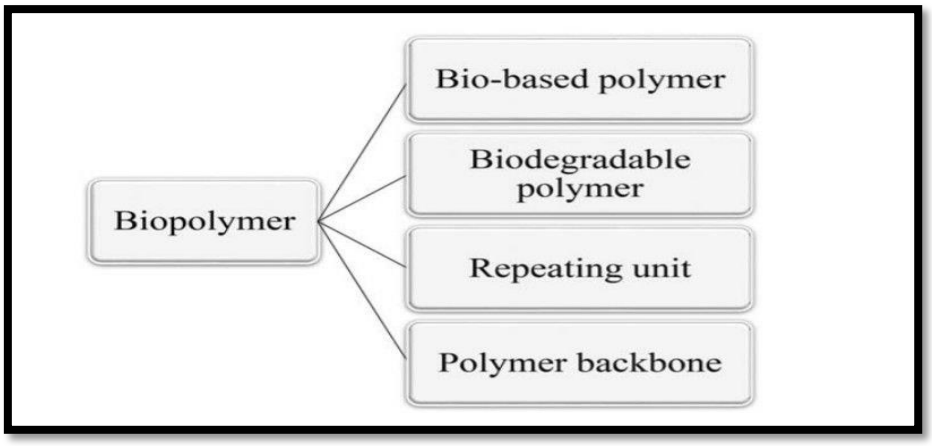

Figure (2-2) Classification of Biopolymers (mazuki et al .,2022)

Biopolymers can be classified in various ways according to different criteria :

Depending on their nature and method of fabrication, bio-based polymers can be classified into three main groups according to their renewable sources: **First group**: Bio-based polymers primarily derived from agropolymers, such as chitosan, lignin, protein, cellulose, and starch .

Second group: Bio-based polymers produced from genetically modified crops or microorganisms, such as polyhydroxyalkanoates (PHA).

Third group: Bio-based polymers obtained from agro-resources or petro-based sources through fermentation and/or conventional chemical methods, such as poly(butylene succinate) (PBS), polyimides, polylactic acid (PLA), and polyurethanes. (mazuki et al .,2022).

Depending on their degradability, they are divided into two main categories: biodegradable and non-biodegradable (Ferreira et al., 2016).

Biopolymers are classified into three main categories based on the nature of their repeating units: proteins, which are composed of amino acids; polysaccharides, which are composed of sugars; and nucleic acids, which are composed of nucleotides (Ye et al., 2012).

According to chemical bonds in the polymer backbone ,The majority of bacterial polymers can be classified into four main classes: polysaccharides, polyesters, polyamides, and inorganic polyanhydrides (such as polyphosphates) (Rehm, 2010)

2.3.3 Polysaccharides

Polysaccharides are a type of biopolymer composed of simple fundamental units known as monosaccharides. These units are linked together through O-glycosidic bonds, arranged either linearly or in a branched manner, resulting in the formation of polysaccharide chains containing more than 20 and up to 60,000 monosaccharide units (Maji, 2019).

The term "exopolysaccharide" was first used by Sutherland in 1972 to describe high-molecular-weight carbohydrate biopolymers produced by bacteria. (Osemwegie et al., 2020).

Exopolysaccharides (EPS) refer to high-molecular-weight biological macromolecules produced by microorganisms and secreted into their surrounding environment (Kumari et al., 2025).

Term of EPS applied as a reference to polysaccharides, which make up about 40 to 95 percent of the polymeric materials that microorganisms release into their environment. Besides, exopolysaccharides differ in terms of molecular weight,

size, glycosidic linkage, extent of branching, and presence of neutral or ionic functional groups. (Escarcega-González et al. 2018).

It considered fundamental components of various forms of life, playing a crucial role in maintaining structural integrity and supporting essential cellular functions (Casillo et al., 2022).

They are among the most widely distributed natural biopolymers and possess an excellent reputation due to their distinctive properties. Firstly, they are economically affordable; secondly, they can be chemically modified to meet specific purposes. (Shariatinia, 2019).

Polysaccharide-based biopolymers exhibit a higher level of stability compared to protein-based polymers, which are more susceptible to aggregation and instability. This is attributed to the chemical structure and physical properties of these materials, such as their thermal stability. Thus, polysaccharide-based biopolymers can provide environmentally friendly and promising stabilizers as alternatives to toxic chemical stabilizers. Additionally, the use of this method presents an eco-friendly and cost-effective option. (Kalina et al., 2015 ; Hassanein et al., 2021).

Exopolysaccharides (EPSs) are generally classified into two main types based on their monosaccharide composition:

- **The first type:** homopolysaccharides, consists of repeated units of a single simple sugar linked together through glycosidic bonds.
- **The second type:** heteropolysaccharides, is composed of two or more different monosaccharide units (Roy et al., 2019).

According to Escárcega-González et al. (2018), exopolysaccharides (EPS) can be classified based on their association with the cell into two main types:

- **Slime polysaccharides:** These are carbohydrate polymers that are loosely attached or freely released from the cell surface, typically forming a viscous layer around the microbial cell.
- **Capsular polysaccharides:** These are carbohydrate polymers that are firmly bound to the cell envelope, forming a compact and well-defined structure known as a capsule.

2.3.4 Bacterial Polysaccharides

Bacterial exopolysaccharides (EPS) are metabolites that are released by diverse bacteria, which are crucial in the survival of microbial cells. The compounds have a myriad of biological roles, including protecting the cells, interacting between the cell and the environment around it, and also protecting against adverse environments like dehydration. They are also involved in minimizing the effects of toxic substances and acclimatization to environmental changes, as well as avoiding the immune system's response to viruses. Also, EPS is important in processes like the adhesion to solid surfaces, cellular aggregation, and the improvement of the cellular interaction. Bacteria-generated exopolysaccharides have their particular benefits over plant, animal, and algal polymerases. These can be continuously manufactured regardless of seasonal changes or weather conditions, hence making them fit in industrial-level production. They come out of the cell easily due to their extracellular viscosity and into the rest of the environment. Therefore, cell-free liquid extraction techniques are not complex and are cheap. (Abdalla et al., 2021).

They are shed into the surrounding environment and accumulate on the outside of the cells. This is based on the fact that they can either be attached to the microbial cell surface or be present in the fermentation medium. Such polymers may be released as part of the cell surface-associated structures (as with capsular EPS) or as a free release into the culture medium (as with slime EPS). When exopolysaccharides are released into the environment, they combine with other biomolecules, including proteins, lipids, and hyaluronic acid derivatives, to create an extracellular matrix. (Escarcega-González et al. 2018).

Halomonas sp. was able to extract high molecular weight exopolysaccharides whose composition is composed of glucose, galactose, mannose, and glucuronic acid (Park et al., 2017; Asgher et al., 2020). Moreover, it was identified that a potent isolate of Bacillus velezensis KY498625 secretes exopolysaccharides of the galactose, glucose, and mannose levels (1.14×10^5 Dalton) (Moghannem et al., 2018).

2.3.5 Biosynthetic Pathways of EPS

Exopolysaccharides (EPS) are synthesized within cells during the late logarithmic or stationary phases of growth. The EPS production process is affected by many stresses, including nutrient imbalances, salinity, temperature variations, pH, and environmental factors (Kaur and Dey, 2023).

The exopolysaccharides (EPS) are synthesized within the cell by a succession of heterogeneous enzymatic modifications that adhere to the same overall principle of the production of activated sugars or sugar acids, formed by different biosynthetic routes. External production is performed by the extension of the polymer chain with the introduction of monosaccharides, which are obtained by the disintegration of disaccharides or trisaccharides (Schmidt et al., 2015).

The mechanism of production of EPS within the cell is very intricate and combines the activities of a great number of enzymes, carriers, and transporter proteins, which are coded by chromosomal or plasmid genes. Glycosyltransferases (Gts) tend to produce exopolysaccharides (EPSs), which bind the sugar monomers into long chains carrying organic molecules bound to proteins and lipids; thus, they are stable and determine viscosity and shape (Nguyen et al., 2024)

Kaur and Dey (2023) explain that the exopolysaccharides (EPS) biosynthesis pathway in the cell is based on the transformation of sugar residues into a variety of monomeric units, which are polymerized and attached to an isoprenoid lipid carrier localized in the membrane. Through this process, the polymers are subjected to necessary changes, and once such changes are made, they are then moved out of the cell and assembled to compose the exopolysaccharides.

This is done in bacteria in a series of steps as follows:

1. Substrate is absorbed or enters the cell using special carriers or through diffusion into the cell.
2. Metabolism takes place through processes such as phosphorylation and conversion of intermediate substrate products.
3. The intermediates undergo anaerobic polymerization, leading to the formation of exopolysaccharides.
4. The polymer is modified by the addition of methyl, sulfate, or other groups.
5. Transport and secretion of the exopolysaccharides outside the cell.

This process is entirely regulated through three different biosynthetic pathways: (1) the Wzx/Wzy-dependent pathway;

(2) the ATP-binding cassette (ABC) transporter system; and

(3) the synthase-dependent pathway (Schmid et al., 2015).

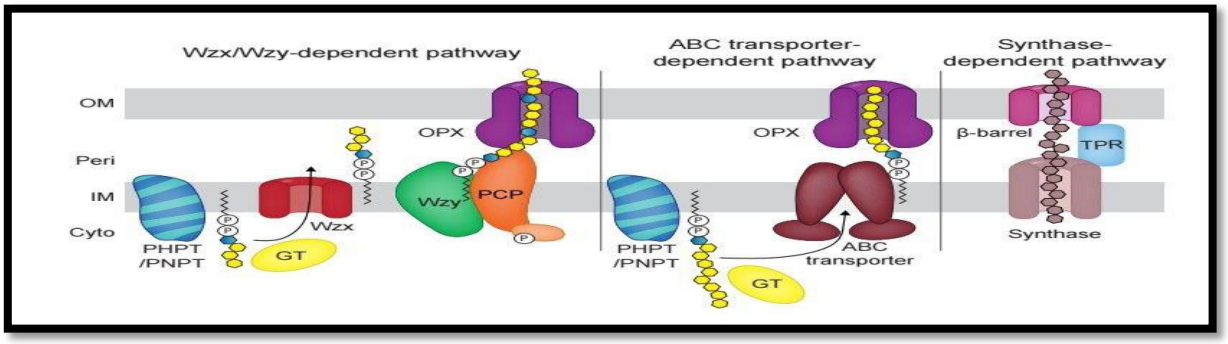

Figure (2-3) An overview of the Wzx/Wzy, ABC transporter, and synthase-dependent pathways for the biosynthesis of surface polysaccharides in bacteria . (Pérez-Burgos& Søgaard-Andersen,2020).

2.4 The concept of nanotechnology

"Nanotechnology is one of the most significant trends of science in the 21st century."(Altammar.,2023).

The start of the nanotechnology adventure began with the nanomolecule acquiring its own existence as an independent material entity."(Loeve .,2010). the term Nanotechnology cover the design, construction and using of functional structures that have one dimension at least measured in nanometres.(Kelsall.,2005).

Nanotechnology is a multidisciplinary science that involves nanoscience, nanophysics, nanoelectronics, nanomaterials, nanochemistry, nanometrology, nanobionics, etc.

Nanotechnology is a new branch of science that includes a set of applications ranging from energy production to industrial production processes, as well as biomedical applications and the engineering of nanomaterials to have distinct compositions and functions, thereby providing new tools and techniques. (Madkour .,2019).

Nanotechnology is a key enabling technology. (Satalkar.,2016). The origin of the grammatical form of the word 'nano,' according to the Oxford English Dictionary, comes from the Classical Latin nanus or the Ancient Greek nanos, meaning 'dwarf.' In 1958, the prefix 'nano' was added to the International System of Units alongside giga, tera, and pico (Boholm., 2016).

"A nanometer is a unit of measurement equal to one billionth (10^{-9}) of a meter. It is smaller than the length of visible light wave and wider than one hundred thousandth of the width of a human hair."(Tripathi.,2019).

The size of a nanometer relative to a meter is comparable to that of a marble relative to the Earth. The building blocks of nanotechnology are nanoparticles, which are defined as dispersions or solid particles with at least one dimension in the nanoscale range .(Mohanraj.,2006).

Nanoparticles have a small size, surface structure, charge, and solubility; therefore, they are considered a better model for studying the significant influence of interactions with biomolecules and cells."(Asha and Narain .,2020).

These nanomaterials exhibit a distinct set of physical ,optical, magnetic, electrical, biological, chemical and catalytic properties. (Aljuhani et al .,2021).

The synthesis of Nanoparticle can be obtained by two basic approaches: the bottom-up and top-down approaches."(Purohit.,2019).

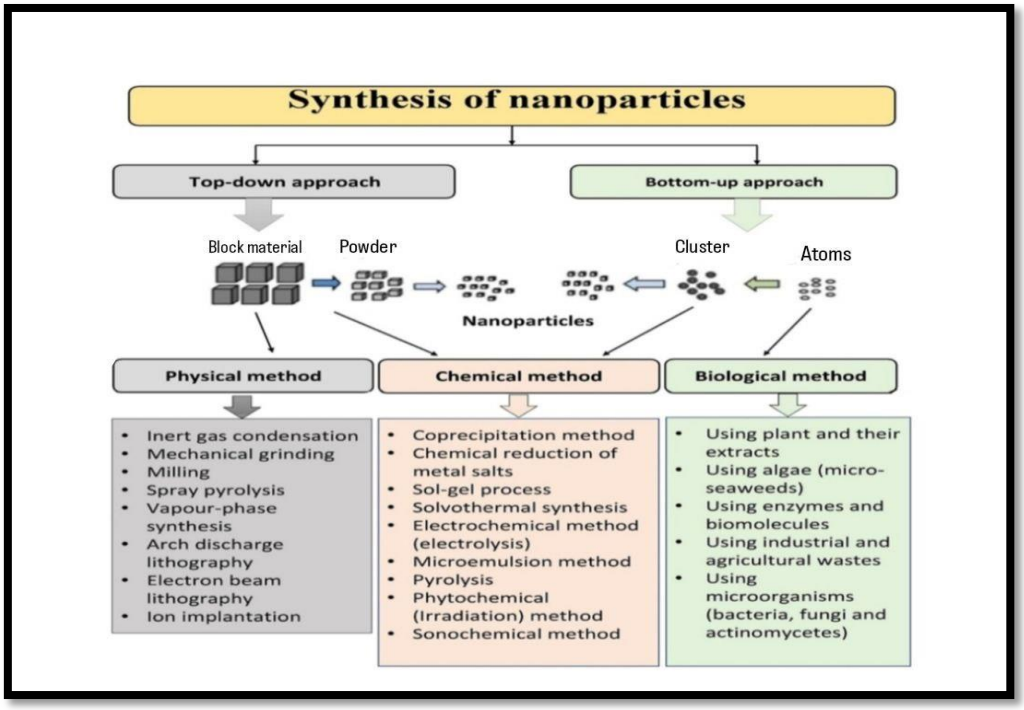

Figure (2-4) Methods of Nanoparticle Synthesis (Adimule et al .,2022)

2.4.1 Biological synthesis of nanoparticles

The birth of nanoscale matter has generated so excitement among researchers and pledges to modification numerous fields of materials sciences in the twenty - one century and beyond. (Shinde, 2012)**.** Biological synthesis is a green chemistry method that links biotechnology and nanotechnology (Rane et al.,2018).

Green nano-biotechnology means using biological passage involving microorganisms, viruses ,plants, or their products, like lipids and proteins with

the aid of different biotechnological tools to synthesizing of nanoparticles, is proper with the principles of green chemistry . Nanoparticles manufactured by this method are characterized by far superior to nanoparticles manufactured with chemical and physical methods in term of diverse aspects. For instance, reduce depend on costly chemicals , minimize consumption of energy , and produce by-products eco-friendly ،Biocompatibility ,safe and non-poison reagents with more stability and suitable dimensions because they are synthesized by one-step bio-procedure (Parveen et al.,2016).

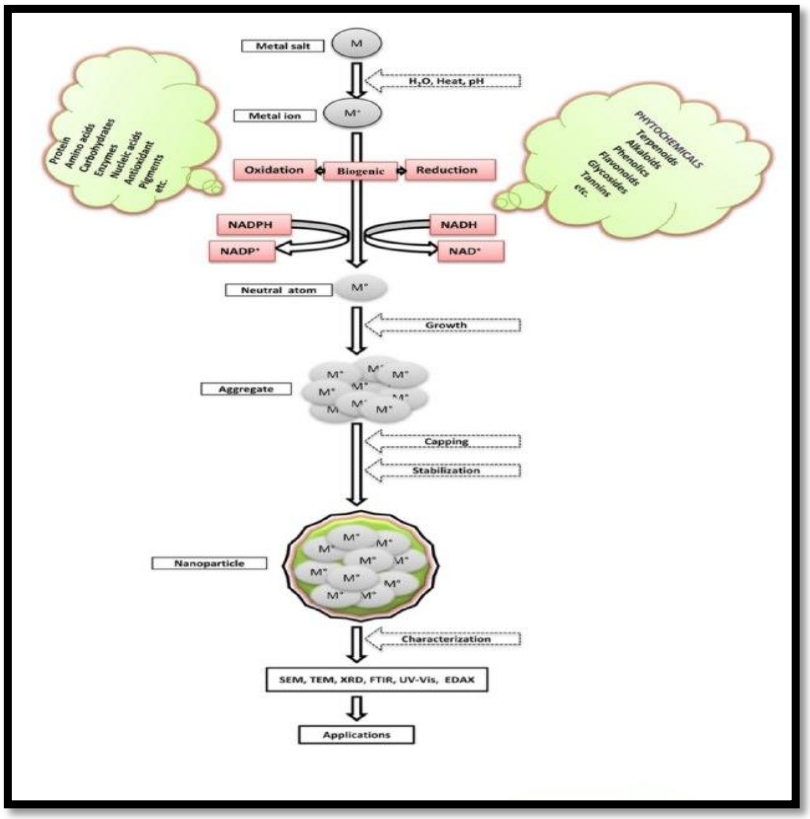

Figure (2-5) Scheme summarizing potential of biological mechanism that mediated nanoparticles synthesis . where symbol of M is metal salt, M+ is Metal ion and M 0 is neutral atom (Hussain et al .,2016).

Making them suitable for a wide range of applications. In the medical field, biologically synthesized nanoparticles are used for diagnostics and treatment, including drug delivery systems that precisely target cancer cells. Additionally, they are utilized in the fabrication of biosensors for detecting diseases such as cancer and bacterial infections. Nanoparticles produced by microorganisms have also demonstrated antimicrobial properties, making them a promising option for developing treatments against antibiotic-resistant bacteria.

Microorganisms, including bacteria, fungi, micro algae,yeast and viruses, are effective tools for synthesizing nanoparticles in environmentally friendly biological ways. The development of nanoparticle synthesis using microorganisms has emerged as an alternative to conventional physical and chemical techniques, which often rely on harsh conditions and toxic chemicals. This makes microbial synthesis more sustainable and cost-effective. These microorganisms have the ability to reduce metal ions and convert them into nanoparticles through intracellular or extracellular processes using natural biological mechanisms (Gahlawat& Choudhury,. 2019).

Bacteria are among the most widely used microorganisms in this field. such as Pseudomonas spp , Bacillus spp and actinomycetes etc can produce nanoparticles of silver, gold, and metal oxides. These bacteria secrete reductase enzymes that convert metal ions into their nanoscale form. The earliest known report of bacteria synthesizing nanoparticles dates back to 1984, when Haefeli studied Pseudomonas stutzeri AG259, a bacterial strain originally isolated from a silver mine. This strain exhibited the ability to synthesize silver nanoparticles." (Punjabi et al .,2015).

The most critical factors influencing the biosynthesis of nanoparticles are pH, temperature, and precursor concentration, as they significantly affect the size,

shape, and functional properties of the resulting nanoparticles. (mohammadi & ghasemi ,2018).

The synthesis of nanoparticles may occur either inside or outside the cells, depending on their site of formation .(Hulkoti & taranath ,2014).

2.4.2 Gold Nanoparticles

Gold (Au), with an atomic number of 79, is a transition metal that naturally occurs as a dense, reddish-yellow element. It belongs to Group 11 of the periodic table and is classified as a noble metal due to its remarkable resistance to most common acids, except aqua regia. Owing to its scarcity in the Earth's crust, the average abundance of gold is estimated at approximately 5 ng/g, while its concentration in natural waters ranges from 0.0197 to 0.197 µg/L (McHugh, 1988; Mandaro, 2009; Devillanova & Du Mont, 2013).

Gold has been used for therapeutic and aesthetic purposes, particularly in the crafting of jewelry, since ancient times due to its chemical inertness, resistance to atmospheric changes, and ability to retain its attractive color (Yang et al., 2015).

Gold is generally known to be non-toxic and biocompatible in a chemical way, and until recently, it was regarded as a mere conventional metal. But the advent of nanotechnology and the discovery of nanoparticles, plus the exploration of the physicochemical characteristics of gold in nanoscale, have made it one of the most attractive materials with sophisticated uses. Nanoscale particles have a unique complex of properties, including size, surface properties, charge, and solubility; this is why they are taken as a more appropriate model of close interaction with biomolecules and cells, which is important. In 1857, Michael Faraday was the first to successfully synthesize gold nanoparticles and observed

their distinctive property of exhibiting a red coloration and its derivatives (Asha and Narain, 2020 ;Hammami et al., 2021).

In recent years, gold nanoparticles have been widely applied across various disciplines, including drug delivery, catalysis, biosensors, cosmetics, and numerous biomedical applications. As the most stable nanoparticles, they are considered a cornerstone of new technologies in the 21st century. Their chemical stability and distinctive properties make them highly promising candidates for a broad range of biological and biomedical applications (Ahmed and Ikram, 2016).

2.4.3 The biological synthesis of gold nanoparticles

The green synthesis of gold nanoparticles has commanded attention because of its rapidity, eco-friendliness, and cost-effective protocol, offering a single-step technique at ambient temperature and pressure conditions, and it is non-pathogenic. The biological synthesis method utilizes a broad range of organisms such as plants, yeast, fungi, bacteria, and actinomycetes, compared with classical physical and chemical methods. (Ahmed and Ikram,2016).

Microorganisms serves as potential biofactory for synthesis of metallic nanoparticles for instance cadmium sulfide, silver and gold. (Husseiny et al.,2007).

According to Shukla and Iravani (2018), the reducing agents and other constituents present within cells serve as stabilizing and capping agents, thereby obviating the need for the addition of external stabilizing or capping substances. These reducing agents are extensively distributed across biological systems.

Table (2-1) Several organisms /microorganisms have been reported to produce gold nanoparticles in previous studies

Organism	Scientific Name	Size in nm	Reference
Plant	*Eucalyptus camaldulensis* *Azadirachta indica* *Magnolia kobus* *Diospyros kaki*	5.5 − 7.5 20-40	(Ramezani et al .,2008) Song et al.,2009
Fungi	*Aspergillus niger*	10-30	(Soni and Prakash .2012). (Zhang et al.,2011)
	Aureobasidium pullulans	6	
	Fusarium sp.	83	
	Fusarium oxysporu	70	
Yeast	*Yarrowia lipolytica*	40–120 nm	(Guerra et al .,2025) (Zhang et al.,2016
	Pichia kudriavzevii	30–140 nm	
	Candida utilis	15–50	
	Magnusiomyces ingens LH-F1.	10-80	
Alage	*Sargassum wightii* Greville	8-12	Singaravelu et al.,2007 Venkatesan et al.,2014 Ramakrishna et al.,2016
	Ecklonia cava	15-55	
	Turbinaria conoides	12-57	
	Sargassum tenerrimum	5-45	
Bacteria	*Ureibacillus thermosphaericus* *Rastrelligerkanagurta* *Selachimorphasp.* *Panna microdon*	50-70 45-80	Xiangqian et al.,2011 Rajasekar et al.,2020
Virus	Cowpea chlorotic mottle virus	8-24 nm	Slocik et al.,2005 Karczewska-Golec et al., 2024) (Iravani and Zolfaghari .2022)
	Bacteriophage M13	20 nm	
	Tobacco mosaic virus	5 nm	
	Cowpea mosaic virus	30 nm	

2.5 Antifungal Activity

2.5. 1 Fungal infections

Fungal infections , also known as mycoses, are caused by pathogenic fungi and encompass a wide spectrum of conditions, ranging from superficial or cutaneous infections which generally respond well to routine pharmacological treatment to invasive systemic infections that can be life-threatening. (Vitiello et al.,2023).

Fungal infections also afflict more than one billion people annually all over the world, of which candidiasis disease causes about a quarter to two-thirds of these infections. Despite the development of the treatment plans, the rates and the number of fatalities in connection with these infections are growing. (Tamo, 2020).

Candidiasis is an infection caused by opportunistic fungi of the genus Candida, the manifestation of which can be mucocutaneous injuries or acute bloodstream infections that can even be fatal. Candida species are found in the different organs of the human body, such as the oropharyngeal mucosa, esophagus, gastrointestinal tract, and genitourinary mucosa. (Arumugam et al., 2024).

There are few treatment options in case of fungi as opposed to bacterial infections, where numerous medications that counter infections can be used. Existing antifungal agents only reflect a few key classes, such as polyenes, azoles, and echinocandins. Candida and Aspergillus are among the most drug-resistant genera of fungi that are extremely difficult to treat or prevent.

The mechanisms of resistance to antifungal agents in pathogenic fungi are a result of genetic plasticity and the capacity of the mentioned organisms to adjust their cellular reactions to adapt to stressful conditions in the environment (Ben-

Ami & Kontoyiannis, 2021). The problem of antifungal resistance is a growing issue in clinical medicine as the number of fungal infections has been constantly increasing, and the selection of therapeutic options is limited. It develops intrinsic resistance mechanisms, including less drug-target binding, high activity of efflux pumps, and fungal cell wall and membrane composition, and acquired resistance mechanisms, including genetic mutations, gene duplication, transposon insertion, aneuploidy, and loss of heterozygosity (Kadariswantiningsih et al., 2025).

Besides, the optimum duration of antifungal therapy has not been defined yet, since it varies based on various factors, such as the immune state of the patient, the type of fungus species and its susceptibility to drugs, and the speed and efficacy with which antifungal therapy is commenced (Vitiello et al., 2023).

Creating new antifungal agents is very challenging, and this has been attributed to the fact that these agents may be poisonous to human beings. This is because the resemblance between fungi and humans is so high in the structure, and it is hard to target fungal pathogens without attacking host cells. (Vitiello et al., 2023).

The mechanisms of antifungal drug resistance should be categorically and thoroughly understood with the aim of coming up with new therapeutic methods that can deal with the existing and ever-increasing threat of fungal diseases.

2.5.2 Biopolymer as Antifungal Agent

As reported by Tarek et al. (2024), Candida albicans and Candida krusei are the most commonly isolated species in the Candida genus, which cover a range of about 70-75 percent of all reported cases of candidiasis in humans and animals.

Many studies have indicated that biopolymers have significant promise to be used as antifungal agents in the treatment of Candida infections.

The antifungal properties of various types of biopolymers against Candida albicans and Candida krusei were tested in the work by Seyfarth et al. (2007). The findings showed that the antifungal activity of all forms was to different extents, which was attributed to variation in the functional groups and surface charge of the polymers. The experiment also found that the antifungal effect is attributed to the fact that the biopolymer can interact with the fungal cell wall and membrane, causing a reduction in membrane integrity, permeability, and leakage of cellular contents, as well as preventing fungal growth.

In Matsubara et al. (2016), the influence of biopolymers issued by Lactobacilli was evaluated at the early phases of Candida biofilm development. The findings indicated that these biopolymers substantially inhibited the growth of fungi and decreased cell adhesion to surfaces and filamentation, which is essential in the structural maturation of the biofilm.

Almost more recently, Hong et al. (2024) illustrated that biopolymer particles are a prospective strategy used to cure candidiasis and mitigate the virulence of C. albicans. These particles successfully and dose-effectively inhibited filamentous growth and reduced abiotic surface adhesion as well as biofilm development important aspects of fungal pathogenicity. Transcriptional regulation of virulence-related genes, such as hypha differentiation gene repression and stress-response gene activation, was linked to this inhibitory effect. Besides, the particles minimized fungal adhesion to human epithelial cells without causing cytotoxicity, which is a notable attribute of a biocompatible particle.

Taken together, these investigations point to a high potential of biopolymers as natural and promising in designing alternative or adjunctive measures to curb Candida infections, with a growing background of antibiotic drug resistance.

2.5.3 Nanoparticles as Antifungal Agents

As (Wu et al., 2025) put it, nanoparticles increase antifungal activity by multiple pathways:

1. Resistance the degradation in acidic or reducing conditions.
2. Changing how the body distributes drugs to reduce toxicity.
3. Having intrinsic antifungal activity, some nanoparticles have direct antifungal activity.
4. Attacking fungal molecular building blocks and interfering with protective biofilms, which add to drug resistance

Yu et al. (2024) have shown that the biosynthesized gold nanoparticles produced by Candida albicans have a bright potential in increasing the efficacies of azole antifungal drugs, such as fluconazole, itraconazole, and voriconazole, by 16- to 32-fold. The mechanistic studies demonstrated that these nanoparticles stimulate the accumulation of drugs in fungal cells, interfere with cellular structure, dissipate membrane potential, trigger the formation of reactive oxygen species (ROS), and deplete ATP, which surpasses fungal innate resistance mechanisms.

Moreover, these nanoparticles as adjuvant therapy led to a high level of healing of the vaginal mucosa of mice infected with C. albicans and indicate good efficacy of these nanoparticles as a therapeutic agent in animal models. Such results suggest that biosynthesized gold nanoparticles are a novel and safe approach, which can be adopted as an efficient adjuvant to extend the lifetime of

the already existing antifungal agents and increase their effectiveness in situations with multidrug-resistant fungal strains. (Yu et al., 2024).

Lotfali et al. (2020) findings showed that the gold nanoparticles (Au-NPs) have the potential to suppress the growth of Candida krusei, which means that it is possible to reduce its growth using them. This effect was, however, relatively dependent on the concentration of the nanoparticles, with a high concentration being needed in order to get a noticeable antifungal effect.

Carmo et al. (2025) have shown that unmoderated and gallic acid-conjugated gold nanorods can be applied to Candida krusei as antifungals. The tests demonstrated that these nanoparticles can fully stop the growth of planktonic cells at quite low concentrations of 1.56 to 3.12 µg/mL. It is interesting to note that the gallic acid-conjugated nanorods eradicated cells in less than eight hours as opposed to the twenty-four hours that the unmodified nanoparticles took. It was also found that at higher nanoparticle concentrations, the biofilms of the fungus were greatly influenced, with significant average decreases in biofilm density and extracellular matrix components and a greater level of porosity. These modifications promoted the penetration of nanoparticles and destabilization of biofilms. Speaking of the mechanism of action, the study reported that gold nanoparticles augment the generation of intracellular reactive oxygen species and reduce the level of ergosterol in the fungal cell membrane, leading to the disruption of membrane integrity and the antifungal effect. The results indicate that gold nanoparticles, especially those functionalized with gallic acid, are a prospective target for planktonic cells and biofilms of C. krusei and can be used as a single antifungal agent or as an adjuvant to facilitate the efficacy of the traditional antifungal treatment.

2.6 Anticancer Activity

2.6.1. Thyroid cancer

The thyroid gland is a butterfly-shaped endocrine gland located in the upper central part of the neck. It secretes essential hormones that regulate the function of various organs in the body, including heart rate, blood pressure, body temperature, and metabolic rates, thereby playing a key role in weight regulation. (Hu et al., 2018).

Thyroid cancer is among the most common malignant tumors affecting the endocrine system. Over the past few decades, its incidence has increased rapidly worldwide. ranks seventh among the most prevalent cancers in women, while it does not fall within the top 15 cancers in men.

There is a gender disparity in thyroid cancer regarding incidence, disease aggressiveness, and prognosis, with women being affected at a rate three times higher than men. Data indicate that less aggressive histological subtypes are more prevalent in women, whereas more aggressive subtypes exhibit a relatively balanced distribution between genders.

Studies suggest that this disparity may be partially associated with sex hormones, particularly through differences in the patterns and levels of estrogen receptor expression in thyroid tissue depending on the tumor histology. It is believed that the higher expression of estrogen receptors in women renders thyroid cells more sensitive to estrogen's proliferative effects, which may contribute to the higher incidence of follicular cellderived thyroid cancer in women compared to men. (Rahbari et al., 2010 ; Xin et al., 2024).

Thyroid carcinomas originating from the follicular epithelium are defined as tumors measuring 10 mm or less in diameter and are classified as pathological stage (pT1) according to the fifth edition of the TNM classification system for malignant tumors. Clinically, these small tumors are often discovered incidentally. (Clerici et al.,2010).

The early stage of thyroid cancer is often asymptomatic. Symptoms typically appear as the disease progresses and may include the development of neck masses, throat or neck pain leading to voice hoarseness, difficulty swallowing, swelling of lymph nodes adjacent to the gland, weight disturbances, and other related signs (Hu et al., 2018).

Patients with thyroid cancer generally have an excellent long-term prognosis, with 10-year survival rates among adults ranging from 92% to 98%. Prognostic outcomes are influenced by factors such as sex, age at diagnosis, histological subtype, and tumor stage. Accurate diagnosis, appropriate treatment, and long-term follow-up are essential to maintaining these favorable survival rates. (Mitchell et al., 2016)

2.6.2 Therapy of Thyroid Cancer:

According to the recommendations of the Society of Nuclear Medicine and Molecular Imaging (SNMMI) and the European Association of Nuclear Medicine (EANM) outlined in the 2022 guideline titled “Procedure Standard /Practice Guideline for Nuclear Medicine Evaluation and Therapy of Differentiated Thyroid Cancer: Abbreviated Version”, the following treatment approaches are recommended for the management of thyroid cancer. Total thyroidectomy is considered the primary and fundamental treatment for most patients, as it allows for complete tumor removal and facilitates the

subsequent application of nuclear therapies. Following surgery, radioactive iodine therapy (^{131}I Therapy) plays a central role, After completion of surgery and radioactive iodine therapy, thyroid hormone therapy with TSH suppression is employed as part of long-term follow-up.

In cases resistant to radioactive iodine or with distant metastases, systemic therapy with targeted agents is recommended.

Conventional chemotherapy is characterized by its lack of selectivity toward the intended target cells, as it generally attacks all rapidly dividing cells. This deficiency in specificity not only limits its therapeutic efficacy but also increases the likelihood of relapse due to the survival of certain tumor cells capable of continued proliferation after treatment. In addition, when such drugs are used repeatedly, they help cancer cells develop resistance to the drugs, thus becoming less responsive to treatment in the long run.

The lack of specificity of chemotherapy in the separation of malignant and normal cells has also resulted in severe side effects on normal tissues, the most notable ones being bone marrow suppression, cardiotoxicity, and both immune and gastrointestinal disorders. All of these side effects adversely affect the quality of life of patients and limit the possibility of increasing the dosages of the drugs when it is required. (Wang et al., 2024).

The existing treatment plan is based on the risk stratification of individual patients, which is determined by the post-surgical histopathological examination, molecular markers, thyroglobulin (Tg) levels, and the outcome of anatomical and functional imaging (Avram et al., 2022; Gulwani et al., 2024).

2.6.3 Anticancer Activity of Biopolymers

The traditional treatment interventions for thyroid cancer, such as surgery, radiotherapy, and chemotherapy, are not very satisfactory because of the early spread of the disease and high chances of recurrence. Also, heterogeneity of tumors and tumor microenvironments complicates the treatment with conventional drugs and makes them resistant to treatment. Moreover, the disease and targeting the complexities of the disease at a molecular level, which is specific to each patient, are not always possible with conventional methods, which makes determining a one-size-fits-all approach useless. (Gulwani et al., 2024).

The spectrum of pharmacological activities of biopolymers , which are antibacterial, antiviral, antifungal, and anticoagulant. Their anticancer potency is, however, the most remarkable in modern-day medical studies. Several biopolymers have been demonstrated to selectively bind to P-selectin receptors, which are highly expressed on the surface of cancerous cells, specifically at specific nanomolar dosages (Etman et al., 2020).

A lot of research has been done on the medical and therapeutic uses of natural biopolymers, particularly in cancer prevention and cure. The results show that certain biopolymers are capable of regulating or stimulating immune responses, and others have direct anticancer effects via epigenetic or through induction of apoptotic pathways (de Sousa et al., 2020). These biopolymers also inhibit the occurrence of the inflammatory cytokines, e.g., IL-6, IL-8, TGF-b, and TNF-a, in addition to increasing the antioxidant capacity, which inhibits the development of the inflammatory microenvironment that facilitates tumor growth.

In addition, biopolymers have been shown to stimulate caspase-3, which is one of the enzymes that cleave cellular components and finally cause the death of cancer cells (Wang et al., 2024).

The in vitro studies have also focused on the direct effects of biopolymers on the growth and proliferation of cancer cells and showed that these can induce apoptosis and inhibit angiogenesis, thus reducing the development of new blood vessels in support of tumor growth (Mawazi et al., 2024).

In the case of assessment of the biological efficacy of these nanoparticles in vivo with a solid tumor model in mice (Ehrlich carcinoma), the treatment showed a significant tumor growth inhibitory effect, a high rate of apoptotic cell death, and large areas of necrosis in the tumor tissue.

The combination of these results justifies the capability of the biopolymer nanoparticles to promote apoptotic pathways in the test cancer models.

Conversely, the normal cells exposed to the biopolymer under cytotoxicity assay conditions, which served as the control group, did not exhibit any perceptible toxic effect, even when the concentration of the biopolymer was high enough to reach 1000 µg/mL, which is a good indication of a high level of biocompatibility with normal cells (Sun et al., 2022).

In line with such findings, Ferreira et al. (2022) have stated that a blended biopolymer system of two natural polymers showed excellent biocompatibility when assessed on the normal fibroblasts of NIH-3T3. No toxic effects were seen under a large range of concentrations up to 15,000 µg/mL, and there was no adverse effect on cell morphology and growth during the time of incubation. This shows the excellent cellular compatibility and stability at room temperature of the biopolymer mixture in question.

Collectively, this line of evidence indicates that the biopolymer holds great anticancer promise using it as a therapeutic platform. Its multifunctional characteristic of being efficient as a cytotoxic agent on malignant cells, limited in cytotoxicity on normal cells, and selective nanostructured targeting makes biopolymers good candidates in the creation of engineered nanotherapeutics, especially in tissue engineering, wound healing, and cancer treatment (Etman et al., 2020).

2.6.4 Nanotechnology-Based Therapy

Nanotechnology is a research area that has made a direct incursion into the medical and pharmaceutical field because of the direct connection of the research to the human organism and its prospects of tackling some of the most dangerous diseases, especially cancer. Due to the special thermal and mechanical characteristics, nanomaterials have also become an alternative therapeutic means to the traditional chemical treatment. Evaluation of the efficacy of nanoparticles against malignant tumors has been enabled by innovations in the field of tissue engineering and ex vivo animal cell culture techniques are one of the most important applications of biotechnology. (Wang et al., 2013; Muddapur et al., 2022).

Nanotechnology helps to maximize the anticancer effect and optimize the delivery and loading of drugs with minimum damage to healthy tissues, and reduce systemic toxicity due to the off-target effect. This can eventually give the best balance between high therapeutic effectiveness and low toxicity. (Liu et al., 2023).

The role of gold nanoparticles (AuNPs) in addressing these challenges lies in their ability to provide a stable and biocompatible surface, possess tumor-

targeting properties, and reduce potential side effects. These nanoparticles utilize several mechanisms, including enhancement of the permeability effect and active targeting, which facilitate increased production of reactive oxygen species (ROS) and improve overall therapeutic efficacy. Research has shown that treating thyroid cancer cells with gold nanoparticles significantly affects protein folding, cell proliferation, migration, and invasion, and reduces cell viability by increasing apoptosis (Froehlich & Wahl, 2021; Lockwood et al., 2025).

The effect of gold nanoparticles (AuNPs) on cell proliferation and invasion in thyroid cancer cells was first demonstrated in the study by Zhang et al. (2015). It was found that the uptake of AuNPs by thyroid cancer cells was easy, and they became localized within vesicles and in the perinuclear region. The cytotoxicity of AuNPs leads to the production of reactive oxygen species (ROS), which results in morphological changes, disruption of the cytoskeleton, and alterations in the expression of genes related to cell growth and division. Collectively, these factors act as a barrier to the proliferation of cancer cells.

The experiment conducted by Li et al. (2017) showed that the biologically synthesized gold nanoparticles have a high cytotoxic effect on thyroid cancer cells, and the toxicity level rises with the concentration of nanoparticles, proving that there is a dose dependence in the toxicity levels. Referring to these findings, therefore, it can be implied that gold nanoparticles can be used as an effective anti-thyroid cancer agent due to their capacity to cause cellular death of malignant cells, and so it is a promising prospective agent in the future in the development of anticancer therapeutics.

Moreover, the pre-test in vivo safety and biodistribution of these gold nanoparticles were tested using the mouse CD-1 model. The findings provided strong evidence of good tumor targeting with limited systemic toxicity, which

forms a good basis for safe and effective use of the gold nanoparticle-based photothermal therapy in the treatment of thyroid cancer. (Amaral et al., 2021).

These findings present promising prospects for the development of targeted nanotherapies that combine efficacy and safety, representing a crucial step toward the innovation of more precise and effective therapeutic strategies for thyroid tumors, while potentially minimizing the side effects associated with conventional chemical and radiological treatments.

Chapter three

Materials and Methods

3.1 Materials

3.1.1 Equipment and Apparatus

Table 3.1: Laboratory Equipment and Apparatus utilized During the Study period.

No	Equipment And Apparatus	Company	Origin
1	trowel	SML	KSA
2	Sensitive Balance	Sartorius	Germnay
3	Test tube	ALS	Canada
4	Gloves	Broche	Malaysia
5	Flasks	Iso Lab	Germany
6	Screw cap bottles	Pyrex	England
7	Oven	Memmert	Germany
8	Autoclave	Hirayama	Japan
9	Burner	Indiamart	India
10	Vortex	Labco	Japan
11	Water path	Memmert	Germany
12	Refrigerator	Vistal	Poland
13	Water Distillatory	GFR	Germany
14	Slides and covers	Superestar	India
15	Parafilm	BEMIS	USA
16	Petri Dishes	Bio zek medical	Holland
17	Light Microscope	Olympus	Japan
18	Standard wire loop	Himedia	India
19	Microwave	Shownic	Korea
20	Biosafety	Lab Tech	France
21	Shaking Incubator	Zenith lab	China
22	Micropipettes	Dragon	China
23	Beaker	General	USA
24	CO2 incubator	Memmert	Germany
25	Centrifuge	Hittich	Germany
26	Hot plate with a magnetic stirrer	Heidolph	Germany
27	Epindroff centrifuge	Epindroff	Germany
28	Vaccum pump	Knflaboport	USA
29	Cooling Centrifuge	Epindroff	Germany
30	Anaerobic sachets (gas paks)	Thermo Scientific	UK
31	Disposable Syringes	Superstar	India

32	Epindroff	Bio neer	Korea
33	Filter paper	Watman No.1	UK
34	Thermo cycler appartus	Prime	UK
35	Laminar flow hood	K & K Scientific Supplier	Korea
36	Electrophoresis	Consort	Belgium
37	Digital gel documentation	Shownic	Korea
38	Deep freezer	The Electron corporation	USA
39	PH- Meter	Radiometer	Denmark
40	Forceps	Himedia	India
41	Sterile tiny plastic bags	Superstar	India
42	box Cool	Tan	UAE
43	Universal Pipette Tips	Globe scientific	Germany
44	Glass rod spreader	John Bolten	England
45	Micro titer reader	Thermo Fisher Scientific Supplier	USA
46	UV-Visible spectroscopy	Shimadzu	Japan
47	Zeta Potential Analyzer	Brookhaven Instruments	USA
48	Atomic Force Microscope	ZEISS Integrated	Germany
49	Vitek2 Compact system	Biomerieux	France
50	Cylinders	Bio Lab	Germnay
51	X-Ray Diffraction	Philips	Holland
52	Fourier Transform Infrared (FT-IR) Spectrophotometer	Zenith lab	China
53	Transmission Electron Microscope (TEM)	ZEISS	Germany
54	FE-Scanning Electron Microscope (FESEM)	ZEISS Gemini SEM	Germany
55	Cell culture plate	Thermo Fisher Scientific	USA
56	Thermogravimetric Analyzer	TA Instruments	USA
57	Vaccum pump	Knflaboport	USA
58	Cork borer	Brand-w	Germany
59	Gel system documentation	Vilberlourmat	France
60	Glass jar	Borosil	India

61	millipore filter 0.22 µm	Sigma- Aldrich	Germany
62	Invert Microscope	Olympus	Japan
63	Elisa reader	Quik Fit	Germany

3.1.2 Biological and chemical material

Table (3.2): Chemical and Biological Materials employed in the Study .

No.	Chemical/biological materials	Manufacturer The	Country of Origin
1	Agarose	Marvel	Korea
2	Vitek2 GP Kit for Gram positive	Biomerieux	France
3	Cycloheximide	Himedia	India
4	Glucose	Barcelona	Spain
5	Agar	KR	Chile
6	Absolute Ethanol	Baker	Germany
7	Ethanol (70%)	local factories	Iraq
8	Normal saline	Schuchard	Germany
9	water Deionized	Bioneer	Korea
10	Primer	Macrogen	Korea
11	MaximeTM PCR PreMix	iNtRON Biotechnology, Inc	Korea
12	DNA Bacteria Kit	Geneaid	Taiwan
13	INEOS Phenol	INEOS	USA
14	sulfuric acid (H_2SO_4)	Himedia	India
15	Date syrup	local factories	Iraq
16	Calcium carbonate	Fisher Scientific	USA
17	Isopropanol	Hosea Chem	China
18	Dichloromethane	Kanto Chemical Co., Inc	Japan
19	Dimethyl sulfoxide	Toray Fine Chemicals Co., Ltd	Japan
20	Chloroform	Shin-Etsu Chemical Co., Ltd.	Japan
21	Acetone	Kumho P&B Chemicals	Korea

22	Sodium chloride	Himedia	India
23	Hydrogen peroxide	BDH	England
24	Gram stain kit	Sybio	S.A.R
25	Fetal Bovine Serum	Gibco	USA
26	Hydrogen tetrachloroaurate (III) trihydrate	Glentham	UK
27	Trypsin/EDTA	Capricorn	USA
28	TBE buffer	Bioneer	korea
29	DNA ladder	Promega	USA
30	PBS	Promega	USA
31	Trypsin/veresin enzyme	Bioneer	Canada
32	Amikacin	ACS Dobfar S.p.A.	Italy
33	MTT Stain	Sigma	USA
34	Master mix	Bio neer	Korea
35	Sodium hypochlorite 5%	Local Iraqi factories	Iraq
36	Green Master mix 2X	Promega	USA
37	Loading Dye	Promega	USA
38	Nuclease free water	Promega	USA
39	Orange Diamond Dye Tm	APM Technica AG	Switzerland
40	Yeast extract	Foodchem International Corporation	China
41	Monopotassium Phosphate (KH_2PO_4)	Shanghai Titop Chemicals Co., Ltd	China
42	Ammonium Sulfate $(NH_4)_2SO_4$	Vinipul Chemicals Pvt. Ltd	India
43	Magnesium Sulfate ($MgSO_4$)	Jost Chemical Co	USA
44	Urea (CH_4N_2O)	Sigma-Aldrich	USA

3.1.3 The media

Table 3-3 : The culture and fermentation media used in this study.

No.	Culture or fermentation Media	The company	Country of Production
1	Starch-Casein-Nitrite Agar (SCN Agar)	Sigma-Aldrich	USA
2	actinomyces agar AA or Act. agar	Sigma-Aldrich	USA
3	Brain Heart Infusion broth (BHI) broth	Himedia	India
4	Nutrient broth	Himedia	India
5	Sabouraud agar	JINAN BABIO BIOTECHNOLOGY CO.,LTD.	china
6	Mineral salt media MSM	according to Dlamini et al. (2020)	
7	Roswell Park Memorial Institute Medium 1640 (RPMI 1640)	Capricorn Scientific	Germany

All ready-made culture media were prepared according to the manufacturer's instructions, while the mineral salt medium was prepared according to the method described by Dlamini et al. (2020).

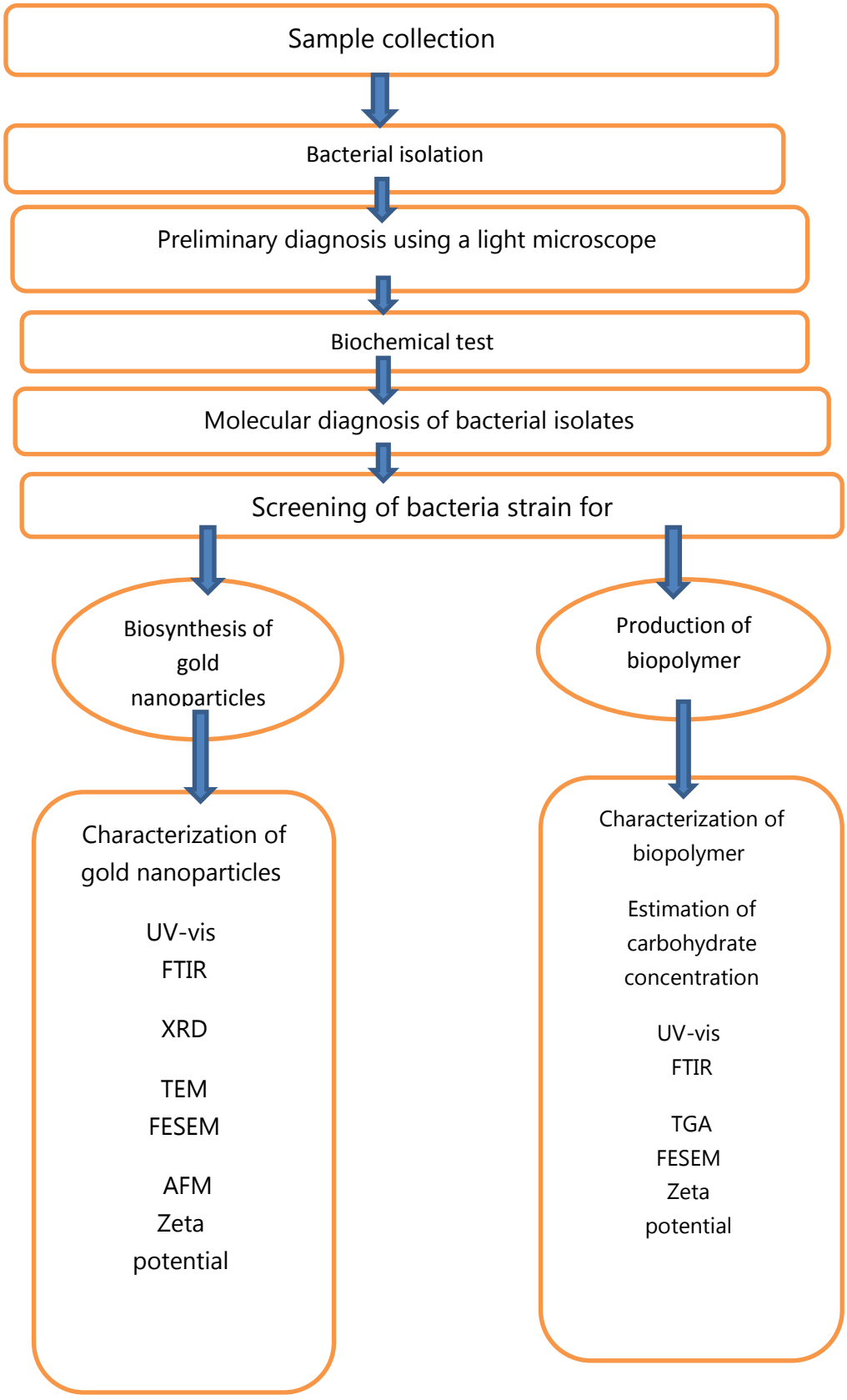
Sample collection
Bacterial isolation
Preliminary diagnosis using a light microscope
Biochemical test
Molecular diagnosis of bacterial isolates
Screening of bacteria strain for
Biosynthesis of gold nanoparticles
Production of biopolymer
Characterization of gold nanoparticles
UV-vis
FTIR
XRD
TEM
FESEM
AFM
Zeta potential
Characterization of biopolymer
Estimation of carbohydrate concentration
UV-vis
FTIR
TGA
FESEM
Zeta potential

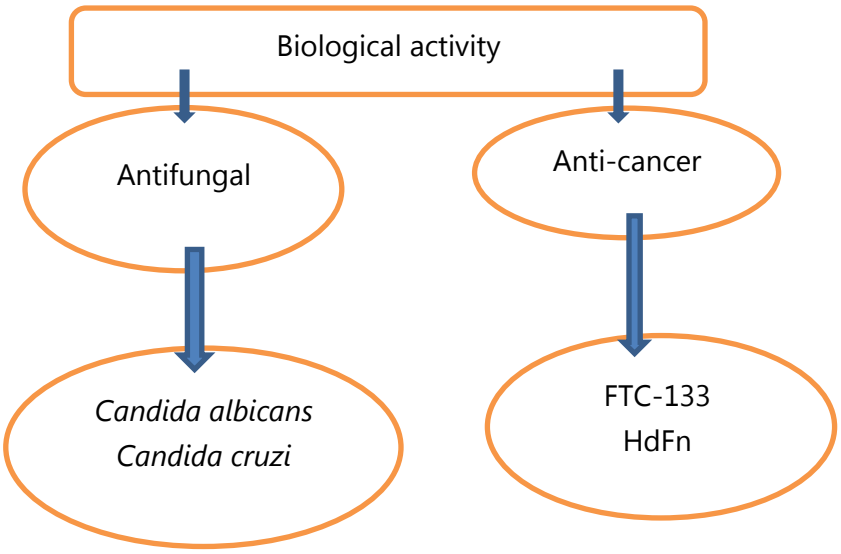

Figure (3.1): A schematic representation of the research study work plan (Prepared by the student)

3.2 Methods

3.2.1 The Sterilization :

Instruments, glassware, and culture media were sterilized before use using standard sterilization methods to prevent microbial contamination, as follows:

A- Direct flame sterilization : All heat-resistant metal instruments, including inoculation loops, spoons, and forceps, were sterilized by direct heating in a Bunsen flame until completely red-hot, and then left to cool before contact with samples or culture media.

B- Dry heat sterilization: Heat-resistant glassware was sterilized using a hot air oven at 180–200°C for two hours, a sufficient time to eliminate all microorganisms, including bacterial spores.

C- Moist heat sterilization: Culture media were sterilized by steam using an autoclave at 121°C and a pressure of 15 psi for 15 minutes. In contrast,

the mineral salt medium used for biopolymer production was sterilized for only 10 minutes due to its simple composition and lack of complex organic compounds.

D- Sterilization by filtration: Heat-sensitive solutions and materials, including RPMI medium used in cell culture, biopolymer solutions, and gold nanoparticle suspensions were sterilized using millipore filters with pore sizes of 0.22 micrometers, to ensure the removal of bacteria and other microorganisms without affecting on components nature of the solutions.

3.2.2 Soil Samples Collecting

Ten soil samples were collected from different areas of the banks of the Tigris River and its branches in Maysan province, including the areas of the city center of Amarah, Al-Majjar Al-Kabir and Al-Kahla District. during the period from 1 November 2024 to 1 May 2025. The samples were taken from a depth of 20 cm. The soil was excavated using a small trowel , and the samples were placed in sterile plastic bags, with each bag clearly labeled with the date and location of collection.

3.2.3 Soil pretreatment for selective isolation of actinomycetes

Samples of soil were taken on riverbank areas at a depth of 20 cm. The samples underwent thermal drying in a hot air oven at a temperature of 60 0 C with a duration of 45-50 minutes, and then treated with the calcium carbonate ($CaCO_3$) at a ratio of 0.05 g/gram of soil. These reagents were used to optimize the selective isolation of actinomycetes from soil samples based on the procedure established by Chandwad et al. (2020). The treated soils were then put in sterile

glass dishes in tightly sealed containers and allowed to incubate at room temperature over a period of two days before the isolation process.

3.2.4 Isolation of Bactereria

After a treatment of the soil, a tenfold serial dilution was done with sterile physiological saline in a ratio of 1:9 until the seventh dilution. The dilutions were inoculated on Starch Casein Agar (SCA) with the help of a sterile glass spreader. To prevent the proliferation of fungi and the contaminating bacteria, the culture medium was spiced with cycloheximide at a concentration of 50 µg/mL and amikacin at 50 µg/mL. Using a pH meter, the pH of the medium was changed to 7.8.

The samples inoculated were separated into two groups based on the conditions of incubation:

1. Group One: Incubation of the samples was followed by aerobic conditions, and further purification of the isolates was done on selective YEGA medium.
2. Group Two: The samples were incubated in an anaerobic environment and then purified on Actinomyces agar.

The plates were incubated at 28-30°C for 10 days. Once colonies started to appear, the growing colonies were subcultured into purification media alone. To obtain pure isolates, the streak plate method was used, and one was incubated at 28-30°C for 6-7 days. The process was continued until pure stocks were obtained, as indicated by Gathuru (2017.).

3.2.5 Identification of bacteria

3.2.5.1 Morphological Examination of Bacteria

Actinomycetes bacteria and other bacterial species were separated using a compound light microscope (Olympus). The microscope was operated at different magnifications, and emphasis was made to use an oil immersion lens at a magnification of 100X to get a magnified image of 1000X, which could be clearly used to view details of the bacterial colonies. Microscopic analysis was done by taking a small smear of a colony and applying it to a glass slide, and then staining it with Gram stain procedure as per the detailed directions of the staining kit. The observed slides were further examined using the microscope to analyze the morphology of the cells, their structure, and staining properties, and also to know whether they were gram-positive or gram-negative.

3.2.5.2 Biochemical Tests

3.2.5.2 .1 Catalase Test:

A clean slide of glass was put in a drop of 3 percent aqueous hydrogen peroxide. The standard procedure of the catalase test required a small portion of the bacterial isolate to be transferred using a sterile loop and combined with the hydrogen peroxide to see whether oxygen bubbles were produced.

3.2.5.2 .2 Vitek 2 Compact system identification of bacterial isolate.

The source states that the Vitek-2 system was used to conduct the bacterial identification test at the Children and Maternity Hospital in Maysan Governorate (Bitew et al., 2017). Gram-positive identification (GPI) cards were applied to identify the bacteria. A sterile loop was used to transfer sufficient pure bacterial colonies, which were then suspended in a test tube with 3.0 mL of 0.45% sterile saline solution. The suspension turbidity was altered to make it 0.5-0.63

McFarland and measured in the DensiCHEK Plus Meter. Subsequently, the bacterial suspension tube was placed into the designated plastic cassette, and the identification card was inserted into its appropriate slot. The cassette was then loaded into the automated Vitek-2 instrument, and after 24 hours, the bacterial identification results were obtained.

3.2.5.3 Molecular Identification

3.2.5.3.1 Extraction of Bacterial Genomic DNA

Genomic DNA extraction was initiated by activating a single colony of the bacterial isolate grown on Actinomyces agar. The colony was inoculated into 10 mL of sterile nutrient broth under anaerobic conditions and incubated at 30°C for 24 hours. Subsequently, DNA was extracted using the Presto™ Mini gDNA Bacteria Kit (Geneaid) according to the manufacturer's instructions, and the resulting genomic DNA was stored at −20°C.

3.2.5.3.2 Measurement concentration and quality of DNA

The concentration and purity of DNA were determined using a NanoDrop spectrophotometer, and the absorbance ratios A260/A280 and A260/A230 were calculated after calibration with the elution buffer.

3.2.5.3.3 Confirmation of the Presence of Extracted DNA

A conventional 0.8% (w/v) agarose gel was prepared to verify the presence of the extracted genomic DNA. The agarose solution was prepared by dissolving 0.10 g of agarose powder in 12.5 mL of 1X TBE buffer, gently mixed, and heated in a microwave oven for approximately 2 minutes until completely clear. After cooling the solution to 50–60 °C, 1 µL of Green Safe dye was added and mixed carefully. To form the wells, the comb was placed at one end of the pre-cast gel tray, and the agarose solution containing the dye was poured into the tray

and left to solidify. Once solidified, the comb was carefully removed, and the gel was transferred to the electrophoresis tank, where 1X TBE buffer was added to cover the gel surface to a depth of approximately 3–4 mm.

For sample loading, 3 µL of the extracted DNA was mixed with 2 µL of loading dye (bromophenol blue) and carefully loaded into the well using a micropipette. Additionally, 5 µL of a DNA ladder was loaded into a separate well for size comparison. Electrophoresis was performed at 80 V for 30 minutes, and DNA bands were subsequently visualized using a gel documentation system (Lee et al., 2012).

3.2.5.3.4 Amplifying of 16S rRNA by PCR

The bacterial isolates were molecularly identified by amplifying the 16S rRNA gene using the polymerase chain reaction (PCR) with the universal primers 27F and 1492R (Tian et al., 2023).

Table (3-4). The sequences of the universal primers used for 16S rRNA gene amplification

Name of primers	Primers Sequences (5-3)
27 F	AGAGTTTGATCMTGGCTCAG
1492 R	ACGGYTACCTTGTTACGACTT

Table (3-5): Components of the polymerase chain reaction (PCR) for 16S rDNA gene amplification

Reagents	Volume (ul)
Master Mix	12.5
Primer forward	1
Primer reverse	1
DNA template	3
Free water	7.5
Total	25

Table (3-6) Thermal cycling program for amplification of the 16S rDNA gene.

Steps	Temperature	Time	No. of cycles
Initial denaturation	94 C	5 min	1
Denaturation Annealing Elongation	94 C 60 C 72 C	1min 1min 1.5 min	35
Final Elongation	72 C	10 min	1

The program of PCR for amplification of the 16S rDNA gene. (According to Kaya .,2011)

3.2.5.3.5 Electrophoresis of PCR products

PCR products were analyzed by agarose gel electrophoresis. agarose gel 1% was prepared in TBE 1X buffer and supplemented with GelRed for nucleic acid visualization. After casting the gel and inserting the comb to form wells, 2 µL of each PCR product was loaded into individual wells after mixing with an

appropriate DNA loading dye. Electrophoresis was performed at a voltage of 80–120 V for 30 minutes. Following electrophoresis, the amplified DNA bands were visualized and documented under UV illumination. (Liu et al .,2022).

3.2.5.3.6 Sequencing of the 16S rDNA gene

Sample was labeled and sent to Macrogen Biotechnology Company (South Korea), where the PCR product was purified and the 16S rDNA gene sequence was analyzed using both forward and reverse primers. The obtained sequences were subsequently compared with the reference gene sequences available in the National Center for Biotechnology Information (NCBI) database (http://www.ncbi.nlm.nih.gov) using the Basic Local Alignment Search Tool (BLAST) (https://blast.ncbi.nlm.nih.gov) in order to identify the closest match for the bacterial isolates.

3.2.6 The production of biopolymer

3.2.6.1 The biopolymer production medium

The biopolymer production medium was prepared according to Dlamini et al. (2020) with some modifications. The medium was prepared by dissolving yeast extract (0.5 g),date syrup (50 g), KH_2PO_4 (2.0 g), (K_2HPO_4 (5.0 g), CH_4N_2O (0.5 g), NaCl (0.1 g), $MgSO_4$ (0.2 g), and $(NH_4)_2SO_4$ (0.2 g), in 1000 ml of distilled water.

3.2.6.2 Biosynthesis of Biopolymer by Bacterial Isolates

The bacterial strain were subcultured in 30 ml of sterile Brain Heart Infusion (BHI) broth using an inoculation loop loaded with a single bacterial colony and incubated at 37 °C for 48 hours under anaerobic conditions . Subsequently, 5% of the bacterial culture was transferred to 500 ml Erlenmeyer flasks containing

the biopolymer production medium and incubated on a rotary shaker at 37 °C and 120 rpm for 72 hours.

3.2.6.3 Extraction and Partial Purification of the Produced Biopolymer

The extracellular biopolymer was extracted using the cold ethanol extraction technique as described by Abu Tawila et al. (2018). The cell-free supernatant obtained from the centrifugation of the liquid culture grown in the salts medium was mixed with cold ethanol and isopropanol at a volumetric ratio of (1:3), and the mixture was left to stand overnight at (4)°C. The resulting precipitate was then collected by centrifugation at 6000 rpm for 30 minutes. The supernatant was discarded, and the precipitate was subsequently washed twice with 75% cold ethanol by centrifugation at the same speed for 10 minutes (Etxabide et al., 2022). Ethanol washing helps in the elimination of soluble impurities like proteins, lipids, and other non-polymeric bodies. Lastly, the weighing of the precipitate was done at room temperature with a sensitive balance.

3.2.6.4 Biopolymer Characterization

3.2.6.4 .1 Solubility Test

The compatibility of the biopolymer was checked in various organic and inorganic solvents by putting 50 mg of biopolymer in 5 mL of the following solvents (water, methanol, chloroform, dimethyl sulfoxide (DMSO), dichloromethane (DCM), acetone, phenol, and 96% ethanol. The mixtures were mixed in a vortex for two minutes. The solubility was assessed visually, and the data were documented as soluble, or insoluble, depending on the clarity of the solution and the formation of precipitates or not .

.

3.2.6.4 .2 Determination of carbohydrate value in the biopolymer.

The concentration of carbohydrates in the biopolymer was ascertained by the phenol-sulfuric acid method (DuBois et al., 1956). The free reduced aggregates of these compounds produce an orange-yellow color when processed with phenol and concentrated sulfuric acid. The test was carried out according to the following steps:

A standard glucose solution (stock solution) with a concentration of 1 mg/mL was prepared by dissolving 100 mg of glucose in 100 mL of distilled water. Different concentrations (0, 10, 20, 40, 60, 80, 100 µg/mL) were prepared by diluting the stock solution with a concentration of 1 mg/mL.

1. 1 mL of 5% phenol was added to the sample and comparison tubes.
2. 5 mL of 95% sulfuric acid was added drop by drop to the sample and comparison tubes. The tubes were kept on ice and then incubated at room temperature for 20 minutes.
3. The absorbance at 490 nm was measured for each glucose tube. A standard glucose curve was plotted by correlating absorbance with carbohydrate concentration (µg/mL).

Table (3-7) Standard glucose concentration and its absorbance.

Glucose conc. (µg /ml)	Absorbation(490 nm)
10	0.23
20	0.27
40	0.42
60	0.51
80	0.67
100	0.80

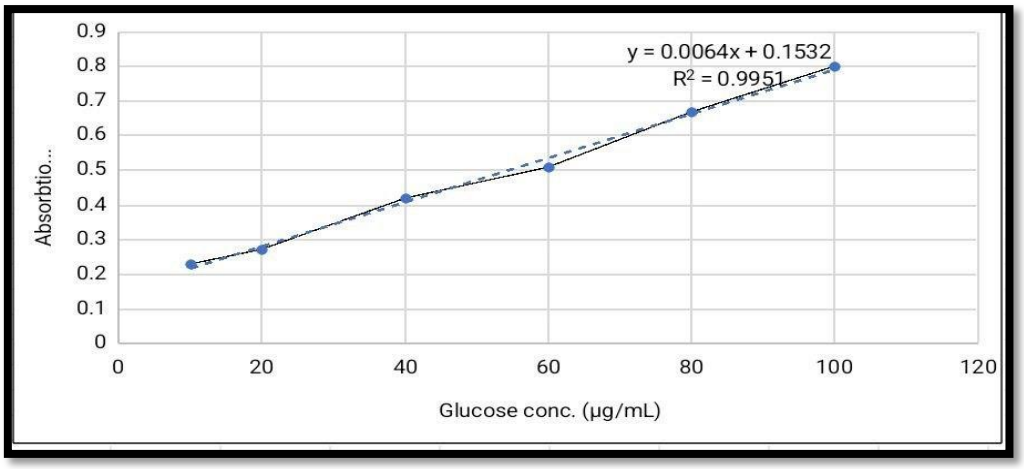

Figure (3-2) Standard glucose curve

Sample preparation: 100 mg of the biopolymer was dissolved in 100 mL of solvent (cold distilled water) with thorough mixing using ultrasonic waves until a homogeneous solution was obtained.

1. The biopolymer sample was treated in the same manner as in the calibration curve procedure.
2. The carbohydrate concentration was determined according to the calibration curve shown in the figure.(3-2)

3.2.6.4.3 Uv of polymer :

For spectrophotometric analysis, the biopolymer was completely dissolved in distilled water, which served as the only suitable solvent. A 2 mL aliquot of the prepared solution was then subjected to absorbance measurement using a UV–Vis spectrophotometer. Distilled water was used as the blank reference to calibrate the instrument and eliminate background interference.

3.2.6.4.4 Fourier Transform Infrared analysis

FT-IR analysis was performed to identify the biomolecules and functional groups involved in the formation of the biopolymer. The samples were prepared in powdered form and mixed with 100 mg of KBr to obtain a homogeneous mixture, which was then pressed into a thin pellet suitable for FT-IR measurements within the wavenumber range of 4000–400 cm^{-1}.

3.2.6.4.5 Thermogravimetric Analysis (TGA)

The thermogravimetric properties of the biopolymer (4.5 mg) were measured using a TGA analyzer (SDT 600 TA Instruments) at a heating rate of 20 °C/min over a temperature range of 25–800 °C. Argon gas was used to maintain an inert atmosphere throughout the analysis.

3.2.6.4.6 Field emission Scanning Electron Microscope (FE-SEM)

To study its morphological structure ,biopolymer was analyzed using a Scanning Electron Microscope equipped (Hitachi, Japan). For sample preparation, 5 mg of the bio-polymer was placed onto a pre-coated silicon slide and fixed using a spin coater. The slide was spun for 60 seconds at a speed of 1000 rpm to ensure a uniform distribution of the sample before being introduced into the analyzer for examination (Rasulov et al., 2017).

3.2.6.4.7 Zeta Potential Analysis

The zeta potential of the biopolymer solution was measured using a HORIBA SZ-100 zeta potential analyzer at 25.2 °C (holder temperature) to investigate the particle aggregation mechanism, either through particle bridging (interparticle association) or charge neutralization.

3.2.7 Biosynthesis of Gold Nanoparticles

The bacterial isolate grown on Actinomyces agar was activated in 30 mL of Brain Heart Infusion (BHI) medium using a sterile metal loop containing a single colony, and incubated under aerobic conditions at 37 °C for 48 hours. After that, the bacterial culture was transferred into 500 mL Erlenmeyer flasks containing nutrient broth and incubated on a rotary shaker at 37 °C at 120 rpm for 24 hours. The grown culture was then centrifuged at 6000 rpm for 40 minutes.

Finally, 50 mL of the bacterial filtrate was mixed with 50 mL of 1 mM $HAuCl_4$ solution at a 1:1 volume ratio between the filtrate and the $HAuCl_4$ solution. A control tube containing only $HAuCl_4$ (1 mM), without bacterial filtrate, was also prepared for comparison with the experimental setup. The reaction mixture was maintained under shaking conditions at 120 rpm, at 37 °C, and in complete darkness (Hamed & Abdel Fattah, 2019).

3.2.7.1 Physical Properties of Synthesized Gold Nanoparticles

The physical characterization of nanomaterials primarily focuses on their size and shape. Additionally, parameters such as size distribution, degree of aggregation, surface charge, surface area, and organic functional groups on the particle surface can be evaluated, as they may influence other properties and potential applications. Furthermore, the crystal structure and chemical composition of the nanoparticles are examined as an initial step following their synthesis (Verma and Maheshwari, 2018).

3.2.7.1.1 UV- vis Spectroscopy

The synthesized nanoparticles were examined using the bacterial supernatant as a reference sample (blank). 2 ml of sample were transferred to quartz cuvettes,

and absorbance was measured utilizing a dual-beam UV-1900 spectrometer in the 400–700 nm range to identify features plasmon resonance peak of the gold nanoparticles .

3.2.7.1.2 Fourier Transform Infrared analysis

The FTIR study aimed to determine whether the produced nanoparticles contained functional groups that could contribute to biosynthesis. The specimens were sited in liquid form within a suitable cell, and measurements were performed at a resolution of 4 cm^{-1} in the 400–4000 cm^{-1} wavenumber range using an FTIR spectrometer.

3.2.7.1.3 X-ray diffraction (XRD) analysis

Is one of the most widely used techniques for characterizing nanoparticles, providing critical information on their crystalline structure, phase nature, lattice parameters, and crystallite size. The composition of nanoparticles can also be determined by comparing the positions and intensities of diffraction peaks with known reference patterns. XRD analysis was performed using an X'pert Pro diffractometer to evaluate the diffraction pattern of bacterially synthesized nanoparticles. The diffraction pattern of the powdered nanoparticles was recorded over a 2θ range of 10°–80°, with a step size of 0.050°, using Cu Kα radiation (λ = 1.54060 Å) under operating conditions of 40 kV and 30 mA. The average crystallite size of nanoparticles was estimated using Scherer's equation, as described by Qais et al. (2019).

3.2.7.1.4 Transmission Electron Microscopy (TEM)

Transmission electron microscopy (TEM) used to study the morphology, size, and distribution of the nanoparticles.

In the case of TEM grid preparation, the nanoparticle suspensions were dropped on the copper grids covered with carbon via the drop-casting technique and were left to dry in air before imaging.

TEM was used to obtain individual images of the nanoparticles as the voltage accelerated to 200 kV.

3.2.7.1. 5 Field Emission Scanning Electron Microscope (FE-SEM)

The morphological features of the nanoparticles synthesized were examined using the iron-equipped scanning electron microscope (Fe-SEM). Before the examination, a drop of the suspension of nanoparticles (small in amount) was deposited on a slide and left to dry. The instrument used in the analysis was the microscope with different magnifications.

3.2.7.1. 6 Atomic Force Microscopy (AFM)

The AFM instrument was used to examine the morphology and size of the fabricated nanoparticles using biofabrication . Prior to AFM scanning, thin layers of the biofabricated nanoparticles were deposited onto clean glass coverslips and allowed to dry at room temperature.

3.2.7.1.7 Zeta potential analysis

The stability of the nanoparticles (NPs) was evaluated using a HORIBA SZ-100 analyzer. The nanoparticles were analyzed at 25.2 °C (holder temperature) within a potential range of −100 to +100 mV. This method allowed for a precise assessment of the colloidal stability of the synthesized nanoparticles.

3.2.8 Biological Activity

The biosynthesized biopolymer and gold nanoparticles in this study were characterized using antifungal and anticancer activities.

3.2.8.1 Antifungal Activity

Clinical isolates of yeast fungi were obtained from the Microbiology Laboratory at Baghdad Teaching Hospital. Vaginal swabs were collected from women of reproductive age (15–50 years) suffering from vaginal infections. Two species of yeast fungi, *Candida albicans* and *Candida krusei* , were isolated, and the isolates were identified and characterized using the VITEK-2 Compact system.

3.2.8.1.1 Preparation of the Dilutions Used in the Experiment

A series of concentrations of 500, 250, 125, and 62.5 µg/mL, diluted sequentially in a 1:2 ratio, were used to accurately study the dose-response relationship between the polymer and the nanomaterial. This concentration gradient determines the lowest concentration that could give a significant inhibitory effect, and based on this, a rough determination of the lowest concentration that can be used to get a significant inhibitory effect is the minimum inhibitory concentration (MIC) that can be determined by the agar well diffusion technique. (Balouiri et al. ,2015).

3.2.8.1.1.1 Preparation of the Biopolymer Serial Dilutions.

According to (Balouiri et al. ,2015), a series of serial dilutions of the biopolymer was prepared using 5 test tubes marked as Tube-0 to Tube-4. Tube-1-Tube-4 Each tube was pre-loaded with 0.5 mL of distilled water. The serial dilution process was done as follows:

1. Tube-0 (Stock Solution): 1 mg of the biopolymer powder was dissolved in 1 mL of distilled water, and the solution was stirred until the solution was fully dissolved to form a stock solution with a concentration of 1000 µg/mL.

2. Tube-1: 0.5 mL of the stock solution was mixed into Tube-1, which had 0.5 mL of distilled water, which led to a 1:2 dilution (i.e., 50 percent of the stock concentration).
3. Tube-2: 0.5 mL of Tube-1 was pipetted into Tube-2 that had 0.5 mL of distilled water, the dilution was 1:4 (i.e., 25% of stock concentration) .
4. Tube-3: 0.5 mL of Tube-2 was added into Tube-3 that had 0.5 mL of distilled water, which yielded a 1:8 dilution (i.e., 12.5 percent of the stock concentration).
5. Tube-4: 0.5 mL of Tube-3 was moved into Tube-4, which had 0.5 mL of distilled water to produce a 1:16 dilution (i.e., 6.25% of the stock concentration).

Each of the tubes was mixed thoroughly after every step of the dilution procedure in order to make the substance homogeneous and ensure uniform distribution in all concentrations.

3.2.8.1.1.2 Preparation of the Nanomaterial Serial Dilutions

Dilutions of the nanomaterial were done in series by centrifugation of the nanoparticle suspension at 6000 rpm for 10 min . The precipitate was then rinsed three times using distilled water to get rid of impurities and was left to dry at room temperature to get the nanomaterial in the form of a precipitate. The weight of one milligram of the nanomaterial was taken and suspended in 1 mL of distilled water to give a stock solution containing 1000 µg/mL. Five labeled test tubes, Tube-0 to Tube-4, were utilized. Tubes 1 through Tube-4 had 0.5 mL of distilled water pre-added in them, and Tube-0 was kept as the stock solution. (Balouiri et al. ,2015 : Aliwi,2023)

The stepwise dilutions were done as follows:

1. Tube-1: 0.5 mL of the standard solution was measured and added to Tube-1, where 0.5 mL of distilled water had been previously added, in a 1:2 dilution (i.e., 50 percent of the standard solution concentration).
2. Tube-2: 0.5 mL of Tube-1 was moved to Tube-2, which had 0.5 mL of distilled water, thus creating a 1:4 dilution (i.e., 25% of the concentration of the standard solution).
3. Tube-3: 0.5 mL was transferred from Tube-2 to Tube-3, which contained 0.5 mL of distilled water, resulting in a 1:8 dilution (i.e., 12.5% of the standard solution concentration).
4. Tube-4: 0.5 mL was transferred from Tube-3 to Tube-4, which contained 0.5 mL of distilled water, resulting in a 1:16 dilution (i.e., 6.25% of the standard solution concentration).

Each tube was gently mixed after each dilution step to ensure homogeneity.

3.2.8.1.2 Evaluation of antifungal activity

The antifungal activity testing of the Candida isolates was performed using the agar well diffusion method, as described by Berkow et al. (2020).

1. Each *Candida albicans* and *Candida krusei* isolate was re-cultured on Sabouraud Dextrose Agar (SDA) and incubated at 35–37°C for 48 hours to obtain fresh growth.
2. A yeast cell suspension was prepared by transferring one colony from each isolate to 5 mL of sterile physiological saline and adjusting the turbidity to conform to the McFarland 0.5 standard, which is approximately equivalent to 1×10^6 to 5×10^6 colony-forming units/mL.
3. Using a sterile cotton swab, each suspension was spread evenly onto the surface of SDA plates.

4. After allowing the plates to dry for 10–15 minutes, 5 mm diameter wells were made in the agar medium using sterile instruments.
5. Each well was filled with 100 microliters of the test sample for each pre-prepared dilution using a micropipette.

3.2.8.2 Anticancer Activity

Two cell lines, FTC_133 and HdFn, were obtained from the IRAQ Biotech Cell Bank Unit in Baghdad and cultured. FTC_133 cells are follicular thyroid cancer cells isolated from a 35-year-old woman. HdFn cells are human dermal fibroblasts from a newborn infant.

3.2.8.2.1 Preparation of the Dilutions Used in the Experiment

A series of the required concentrations (25, 50, 100, 200, and 400 micrograms/ml) for both the polymer and the nanomaterial were prepared, starting from a standard solution of 1000 micrograms/ml, using the method of sequential dilution with sterile distilled water.

3.2.8.2.2 Culture of FTC-133 and HdFn cell line

The method described by Capes-Davis & Freshney (2021) was followed for the culture of cell lines, as detailed below :

1. Cells from each cell line were cultured into culture vessels with a surface area of 25 cm^2 containing RPMI-1640 medium supplemented with 10% fetal bovine serum (FBS).
2. The vessels containing the cell suspension and culture medium were incubated in a 5% CO_2 incubator at 37°C for 24 hours.
3. After 24 hours of incubation, and upon confirmation of cell growth and absence of contamination, secondary subcultures were performed.

4. An inverted microscope was used to determine the alteration of cells in terms of viability, to check whether cells have not been contaminated, and to check whether the cells are in a range of 500-800 x 103 cells/mL.
5. A biosafety cabinet was used to transfer the cells and dispose of the used culture medium.
6. The cells were washed twice in PBS, which lasted 1-5 minutes each time, and the solution was removed.
7. An adequate portion of trypsin/versene was added to the cells, and then the cells were incubated at 37°C for 30-60 seconds till the cells separated into single cells. The enzyme reaction was next neutralized by the addition of fresh culture medium with 10% FBS.
8. A centrifugation was performed on the cells collected into centrifuge tubes at an appropriate speed (usually 1000-1500 x g) within 10 minutes at room temperature to pellet the cells and eliminate trypsin and the medium used. The supernatant was discarded, and the cell pellet was resuspended in fresh culture medium containing 10% FBS.
9. Cell counting was performed using a hemocytometer after mixing a defined volume of the cell suspension with an equal volume of Trypan Blue. Cell number was calculated using the following equation:

$$C = N * 10^4 * F \backslash ml$$

Where:

C = number of cells per mL of suspension,

N = number of cells counted on the hemocytometer,

F = dilution factor.

10.Cell viability was calculated using the equation:

$$\text{Live cells Viability} = (\text{live cells})/(\text{dead cells}) \times 100$$

11. The cell suspension was then distributed into new culture vessels and incubated again at 37°C in a 5% CO_2 incubator for 24 hours.

3.2.8.2.3 Cytotoxicity Assay of Biosynthesized Gold Nanoparticles and Biopolymer in Cancer Cell Line

The method described by Capes-Davis and Freshney (2021) was followed to evaluate the cytotoxicity of different concentrations of the biopolymer and gold nanoparticles prepared in this study:

1. The contents of a tissue culture flask with a surface area of 25 cm^2 were treated with a Trypsin/Versene solution after discarding the used culture medium. The flask was gently agitated to ensure uniform distribution of the enzyme over the cell surface.
2. The flask was then incubated at 37°C for 10 minutes to facilitate the detachment of the cells from the surface.
3. Then, 20 mL of culture medium with fetal bovine serum (FBS) was added to inactivate the trypsin. The cell suspension was swirled to dissolve any cell clumps.
4. Subsequently, 0.2 mL of cell suspension was added to the well of flat-bottom tissue culture plates by using the automated micropipette.
5. The plates were incubated at a temperature of 37 °C for 24 hours to enable the cells to adhere to the surfaces of the wells.
6. Following incubation, 0.2 mL of different concentrations of the previously prepared extract was added and substituted the old medium. Each

concentration was conducted in three replicates, and three control replicas with untreated cell suspensions were performed.

7. The plates were subsequently incubated again at 37°C over the next 24 hours.
8. At the end of the exposure time, the plates were taken out of the incubator, and 100 µL of crystal violet staining solution was added to each of the wells with cells.
9. The plates were once more left to incubate for 20 minutes, after which viable cells were expected to absorb the dye.
10. The contents were then disposed of, and the wells were washed using distilled water a few times to remove any excess stain.
11. Lastly, the optical density of the stained cells was obtained at a wavelength of 492 nm using an ELISA reader to obtain the percentage of viable cells as well as compare the cytotoxic effect of the extract to the control treatments.

The percentage cell inhibition was determined by the following equation:

Percentage of cell inhibition = (absorbance reading of control cells - absorbance reading of treated cells for each concentration/absorbance reading of control cells) x 100

This percentage is used to show the level of decrease in absorbance, which is caused by the effect of the tested substance when compared to the control sample. It is a measure of the level of cytotoxicity or the inhibitory effect caused by the treatment.

3.2.9 Statistical Analysis

Statistical analysis of data was provided with the help of GraphPad Prism Version 6, and ANOVA was applied to find out the difference between groups. Mean comparisons were performed using the Duncan Multiplex test to identify statistically significant differences at $P \leq 0.05$.

Chapter Four

Results and Discussion

4.1 Isolation of Bacteria from Soil Samples

In this study, soil samples were collected from riverbank areas adjacent to the Tigris River in Maysan province for the purpose of isolating Actinomycetes. The cultured samples were divided into two groups: one incubated aerobically and the other under anaerobic conditions. Subsequently, isolates from each group were selected for morphological and molecular identification. The results showed that the aerobic isolates belonged to the genus Bacillus, which is characterized as a rod-shaped aerobic bacterium known for its ability to withstand harsh environmental conditions due to its capacity for spore formation (Farrar & Reboli, 2006).

In contrast, the anaerobic isolates were found to belong to the genus Schaalia, as species of this genus are typically oxygen-loving at low concentrations to anaerobic, slow-growing, and exhibit a distinctive branched, filamentous form (Cronin et al., 2023). Actinomycetes were distinguished from Bacillus isolates based on differences in colony morphology and structure, with colony textures ranging from powdery to chalky, and their ability to produce and form filamentous structures, a characteristic feature of this bacterial group. Soil is a rich and highly diverse ecosystem, exhibiting the highest levels of microbial diversity compared to other natural ecosystems. This exceptional diversity is primarily attributed to its high organic matter content and the ability of soil microorganisms to adapt to a wide range of environmental conditions. (Prashanthi et al, 2021).

4.2 Identification of Bacterial Isolates

4.2.1 Microscopic Observation of Bacterial Isolates

Both types of isolates showed a positive Gram stain. The anaerobic isolates were characterized by distinct filamentous branching forming a network of intertwined threads, a characteristic morphological feature of actinomycetes, and were observed to be non-spore-forming (Figure 4.1).

In contrast, the aerobic isolates did not exhibit these characteristic filamentous structures and appeared different in their structure and morphological characteristics. Figure (4.2) .

Figure (4.1) The anaerobic isolates observed under the microscope.

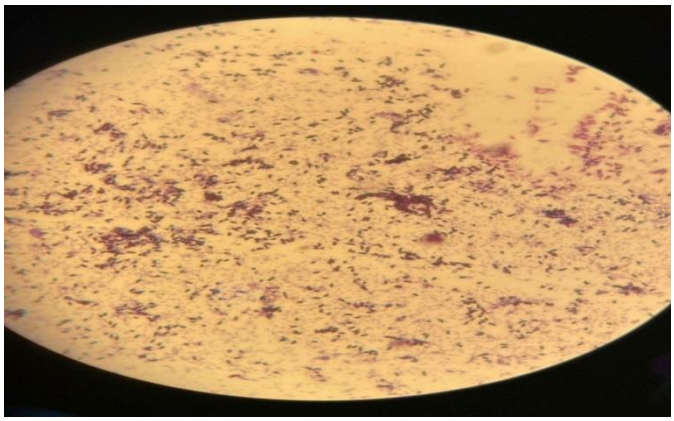

Figure (4.2) the aerobic isolates observed under the microscope.

4.2.2 Biochemical Tests

4.2.2.1 Catalase Test

The results of the catalase test showed that the anaerobic bacterial isolates were negative for the catalase test, as no bubbles were observed when hydrogen peroxide was added to the bacterial culture.

According to UK Standards for Microbiology Investigations (2025), most Actinomyces species are catalase negative.

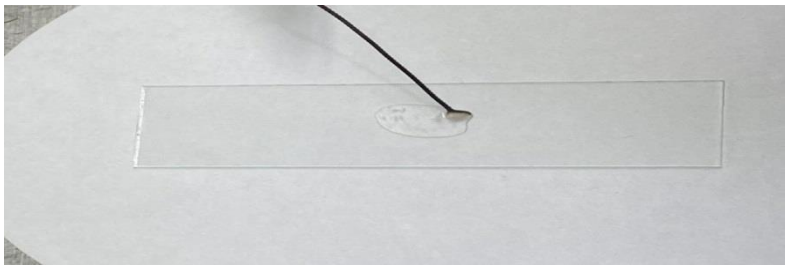

Figure (4.3) Catalase test result of anaerobic bacterial isolate

4.2.2.2 Using the VITEK-2 Compact System

The results obtained from the VITEK-2 Compact system indicated that the tested anaerobic bacterial isolate did not match any known species in the stored database, and therefore, were not accurately identified.

4.2.3 Molecular Identification

4.2.3.1 Extraction and purification of DNA from the bacterial isolate

In the present study, genomic DNA was extracted and purified from the selected anaerobic bacterial isolate.

The concentration and purity of the extracted DNA were assessed using a nanodrop spectrometer. Purity was assessed based on absorbance ratios at 260/280 nm and 260/230 nm. The result indicate in table 4.1 :

Table(4.1) concentration and purity of DNA assessment by NanoDrop spectrophotometry.

Concentration	260/280	260/230
186.1 ng/uL	1.9	2.0

The results indicated a 260/280 ratio of 1.9, which falls within the optimal range for DNA purity and suggests the absence of protein contamination. The 260/230 ratio was 2.0, a value within the acceptable range indicating minimal contamination by salts or organic solvents. Overall, these measurements confirm that the DNA sample was of high quality and purity.

4.2.3.2 Amplification of the 16S rDNA Gene Using Polymerase Chain Reaction (PCR)

The use of 16S rDNA sequences for studying bacterial taxonomy and evolution is among the most widely applied molecular markers. This has been explained by the biological peculiarities of the 16S rDNA gene, which are:

1. It is found as a multigene family in almost all bacterial species.
2. It has been found that the role of the 16S rDNA gene has been very conserved over the years, and thus, random mutations in the gene sequence have been used as a very specific measure of estimating evolutionary divergence.

It is long enough (about 1,500 base pairs) to give informative phylogenetic resolution (Janda & Abbott, 2007).

The molecular identification of the bacterial isolate was done by amplification of the 16S rRNA gene using universal primers and polymerase chain reaction (PCR). Gel electrophoresis of the PCR products using agarose gel showed that the DNA fragment was about 879 base pairs, which was calculated by using a molecular size marker (DNA ladder) with a 1500 bp DNA band.

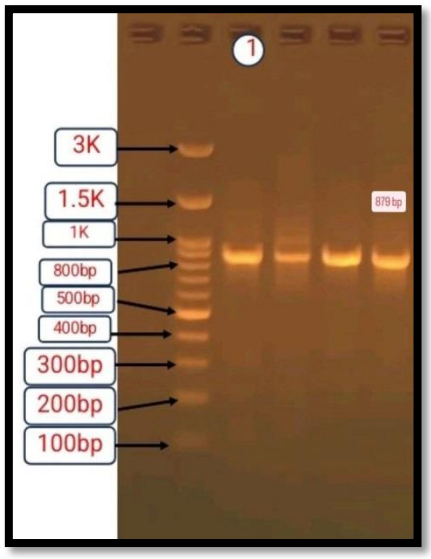

Figure (4.4). The results of PCR products, (16S rDNA gene) after gel electrophoresis .

4.2.3.3 Analysis of DNA Sequencing

Following the amplification, purification of the PCR products was done, and the sequences formed were aligned and analyzed. The data obtained with DNA sequencing of the target isolate were analyzed with the help of the BLAST tool and were compared with the reference strains, which are regarded as one of the most valuable world repositories of nucleotide sequences of various organisms (Abd-Elnaby et al., 2016).

The analysis has revealed that the similarity of the isolate under study and the *Schaalia naturae* sequences in the database was high, i.e., there was about 98 percent sequence identity, an E-value of 0.0, and a few gaps. The results suggest high genetic correspondence and prove the accuracy of the molecular identification of the isolate.

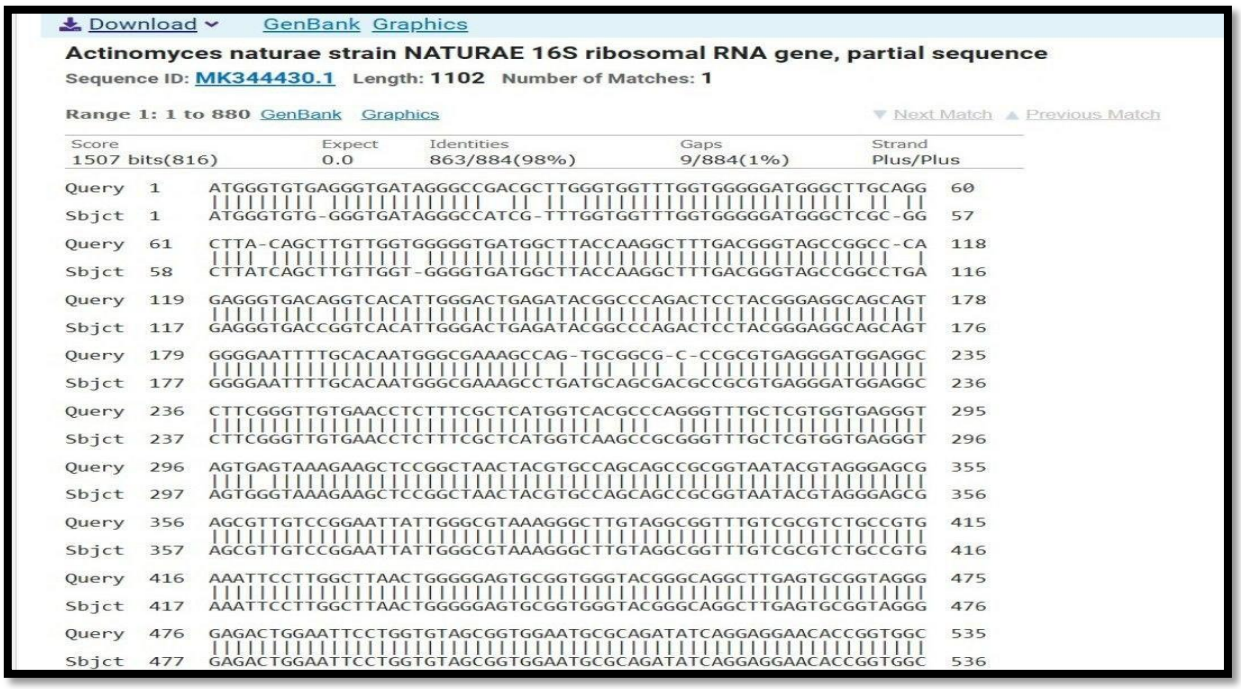

Figure (4.5). BLAST alignment of the 16S rRNA gene sequence of the studied bacterial isolate

A phylogenetic analysis of the 16S rRNA gene sequence was done to further enhance the accuracy of identification. The resultant phylogenetic tree also put the isolate studied in the same clade as Schizobactera naturae, as well as the other closely related members of the family Actinomycetaceae. Green branches indicate a sequence with the most similar evolutionary relationship to the isolate under study, and it can be easily visualized that its phylogenetic location is therefore suitable as a taxonomic assignment.

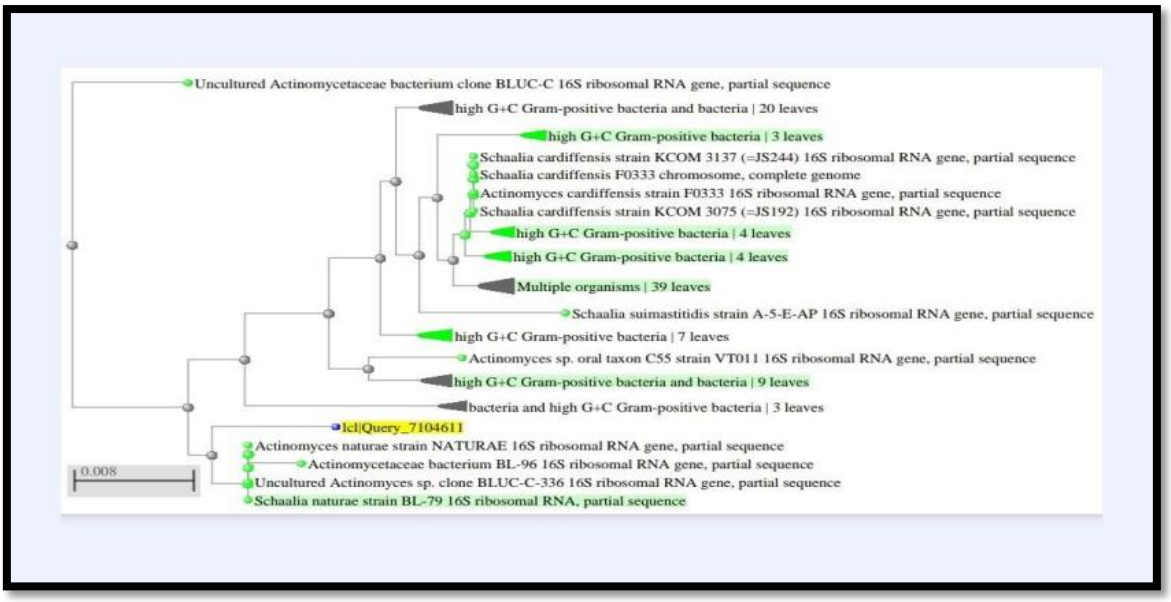

Figure (4.6). The phylogenetic tree of the studied bacterial isolate based on 16S rRNA gene sequence.

According to the overall outcomes of the BLAST analysis and phylogenetic analysis, the isolate was confirmed to be the species of *Schaalia naturae*.

Molecular identification of bacteria in the soil demonstrated in this study a strong variability in bacterial composition in the various environments studied. Actinomycetes are among the prokaryotic microorganisms that are most actively studied and investigated because of their biological significance, especially their capacity to produce secondary metabolites.

The Actinomycetes are broadly distributed in a variety of natural environments, such as soil, water, desert areas, limestone, volcanic caves, marine sponges, and marine sediments (Khan et al., 2023).

Indicatively, in the article by Liu et al. (2022), the authors illustrated that the saxaul forest ecosystem in the Gobi Desert of Mongolia is a unique ecological environment where a staggering variety of bacterial communities can be

cultivated. The article has given a thorough description of cultivable isolates identified in the samples of soils of the saxaul forest located in South Gobi aimag, Mongolia, and evaluated their chances of forming antibacterial molecules. Using culture-dependent environmental isolation techniques, the researchers rediscovered 172 strains of actinobacteria, identified and classified 22 genera and 13 families of these bacteria, and phylogenetically classified them in the harsh desert setting, a high level of microbial richness, and adaptability of these bacteria.

Likewise, the article by Shrestha et al. (2021) also came to the conclusion that the geographical diversity of Nepal offers the most appropriate conditions to the existence of many actinomycete species. Their isolation and characterization had borne 12 isolates of Micromonospora sp., seven isolates of Streptomyces sp., and nine isolates of Nocardia sp.

Ait Assou et al (2023) have provided the first study of this sort in Morocco and have tried to investigate the microbial diversity of actinomycetes in lead- and cadmium-contaminated mining soils in Midelt and contrast them with the worldwide levels in the natural background. The morphological, chemotaxonomic, biochemical, and molecular analysis results showed that a huge percentage of the isolates belonged to the genus Streptomyces, besides other suitors belonging to Amycolatopsis, Lentzea, Actinopolymorpha, and Pseudonocardia. It is interesting to note that Actinopolymorpha was the first organism known to inhabit a heavy-metal-enriched habitat. The authors of the study were able to isolate and characterize 145 actinobacterial strains using morphological, chemotaxonomic, biochemical, and molecular methods.

All in all, the studies that have been reviewed show that there are considerable variations in the structure of bacterial communities between environments. The

results of the current research are not similar to those of others, As the *schaalia naturae* was isolated from soil for the first time in this study, it had previously been recorded only in non-human and non-animal environments. Rao et al. (2012) first isolated it in a study of the microbial community of a contaminated site of chlorinated-solvent-contaminated groundwater in Louisiana, USA, in a study that intended to analyze the microbial community of the contaminated site. The outcomes of the present research thus broaden the ecological spectrum of this species that has always been perceived in terms of human and animal pathogenicity.

These observations serve to highlight that the microbial community is directly dependent on the soil properties and the environmental factors around, such as temperature, pH, nutrient levels, and soil salinity.

4.2.3.4 Registration of the New Bacterial Strain in the GenBank Database

The genes of the bacterial isolate in question were compared to the genetic sequences that are presented in the GenBank database by matching and aligning the 16S rRNA gene sequences with the ones in the database. bacterial isolate was registered in the GenBank database as a new strain under the name *Schaalia natura* strain RFAT2. The length of the submitted sequence was 879 nucleotide bases, and the studied isolate showed similarity to bacterial sequences listed in GenBank with a similarity percentage of 97.62%. The sequence was deposited under the accession number PV945972.

4.3 Production of biopolymer

4.3.1 Production of Biopolymer by *Schaalia natura* strain RFAT2 in Modified Mineral Salts Medium

The Mineral Salts Media was used for biopolymer production according to Dlamini et al. (2020), with glucose replaced by date syrup as an additional carbon source. The bacterial isolate demonstrated the ability to produce a biopolymer in this medium. When cultured at 37 °C for 72 hours under shaking conditions (120 rpm), visible precipitates formation was observed in the culture medium, appearing as a viscous and gelatinous material, preliminary indicating successful production of the polymer by the bacterial strain .

A B

Figure(1-3) mineral salt media A- before adding of date syrup B- after adding of date syrup**.**

4.3.2 Optimization of biopolymer Production Using Natural Carbon Sources

There are number of factors that can affect the quantity and functional performance of the produced biopolymer may include the microbial strain, medium composition, and conditions of the culture. All these factors make it possible to produce new biopolymers with increased biological activity. (Jurášková et al., 2022; Zaghloul and Ibrahim, 2022).

The major limitation in the commercial use of biopolymers is their high cost of production, which is why scientists are turning to the use of cheaper alternative sources of carbohydrates, specifically, simple sugars that are readily available, as inexpensive substrates in the microbial biosynthesis of biopolymers (Bhatia, 2023) .

Growing the bacterial strain on date molasses-enriched media rather than glucose as the carbon source enhanced the productivity of the bacterial isolate. The findings indicated that the yield of polymer improved to 4 g/L, which agrees with the results of Hamel (2025).

On the contrary, the production level of the same strain was noted to be 1 g/L when glucose powder was employed as a source of carbon, as shown in Figure 4-7.

Similar results were reported in the study by Obeid (2025), where the biopolymer extracted using 96% ethanol appeared as a white powder with an approximate weight of 1 g/L, as shown in Figure (4-7).

Figure (4-7). The polymer produced by the bacterial strain when glucose powder was used as the carbon source.

4.3.3 Extraction of the Biopolymer Using cold Ethanol and Isopropanol

The biopolymer produced by the bacterial isolate was extracted using cold ethanol and isopropanol after optimizing the production conditions. Yields of 4 g/L and 0.5 g/L were obtained, respectively (Figure 4-8), indicating that extraction with cold ethanol resulted in a higher biopolymer yield compared to extraction with isopropanol (Figure4-8).

These findings are consistent with the results reported by Al-Zaidi (2023), where the use of 96% chilled ethanol for extracting the biopolymer from *Pseudomonas aeruginosa* produced higher yields compared to isopropanol extraction. The recovered bioproduct appeared brown in color due to the influence of date molasses, in contrast to the white biopolymer obtained when glucose was used as the carbon source, as shown in Figure (4-9).

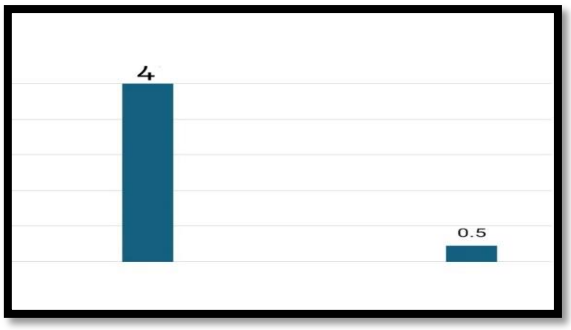

(A) (B)

Figure (4.8). The product of two extraction methods (A - using ice-cold ethanol, B - using isopropanol) of the biopolymer produced.

Figure (4.9). The polymer produced by the bacterial strain when was used date molasses as the carbon source.

A B

Figure (4.10). Biopolymer extracted . A: Before drying, B: After drying

Upon the addition of ethanol, the solubility of highly polar and high-molecular-weight components such as sugars, salts, and proteins—decreases, leading to precipitation. This effect is attributed to the higher polarity of ethanol compared to isopropanol, which makes it more effective in lowering the dielectric constant of the aqueous medium upon addition. The reduction in dielectric constant consequently decreases the solubility of polar or charged biopolymers in water, promoting their aggregation and precipitation with greater efficiency. This increases the aggregation and precipitation of biopolymers (Tai et al., 2020).

The behavior of the solubility of various mono- and disaccharides like glucose, fructose, and sucrose in aqueous-ethanol systems was verified by a study by Gong et al. (2011). Such findings normally indicate that the solubility of sugar reduces with lower temperature or with the rising ethanol level.

Chilled ethanol is better compared to chilled isopropanol at lowering the solubility of heavy and high-molecular-weight molecules by lowering the thermal movement of water molecules, and stabilizing them in the medium. It helps to isolate and fall off these polymers more effectively (Tai et al., 2020).

The salt solubility in the reaction medium when cold isopropanol is employed is lower, and isopropanol will also co-precipitate salts and organic impurities in the reaction mixture with the polymer.. This results in a lower actual yield of the extracted polymer (Majem et al., 2016). This indicates that increasing the ethanol content in the supernatant, combined with lowering the solution temperature, contributes to the removal of a greater amount of sugary impurities. The findings of Ku et al. (2003) demonstrated that polysaccharides are more prone to precipitation in mixtures of water and chilled ethanol.

4.4 Biopolymer Characterization

4.4.1 Solubility Test

The results of the biopolymer solubility test indicate in the table (4.2).

Table (4.2) The Solubility of biopolymer in different solvents .

The solvents	The results
water	Completely soluble
96% ethanol	Insoluble
chloroform	Insoluble
dimethyl sulfoxide (DMSO),	Insoluble
dichloromethane (DCM),	Insoluble
acetone	Insoluble
phenol	Insoluble
methanol	Insoluble

As a general rule, biopolymers that contain a sufficient number of electronegative atoms or functional groups capable of forming hydrogen bonds with water molecules tend to be soluble in water while remaining resistant to dissolution in organic solvents. The ability of a biopolymer to dissolve in water provides a wide range of medical and industrial applications. The solubility of a biopolymer is determined by the balance between hydrophilic and hydrophobic groups in its chemical structure.

If hydrophilic groups (such as carboxyl or amino groups) constitute the majority of the biopolymer's structure, it will readily dissolve in polar solvents such as water. In contrast, if hydrophobic groups (such as alkyl or phenyl groups) are present in higher proportions, the polymer becomes soluble in non-polar solvents such as acetone, chloroform, and benzene. Patil & Shirsath (2015).

Solubility tests of the biopolymer in water and in a range of organic solvents, such as methanol, chloroform, dimethyl sulfoxide (DMSO), dichloromethane (DCM), acetone, phenol, and 96 percent ethanol, indicated that only in distilled water did the biopolymer dissolve and show no ability to dissolve in the organic solvents tested. The findings of Sasikumar et al. (2017), Al-Zaidi et al. (2023), and Obeid (2025) are in line with this result.

Such a behavior is explained by the existence of hydroxyl and carbonyl groups, which are detected with the help of FTIR spectra, which are characteristic of biological materials and carbohydrate derivatives. The existence of these functional groups generates hydrogen bonds between the polymer chains; the intermolecular bonds formed in the course of time are eventually destroyed, and polymer chains begin to interrelate with water molecules through new hydrogen bonding, The presence of these hydrophilic functional groups within the polymer structure is the reason why there is a low affinity for the use of organic solvents, which include acetone, methanol, and 96 percent ethanol, which explains the lack of solubility observed. (Angelin & Kavitha, 2020).

4.4.2 Estimation of carbohydrate concentration in the biopolymer

One of the easiest and most frequent methods of determining the carbohydrate level is the phenol-sulfuric acid method (Yadav et al., 2024).

The carbohydrate measurement technique in colorimetric methods is the sulfuric acid phenol method, which is also known to be an accurate, simple, stable, and sensitive method (Dubois et al., 1956). This procedure is based on the fact that carbohydrates react with sulfuric acid and phenol to give a product of color, and its absorbance is quantified at 490 nm. Experimental conditions, including wavelength, reaction time, temperature and range, have to be controlled in order to achieve the correct results. Also, the preparation of a monosaccharide such as glucose to produce a standard curve is an important procedure when determining the sugar content (Yue et al., 2022).

The carbohydrate concentration in the biopolymer sample produced from the bacterial strain was estimated using the sulfuric acid phenol method. To calculate the percentage of carbohydrates, the absorbance of a standard glucose solution was measured using a UV-visible spectrophotometer. The results are presented in Table (4.3).

Table (4.3). Determination of carbohydrate concentration in the biopolymer using phenol–sulfuric acid method

Parameters	The measured values	Unit of measurement
Absorbance of sample	0.70	nm
Concentration of sample	80	mg/ml
Absorbance of standard	0.67	nm
Concentration of standard	80	mg/ml

By applying Equation No. ….....(1)

Total sugar concentration = A . test / A.STD * Conc. of STD* 100

The carbohydrate concentration in the biopolymer sample was 83.5%. Here, (A. test) represents the absorbance of the biopolymer sample, while (A.STD) represents the absorbance of the standard glucose solution. Additionally, (Con of STD) represents the concentration of the glucose solution.

The results are in approximate agreement with those reported in the study by Giri et al., 2015, where the carbohydrate concentration in the biopolymer was 88.3%. They are also in approximate agreement with the findings of Ibrahim et al., 2024, which indicated that the carbohydrate concentration in the biopolymer was 87.5%.

The variation in carbohydrate concentration in biopolymers produced by bacteria highlights the influence of various factors such as strain, carbon source, pH, temperature, sample size, and incubation time Kavitake et al., 2022 ;Oztekin et al., 2025.).

4.4.3 (UV-Vis) spectroscopic analysis of biopolymer

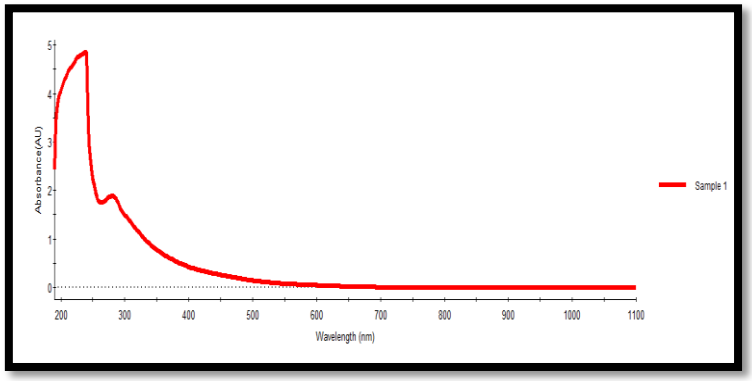

Figure (4.11) The UV–Vis spectrum of the biopolymer exhibited a distinct absorption peak at 204 nm, along with a shoulder peak observed in the 260–280 nm.

Ultraviolet-visible (UV-Vis) spectroscopic analysis is a widely used tool for analyzing chromophoric atomic groups, due to its ability to absorb energy through electronic transitions. The spectrum primarily shows absorption in the 200-400 nm range, with a gradual decrease in absorption beyond that, indicating light absorption at shorter wavelengths (in the ultraviolet range), followed by a slowdown in absorption as the wavelength increases into the visible region. Main peak at 200-300 nm: The spectrum shows a strong absorption peak in this range, indicating the presence of chemical bonds that absorb light in this region. Functional groups such as amino, carboxyl, or aromatic groups are responsible for this absorption. These electronic transitions within the functional groups contribute to UV absorption in this range.

Absorption regions of the spectrum that can be found between 190 and 230 nm are mostly due to either $n \rightarrow \sigma^*$ or $n \rightarrow \pi^*$ transitions, which are found in functional groups such as amines, carboxylates, carbonyls, and esters. In the 260-280 nm range, most of the absorption can be attributed to $\pi \rightarrow \pi^*$ electronic transitions of aromatic and polycyclic molecules, which are typically found in most conjugated molecules such as proteins (Gao et al., 2009; Trabelsi et al., 2009).

The UV-Vis spectroscopy data illustrate a significant concentration of absorption band between the 200-230 nm range due to $\pi \rightarrow \pi^*$ electronic transitions related to the presence of C=C double bonds or carbonyl (C=O) groups. In addition, in the 270-290 nm region, a shoulder exists due to $n \rightarrow \pi^*$ transitions, which typically indicates non-bonding electrons associated with either an oxygen atom or a nitrogen atom. This leads one to postulate that carbonyl (C=O) or amide (C=C) groups make up part of the overall structure.

There are also absorption peaks in the FTIR spectrum at 1740 cm^{-1} and 1622 cm^{-1} that support the presence of the above-mentioned functional groups.

After 350 nm, there is a gradual decrease to near zero in the amount of light absorbed, which provides evidence for the biopolymer being optically clear, uncolored, and without extended chromophoric groups or large aromatic structures in the ultraviolet-visible portion of the electromagnetic spectrum. The results of UV-Vis spectroscopic analysis in this study are consistent with those reported by and Trabelsi et al. (2009) and Al-Assdy et al. (2025) Functional groups such as amino or carboxyl groups suggest that the polymer may interact with proteins or cells in biological or medical environments, which could be beneficial in biological or medical applications .

4.4.4 Fourier Transform Infrared analysis of biopolymer

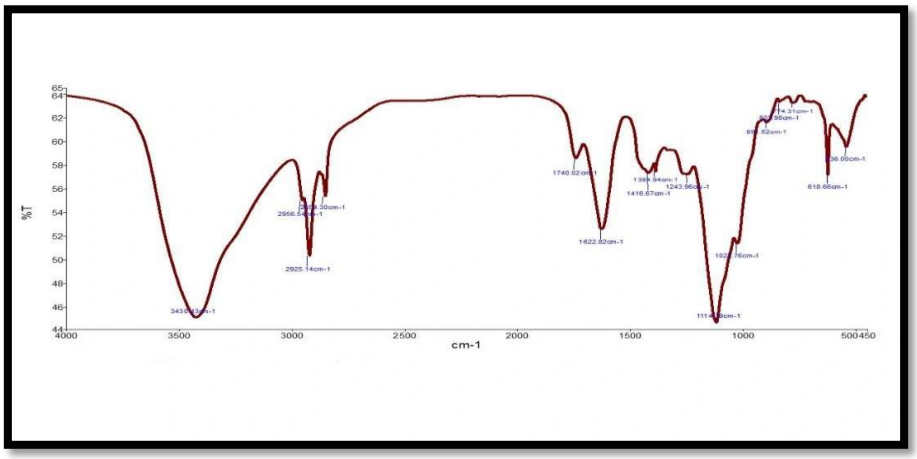

Figure (4.12). The result of the FTIR spectrum of polymer produced by the bacterial strain .

Table (4.4) The absorption bands of the FTIR spectrum and their functional groups

Wave number	The functional group	Description	References
3430 cm^{-1}	O-H	The peak at ~3430 cm^{-1} indicates the stretching vibration of the hydroxyl (O-H) group, and is considered an important marker in the FTIR spectrum of biomolecules and sugar derivatives. This type of vibration is often associated with water or hydroxyl groups in biopolymers such as starch or cellulose.	Nikolić et al., (2014)
2956 and 2925 cm^{-1}	C-H	These peaks at these frequencies indicate stretching vibrations of the aliphatic C-H bonds, which are commonly found in compounds containing saturated or unsaturated carbon chains, such as sugars or organic polymers. In glucose, for example, these peaks represent C-H vibrations in the carbon chains.	Mahmoud et al.. (2014)
1740 cm^{-1}	C=O	The peak at ~1740 cm^{-1} reflects the stretching vibration of the carbonyl group, and is found in glucose ester compounds (such as gluconic acid or its derivatives).	by Geitel et al. (2020),
1622 and 1384 cm^{-1}	C-O-C C-O-H	These peaks indicate bending vibrations of the C-O-C and C-O-H groups, which are commonly observed in carbohydrate-based polymers such as cellulose or hydroxyethyl cellulose. These peaks may suggest intramolecular interactions between oxygen and	Mohsin et al., (2022)

		carbon.	
1114 and 1022 cm^{-1}	C-O and C-C,	These peaks reflect vibrations of the C-O and C-C groups, which are indicative of the bonds between carbon and oxygen within the polymer structure. Such vibrations are common in carbohydrate-based polymers like starch or cellulose.	Acemi et al. (2019)
1022 cm^{-1}	C-O or C-C	The peak at 1022 cm^{-1}, on the other hand, corresponds to vibrations in the C-O or C-C bonds within the polymer structure. It indicates hydroxyl groups or interactions between the sugar and other elements in the polymer. This is typical for biopolymers such as starch	Acemi et al. (2019)

According to these results, the FTIR spectrum demonstrates various interactions between functional groups such as hydroxyl (O-H), carbonyl (C=O), and ether (C-O-C) in the biopolymer. This indicates that the polymer is derived from a sugar, such as glucose, cellulose, or one of its derivatives, like gluconic acid.

4.4.5 Thermogravimetric Analysis (TGA).

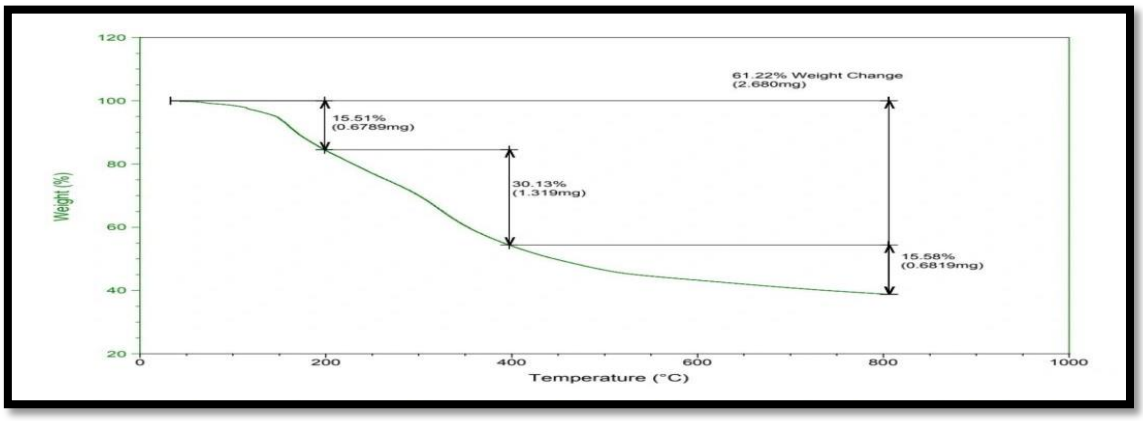

Figure (4.13). The result of thermogravimetric analysis of The biopolymer produced by the bacterial strain .

Thermogravimetric analysis (TGA) measures how much the mass of a sample changes as the temperature increases, generating a thermogram that shows relative weight loss against increasing temperature (°C). (Loganathan et al.,2017).

This analysis, conducted on the biopolymer isolated from the bacterial strain (shown here), demonstrates that three distinct regions exist for relative weight loss versus increasing temperature (°C).

Region 1 (0–200°C): The weight loss within this region stands at 15.51 percent of the initial weight, which is equivalent to 0.6789 mg.

Region 2 (200–400°C): clearly demonstrates a significant enhancement in the loss of mass as compared to the first region and thus indicates that the polymer is currently undergoing an active stage of thermal decomposition with the participation of its fundamental structural units. The overall weight loss in this area was 30.13% of the original mass (the equivalent of 1.319 mg), which indicates that a part of the structure of the polymer is relatively thermally unstable.

Region 3 (400–800°C): Here, the mass of the polymer keeps on decreasing, but more slowly than in the previous two stages.

This process is probably the ultimate degradation or higher chemical dissolution of the polymer. The total mass loss in this area was 15.58 percent. of the original polymer weight, or 0.6819 mg.

This is the last step, whereby the polymer is gradually and continuously degraded in terms of mass, which is the final degradation mechanism.

A slight weight loss was observed during the first stage, which may be attributed to the loss of volatile substances, including moisture and water.

In contrast, a significant decrease in weight occurred during the second and third stages, indicating the decomposition of one of the main components. This component may be a volatile organic substance or the loss of active functional groups.

These results are consistent with the findings of Liyaskina et al. (2021), who reported that the major weight loss in the polymer began at 57 °C, with the degradation rate gradually increasing to reach 15% at 200 °C and 60% at 300 °C.

The decomposition rate was calculated using the equation:

$$\{W_1 - W_2\} / \{T_2 - T_1\}* \text{ heating rate}$$

Substituting the values: {98 - 37}/{800 - 150} * 20 *100% = 1.87% min Thus, the material exhibits a decomposition rate of 1.87% per minute. The value of the decomposition rate is smaller, which means that the material is more resistant to thermal degradation.

The thermogravimetric (TGA) results show that the biopolymer experiences a total mass loss of 61.22 % (which is equal to 2.680 mg) throughout the heating process, and about 38.78 mass remains constant up to 800 degree. This fraction of residue denotes the existence of thermally stable structural elements in contrast to the high mass loss that results in the low and middle temperature stages due to progressive thermal decomposition.

,According to the observed degradation percentages, the thermal stability of the biopolymer can be classified as low to moderate, as evidenced by the significant mass loss at intermediate temperatures. This is because the material is not highly

resistant to thermal decomposition and loses most of its organic components before reaching higher temperature ranges.

This result is consistent with the study of (Blanco & Siracusa, 2021), which indicated that the residual mass observed at high temperatures in the thermogravimetric analysis (TGA) curve is generally attributed to the presence of thermally stable structural elements that do not undergo further decomposition under the applied conditions. The study also confirmed that the presence of distinct degradation steps and residual mass at high temperatures indicates that the polymer exhibits moderate thermal stability, which aligns with the behavior observed in the present study .

The results of this experiment demonstrate that there is a relative measure of consistency with the findings obtained by Corazzari et al. (2015), who have explored the thermal properties of chitosan with the help of TGA. The study under consideration proved that chitosan experiences three major phases of thermal degradation: the first stage is moisture loss at low temperatures, then there is a structural decomposition phase at the middle temperatures, and the last stage is a deep degradation at higher temperatures.

The results of the research provide a definite correspondence to the overall thermal characteristics used by Gola et al. (2023), who examined the thermogravimetric dissolution of PNIPA-based polymers. The authors also mentioned that the samples studied pass through three major steps of thermal decay, also referred to as a triphasic degradation pattern, where the first step involves a slight loss of moisture, the second step involves intermediate structural degradation, and the third step involves high mass degradation, where the greatest mass loss occurs.

But the percentage figures of mass loss in the two studies are not the same, and this can be ascribed to the fact that the chemical structures of the two polymers are not identical, and the nature of the bonds between the atoms in the two polymers is different.

4.4.6 Scanning electron microscopy (SEM) of biopolymer

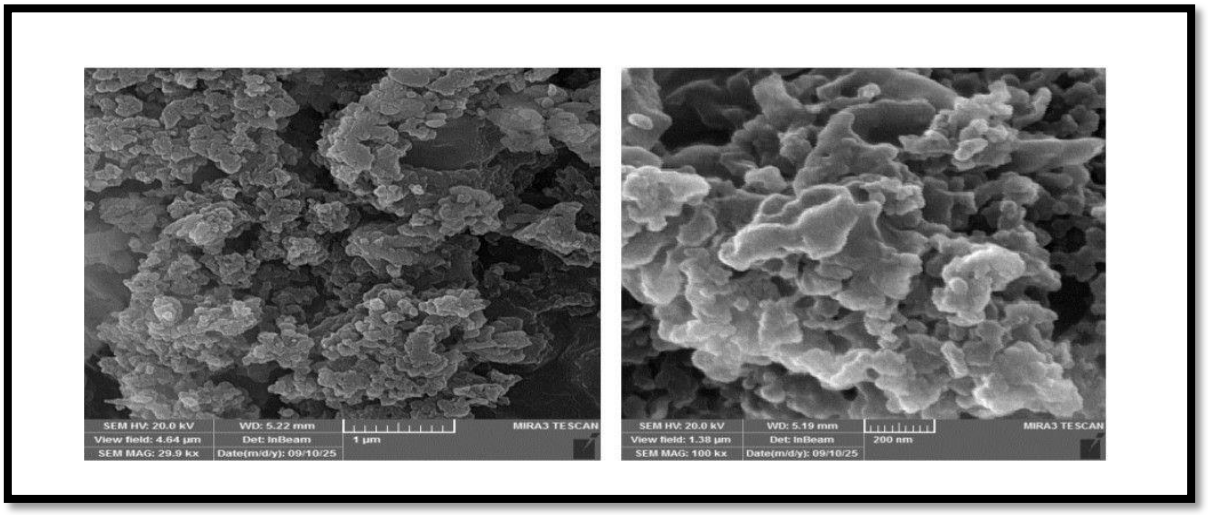

Figure (4.14): SEM images of the biopolymer.

The Scanning Electron Microscope (SEM) is a very powerful and useful imaging method, which involves the utilization of electrons and an electron beam to produce high magnifications of the surface morphology of biopolymer materials. The study of the surface morphology and structure of polymers is an invaluable tool that is analyzed using SEM. It enables the researcher to visualize and examine details on a micro- and nano-scale that will give important information on structural and property characteristics of the polymer. (Goldstein et al., 2017).

To examine the morphological features of the surface and structural composition of the polymer, scanning electron microscopy (SEM) was applied. The outcome of the SEM analysis showed that the biopolymer has a rough and porous surface

structure that is typical of biopolymers, with the size of particles ranging between about 200 nanometers and a few micrometers. Polymer has a diverse surface topography and its surface is uneven with numerous protrusions, folds, sharp edges, irregularly shaped particles, both small spherical particles and non-uniform forms. Such shapes can be termed irregular because of the absence of geometric clarity.

It was noticed that the polymer particles became irregular or aggregated, which indicated that there was partial agglomeration of molecules after the addition of cold ethanol. The effect of the ethanol on the polymer formation might be the cause of this aggregation. The polymer has specific surface roughness, i.e., little protrusion or secondary bumps on the surface of this polymer.

Agglomerates are created in the form of broken layers/sheets that coat the substrate surface all over. The results of this study align with previous studies on the morphology of biopolymer produced by bacteria. The polymer produced in the study by Derdak et al. (2022) showed clear porosity, and the porous nature of some EPS (exopolysaccharides) may contribute to its increased water retention and solubility, facilitating rapid swelling.

Previous studies presented varying forms of polymer structures. Spherical structures were observed in the study by Zaghloul et al. (2023), while Wang et al. (2015) recorded the appearance of network-like porous structures and sheet-like compact structures. These morphological differences may arise from variations in sample extraction methods, purification procedures, and the inherent physical and chemical properties present in the biopolymer composition.

4.4.7 Zeta Potential Analysis of biopolymer

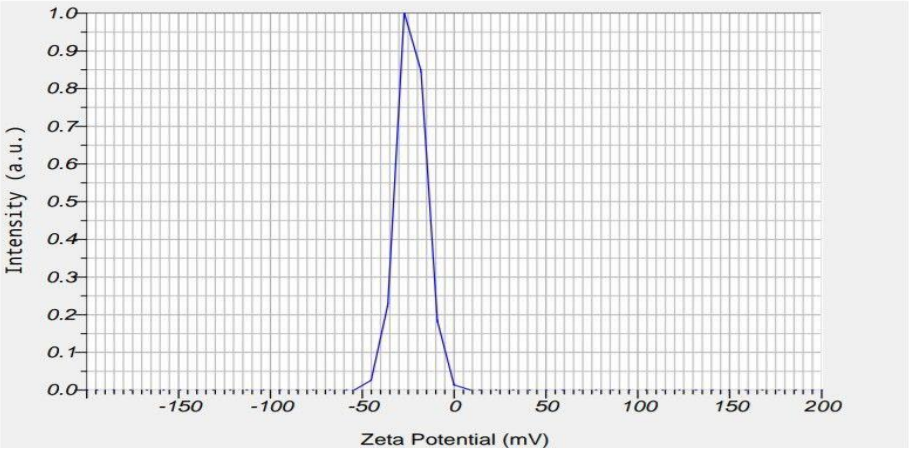

Figure (4.16). The result of Zeta Potential Analysis of biopolymer

The Zeta potential analysis was used to determine the charge present on the surfaces of particles suspended in the solution and to assess their stability based on the magnitude of those charges. High Zeta potential values, whether positive or negative (Zeta potential > +_30), indicate increased stability of the particles. Higher values of zeta potential of these particles are explained by the fact that intense repulsive forces are formed, and particles do not stick together or agglomerate (Manzoor et al., 2021).

The Zeta potential value of the bio-based polymer sample was Zeta potential = -23.2 mV and temperature = 25.2°C. This negative figure shows that the particle surface has a negative charge, which is an indicator of the functional group OH or COOH that is found on the particle surface. This is also evidenced by the FTIR analysis.

Practically, a value of this value implies moderate stability of the particles in the colloidal medium. The negative charge on the surface gives the sample an electrostatic repulsion and does not allow the agglomeration to occur

immediately, but the stability is not high enough to ensure stability in the long-run. (Németh et al.,2022).

But they can be susceptible to aggregation during the course of time or when the environmental factors are altered, and this may necessitate a pH adjustment or the incorporation of stabilizers to make it more stable.

The findings of this paper were more or less the same as those of Ahmad et al. (2020), in which the Zeta potential value of the bio-based polysaccharide polymer was -25.38 +/-3.13 and they were more or less the same as the results of the study by Hassan et al. (2022), where the Zeta potential value of the bio-based polysaccharide polymer was -25.2.

Biopolymers that are based on polysaccharides have a higher stability level than the polymers of proteins that are more prone to aggregation and instability. This is due to one of the chemical structures and the physical characteristics of these materials, which include thermal stability. (Kalina et al.,2015).

The surface charge of the particles affects their interactions with the living organisms, like bacteria and cells, because it is also capable of producing different interaction behavior due to the charge that exists on the surfaces of the particles and the electrostatic forces between the particles and the bacteria.

This may result in either mutual electrostatic repulsion (no effect) or electrostatic attraction (resulting in an effect) between the particles and living organisms (Dhamecha et al., 2015).

4.5 Effects of biopolymer

4.5.1 Antifungal Activity

The results of the biopolymer efficacy evaluation against Candida spp. showed that the antifungal effect of the biopolymer is concentration-dependent and varied between the two fungal isolates. The isolates exhibited clear sensitivity to the biopolymer at concentrations of 500, 250, and 125 µg/ml, while relative resistance was observed at a concentration of 62.5 µg/ml. These results indicate that the fungal response to treatment is directly proportional to increasing concentration, with the inhibitory effect increasing as the biopolymer concentration rises.

The largest zone of inhibition was 29 mm for the *Candida albicans* isolate at 500 µg/mL, whereas the smallest zone of inhibition was 13 mm for the *Candida krusei* isolate at 125 µg/mL, as shown in Table (4.5).

Table (4.5) Effect of biopolymer on candida spp . isolates uses different concentrations

Concentration	***Candida albicans***	***Candida krusei***
500	29 mm	26 mm
250	17 mm	16 mm
125	14 mm	13 mm
62.5	R	R

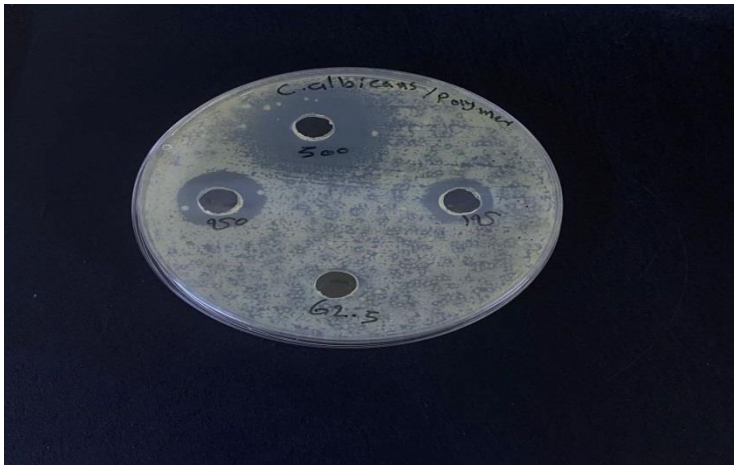

Figure (4.17) Effect of biopolymer on C. albicans

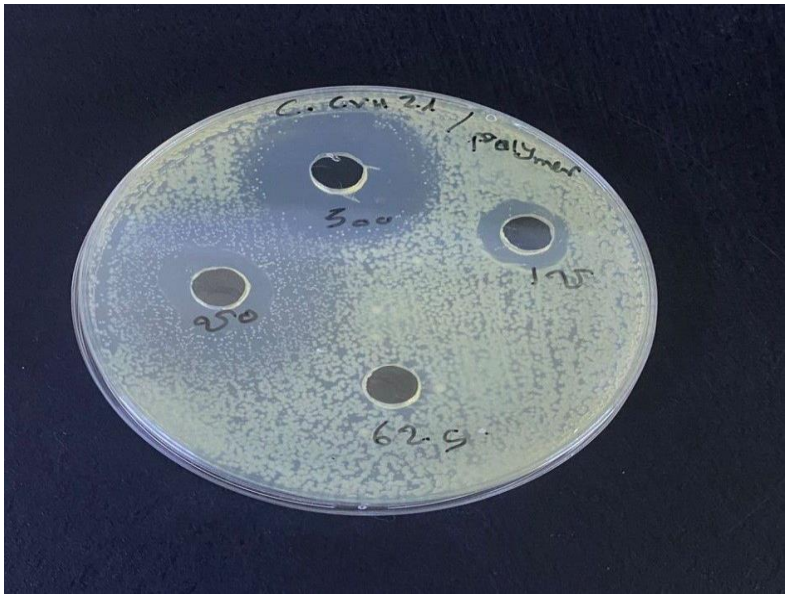

Figure (4.18) Effect of biopolymer on C. krusei

The results showed that the fungal isolate *Candida albicans* was more sensitive to the biopolymer than the isolate *Candida krusei.*

Findings of the research are similar to those of Shih et al. (2019), in which the biopolymer showed explicit activity against C. albicans. This was attributed to several important processes, such as:

1. Damage to cell membranes: The biopolymer reacts with the phospholipids that constitute the cell membrane, causing the membrane to be permeable and thus to degrade and cause disintegration of essential cellular constituents.
2. Prevention of biofilm formation: Biofilm formation is a major defense system of fungi to live in adverse conditions.
3. Gene expression: This biopolymer changes the expression of genes that are involved in cell wall synthesis in Candida spp.

A variety of morphological and molecular studies were used to identify these mechanisms, which proved the fact that the biopolymer has a direct impact on the cell membrane integrity and crucial fungal functions.

Moreover, the findings of the current research are in line with the results of the article by Peña et al. (2013, in which the growth of C. albicans growing on the Yeast Extract Peptone Dextrose (YPD) medium was inhibited by the biopolymer at a concentration of 1000 µg/mL.

Weakening of the cell membrane through the application of high levels of the biopolymer causes the nutrient balance to be broken, which in turn inhibits respiration and fermentation and increases the flow of proteins, leading to eventual fungal growth inhibition.

The difference in the effective concentration of the two studies can be attributed to the fact that the experimental conditions differ, mostly with the difference in the culture medium used.

The medium constituents have a great influence on the growth of fungi and how Candida albicans responds to antifungal agents. SDA medium is also favoured by fungi because it contains dextrose, and its pH is low, hence increasing the

effectiveness of the biopolymer with decreased concentrations (500 µg/mL). Contrarily, YPD medium supports a greater proportion of nutrients, which could render the cells more resistant, thereby necessitating more amounts of the biopolymer (1000 µg/mL) to produce the intended effect.

The findings of the research by Muangsawat et al., 2024 showed that the biopolymer has a high level of efficacy against Candida albicans, irrespective of the presence or absence of the fungus with efflux pumps. Efflux pumps are responsible for the resistance of C. albicans to conventional antifungals such as azoles.

Therefore, the biopolymer can be considered a promising alternative to traditional antifungal agents in cases where the fungus exhibits resistance due to efflux pumps.

The results of the biopolymer's effect on the *Candida krusei* isolate were consistent with :

The findings of Tarek et al. (2024). The biopolymer demonstrated a strong antifungal effect against C. krusei by physically destroying the fungal cell wall and reducing the expression of genes associated with drug resistance.

And The results of the study by Seyfarth et al., 2008 showed the same inhibition outcomes as those observed in our study, where the inhibition zone diameter was 16 mm against C. krusei grown on Sabouraud Dextrose Agar at a concentration of 1000 µg/mL.

The difference in the concentrations used between the two studies can be attributed to variations in experimental conditions, such as slight differences in the composition of the culture medium or preparation methods, which can affect the fungal response to the biopolymer. Additionally, one of the key factors

influencing these results is the time gap between the two studies. Over time, improvements in the preparation methods of the biopolymer are likely to have occurred, increasing its effectiveness at lower concentrations. Furthermore, the increased sensitivity of fungal isolates to the biopolymer may have contributed to achieving the same inhibition results at lower concentrations.

The reasons for the resistance of fungal isolates to the biopolymer at low concentrations are attributed to several factors, such as insufficient effect on the cell membrane, biofilm formation by fungal cells, the fungal defensive response, or environmental interactions . Al-Zaidi (2023).

The results of this study showed that the biopolymer synthesized from the bacterium *Pseudomonas aeruginosa* did not exhibit any effect on fungal isolates of the Candida spp. species.

4.5.2 Anticancer Activity of biopolymer

The cytotoxicity of the biopolymer was assessed by exposing the cells to varying concentrations of the biopolymer (25, 50, 100, 200, 400 µg/mL) for 24 hours at 37°C. Each concentration was tested in triplicate.

The results indicated that the biopolymer exhibited inhibitory effects on the growth of FTC_133 thyroid cancer cells starting at a concentration of 25 µg/mL, with an inhibition rate of 6.14%. This inhibition rate increased progressively to 47.73% at 400 µg/ml.

Table (4.6) Statistical analysis results of survival (viability) rates in the FTC-133 cell line under the influence of different concentrations of biopolymer.

Concentration	Mean
400	52.27 +- 2.25
200	63.58 +- 3.71
100	72.99 +- 2.62
50	86.41 +- 2.37
25	93.86 +- 0.81

In contrast, normal human dermal fibroblast cells (HdFn) showed lower cytotoxicity compared to the cancer cells when exposed to the biopolymer. The inhibition rate for HdFn cells at 25 µg/mL was 3.67%, which increased to 23.19% at 400 µg/mL.

Table (4.7) Statistical analysis results of survival (viability) rates in the HdFn cell line under the influence of different concentrations of biopolymer.

Concentration	Mean
400	76.81 +- 1.15
200	86.92 +- 2.36
100	94.25 +- 0.48
50	95.33 +- 0.29
25	96.33 +- 0.13

The results indicated that the cytotoxicity of the biopolymer increased with higher concentrations in both FTC-133 and HdFn cells.

The lethal concentration for 50% of the test population (LC50) was as follows: FTC-133: 120.2. HdFn: 235.5.

LC50 represents the concentration that causes 50% inhibition of the targeted cells. The results indicate that the polymer affects FTC-133 cells at a lower concentration (120.2) compared to HdFn cells, which require a higher concentration (235.5) to achieve the same level of inhibition. This suggests that the polymer exhibits greater cytotoxicity toward cancer cells than toward normal cells, as it induces a higher rate of cancer cell death at lower concentrations. Consequently, this polymer may be considered a promising material for targeted cancer therapy.

The HillSlope values were as follows:

HdFn: -2.823

FTC-133: -0.9134

The HdFn cell HillSlope value implies a steep and strong response to the concentration of the biopolymer. The negative value is greater, indicating that there is a rapid change in cell viability even with minor changes in concentration, showing the high sensitivity of the said normal cells to the biopolymer.

Contrarily, the HillSlope value of FTC-133 cells indicates a weaker reaction to changes in concentration. This means that the cancer cells have a slower rate of viability reduction and less intense fluorescence than normal HdFn cells, which is an indication that FTC-133 cells are not sensitive to the biopolymer.

This paper confirms the results of previously published articles because Sun et al. (2022) also assessed the cytotoxicity of a composite biomaterial against FTC-133 thyroid cancer cells, with an IC 50 of 148 µg/mL. Comparatively, the findings of the current study have shown that the IC 50 of the tested biopolymer on the same cell line is 120.2 ug/mL.

Considering that a decrease in the value of LC 50/IC 50 represents an increased cytotoxic potential against cancer cells, the results imply that the biopolymer utilized in the present study has a higher inhibitory potential on FTC-133 cell growth than the composite biomaterial tested by Sun et al. Such a difference can be explained by differences in test conditions, differences in polymer composition, structural features, and interaction mechanisms with cancer cells.

Moreover, the lower cytotoxicity of the lauded biopolymer against normal cells in this research is in tandem with the results provided by Wadhwa et al. (2019), who observed low cytotoxicity of the biopolymer against normal cells in contrast to cancer cells.

Al-Zuwaini et al. (2025) also showed that the human dermal fibroblasts (HDFn) had a cell viability of 66% when exposed to the cells to 400 µg/mL of biopolymer nanoparticles. These findings suggest the absence of high toxicity on normal cells as compared to cancer cells. Likewise, the HDFn cells also had a viability of 76.8 percent at the same concentration in the determination of cytotoxicity of the biopolymer. These results follow the overall trend mentioned by Al-Zuwaini et al. (2025) and prove the relative selectivity of the biopolymer to cancer cells and the low toxicity to normal cells.

Moreover, the results of Cheng et al. (2013) showed that the biopolymer exhibited no detectable toxicity toward human red blood cells even at high

concentrations. This demonstrates the good biocompatibility of the biopolymer with healthy cells and supports its safety for use on normal cells at concentrations capable of exerting inhibitory effects on cancer cells.

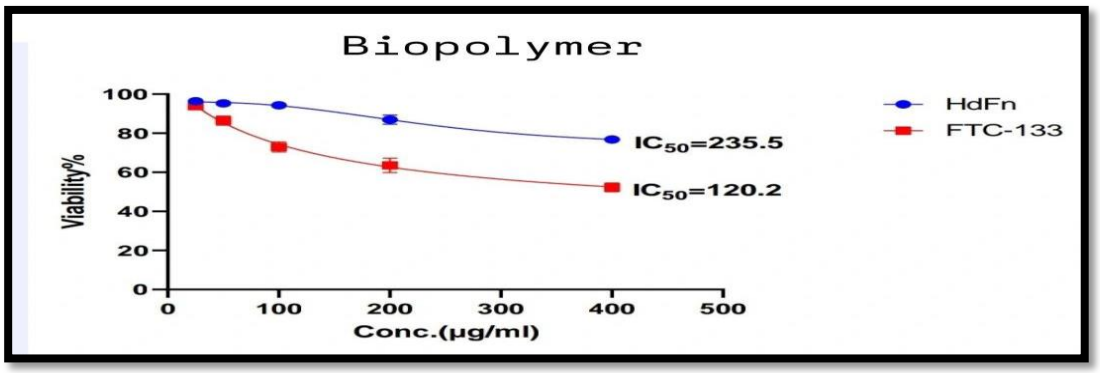

Figure (4.19) Curves IC50 of biopolymer for FTC_133 and HdFn

4.6 Biosynthesis of Gold Nanoparticles

The findings of the current research proved the capability of the bacterial isolate found in soil to biosynthesize gold nanoparticles (AuNPs). Following incubation, the trivalent gold ions (HAuCl 4) bioreduction of the aqueous solution was tracked by visually observing a color change. Three hours after incubating, the solution turned deep purple, which confirmed the depletion of gold ions (AuIII+) to both elemental gold (Au^0) and the creation of gold nanoparticles (Hamed & Abdel Fattah, 2019). This has been regarded as a starting point for the successful biosynthesis of nanoparticles.

This change of color can be attributed to the phenomenon of Surface Plasmon Resonance (SPR) that takes place due to the interaction of nanoparticles and light, and it gives a first visual stimulus of nanoparticle formation (Sidhu & Nehra, 2020).

Surface Plasmon Resonance is present in most metals, and in this case, gold and silver at the nanoscale, which results in the creation of different shapes, including spherical, circular, triangular, and pentagonal (Roy et al., 2016; Amendola et al., 2017; Yuan et al., 2019).

(A) (B)

Figure (4.20). Biosynthesis of gold nanoparticles A - Before the color change B - After the color change

4.7 characterization of gold nanoparticles

4.7.1 (UV-Vis) spectroscopic analysis of gold nanoparticles

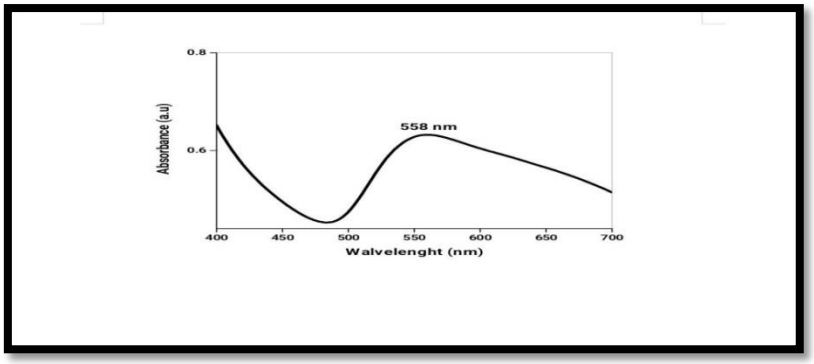

Figure (4.21). The UV-Vis Spectroscopy of gold nanoparticles

NanoUV-Vis UV-Vis Spectroscopy is a very flexible instrument that has numerous applications and is used to comprehend and monitor the dynamics of reactions during the synthesis of nanoparticles and their formation(Calderón-Jiménez et al., 2017).

Monitoring of the color change was done using a UV-Vis spectrophotometer (Thermo Scientific, Multiskan Spectrum) at a wavelength of 300 to 800 nm after the formation of the gold nanoparticles (GNPs). Gold nanoparticles exhibit surface plasmon resonance (SPR) at 510-560 nm in aqueous solutions, depending on the shape and size of the nanoparticles. Gold nanoparticles were formed at different concentrations of the gold salt, as evidenced by the appearance of peaks between 530 and 560 nm. Sharp peaks represent unification of the particle size (monodispersity), whereas those that are broad represent variation in the size (polydispersity). In addition, a higher peak height is associated with the concentration of nanoparticles formed, whereas an increase in wavelengths means that particles are bigger (Srinath and Rai, 2015).

The variation of the color of the gold nanoparticle solution is explained by the phenomenon of the surface plasmon resonance (SPR) since these nanoparticles behave in the visible range of the electromagnetic spectrum. It, therefore, absorbs part of the visible wavelengths, reflects another part, and the reflected portion gives the material the characteristic color. (Rajasree and Suman, 2012).

In this research, it was noted that:

1. The peak of absorption of the synthesized gold nanoparticles was 558 nm. This supports the creation of gold in the Au 0 state. The high value at 558 nm relative to 520-530 nm in small and homogeneous-sized gold nanoparticles indicates that the particles may be relatively large or

partially aggregated (as indicated by the zeta potential value of -8) or that the surface layer has a high refractive index.

This result is consistent Approximately with that reported by Alewi (2023), in which the absorption peak of gold nanoparticles synthesized using the supernatant of *Penicillium citrinum* isolate MEBP016 was observed at 551 nm. Similarly, this finding is in agreement Approximately with the study by Abbood (2025), where the absorption peak of biosynthesized gold nanoparticles produced from the supernatant of *Acinetobacter baumannii* was recorded at 560 nm.

2 .Absorption Intensity (0.6 a.u.)

Absorption value of 558 nm = 0.6 (a.u. = absorbance unit). This value is a pointer that the concentration and distribution of the gold nanoparticles in the solution are moderate. Sultani et al. (2015) also recorded an absorption peak of 550 nm in the case of gold nanoparticles mediated by Streptomyces fulvissimus, and Balagurunathan et al. (2011) measured a peak at 549 nm when using *Streptomyces viridogens* strain HM10. The slight differences in the maximum absorption values can be attributed to variations in particle size distribution and experimental conditions, but these values remain within the expected range for the surface plasmon resonance (SPR) properties of gold nanoparticles. Results from Fourier Transform Infrared (FTIR) spectroscopy supported the UV-Vis spectral findings, revealing the presence of functional organic groups (O–H, C=O, N–H, C–O–C) on the nanoparticle surface. These groups are likely involved in the reduction of gold ions and the stabilization of the nanoparticles, explaining their stability and the observed shift in the absorption peak within the visible-ultraviolet spectrum.

4.7.2 Fourier Transform Infrared analysis of gold nanoparticles

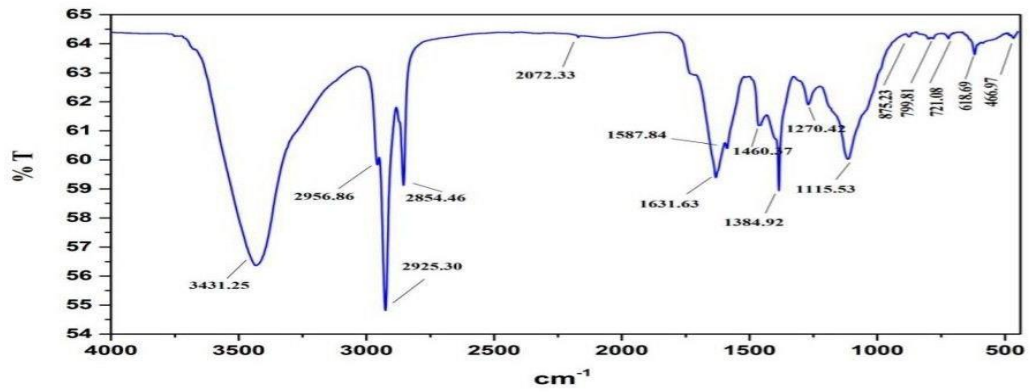

Figure (4.22). The FTIR spectrum of gold nanoparticles

FTIR analysis is used to identify potential interactions between bacterial proteins and metal compounds responsible for the formation of nanoparticles by bacteria (Fouda et al., 2022).

Pure gold does not exhibit significant infrared absorption, which is why FTIR analysis is primarily used to detect the organic molecules attached to the nanoparticle surface, such as stabilizing or reducing agents. Therefore, the peaks observed at specific frequencies in the FTIR spectrum (~3431 cm^{-1}, ~2956–2854 cm^{-1}, ~1631–1587 cm^{-1}, etc.) are attributed to the vibrations of the organic molecules (not the gold itself) that coat the nanoparticles, confirming the presence of functional groups such as -OH, -C-H, -C=O, and others, which are not directly associated with the gold (Pasieczna-Patkowska et al., 2025).

The functional groups associated with the nanoparticles were identified based on the reference table (Merck, 2020).

In the FTIR spectrum, the horizontal axis (X) represents the wavelengths or frequencies in units of cm^{-1}, while the vertical axis (Y) represents the percentage of transmittance or absorbance (%T).

Table (4.8). Functional groups of nanoparticles identified by FTIR analysis according to (Merck, 2020)

Wave number	the functional group	Description
3431.25 cm^{-1}	(O–H)	This peak typically represents the absorption of water molecules or hydrogen bonds that may be present on the surface of the nanoparticles or within the sample itself. It may indicate the presence of water molecules bound to the surface of the gold nanoparticles.
2956.86 cm^{-1} and 2854.46 cm^{-1}	(C–H)	These peaks represent C–H bond vibrations in organic groups or hydrocarbons that may be present on the surface of the gold nanoparticles. These groups could result from interactions between the nanoparticles and chemical or organic compounds during the preparation process.
2925.30 cm^{-1}	C–H	This peak is also related to C–H bond vibrations and may be associated with another set of organic compounds present in the sample.
2072.33 cm^{-1}	(C≡C)	This peak may indicate changes in the chemical interaction on the surface of the

		gold nanoparticles, or it could represent carbon-carbon (C≡C) bonds or compounds that absorb at this frequency.
1587.84 cm^{-1} and 1631.63 cm^{-1}	C=C	These peaks typically represent C=C bond vibrations. This suggests the presence of unsaturated groups or aromatic bonds associated with organic compounds in the sample.
1460.37 cm^{-1}	CH_2	This peak represents CH_2 bond vibrations in organic compounds.
1270.42 cm^{-1} 1115.53 cm^{-1}	C–O C–N	The peak at 1270.42 cm^{-1} may be related to C–O bond vibrations, while the peak at 1115.53 cm^{-1} may indicate C–N bonds in the organic compounds present on the surface of the gold nanoparticles.

As the study conducted by Bharadwaj et al. (2021) states, the FTIR spectrum of the gold nanoparticles covered with plant extracts recorded a specific peak at 3431 cm^{-1}, which is representative of O-H bond vibrations, meaning that the nanoparticles had hydroxyl groups on their surface. Also, a peak at 2956 cm^{-1} was present, which indicates the presence of C-H bond vibrations, and it indicates the existence of hydrocarbon groups. These results prove the hypothesis that the organic compounds in the surface not only function as effective stabilizers of the gold nanoparticles but may also serve as reducing agents, as the functional groups of OH and CH may also help in reducing the gold ions (Au^{3+}) to metallic gold nanoparticles (Au^0) to increase the stability of the nanoparticles.

Even though the value of the spectral peaks in the results of Zhou et al. (2010) and ours slightly differ, it is clear that the two spectra have similar functional groups, such as C=O, C-O, and C-N. The 1587 cm^{-1} peak in our experiment may also be compared with that of 1637 cm^{-1} in the Zhou et al. experiment, both of which are C=O vibrations. Moreover, the peaks at 1115 cm^{-1} and 1270 cm^{-1}, which indicate C O and C N in our case, are comparable to 924 cm^{-1} and 1146 cm^{-1} in the Zhou et al.(2010) discussion, which show C O.. These peaks can be considered as distinct markers for identifying the ligands on the surface of gold nanoparticles.

The functional groups visible in the FTIR spectrum indicate their dual role in the biosynthesis process, acting as reducing agents responsible for converting gold ions into nanoparticles, in addition to their role as stabilizers that coat the surface of the particles and prevent their agglomeration, thus enhancing their stability and biological properties.

4.7.3 X-ray diffraction (XRD) analysis of gold nanoparticles :

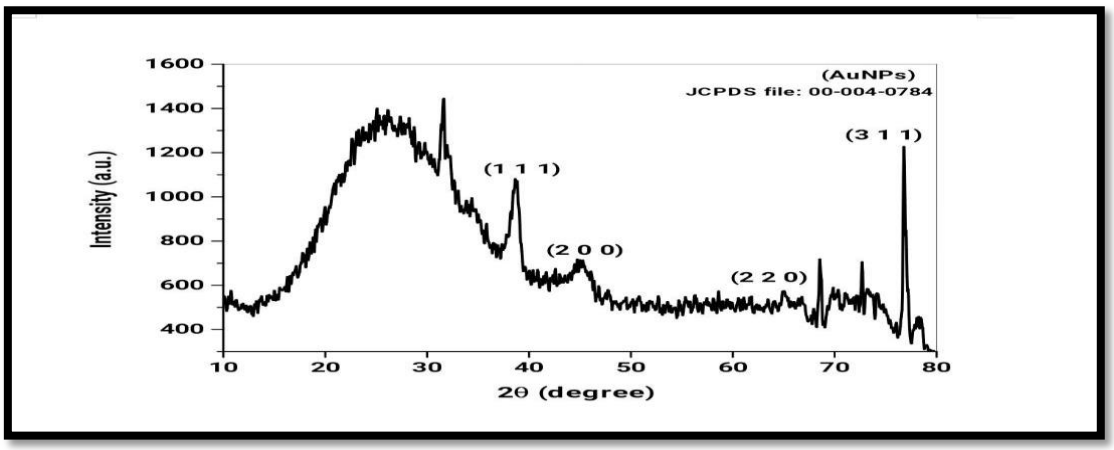

Figure (4.23). X-Ray Diffraction (XRD) of gold nanoparticles

The results of X-ray diffraction (XRD) analysis of the biosynthesized gold nanoparticles from bacterial extract showed that the obtained values correspond with the Bragg reflections at the 2θ angle with JCPDS reference file number (00-004-0784) for gold nanoparticles. This indicates that the synthesized gold nanoparticles are crystalline in nature and tend to have a face-centered cubic structure.

The gold nanoparticles underwent X-ray diffraction (XRD) analysis to confirm their crystalline structure and determine the average particle size of the biosynthesized nanoparticles using the Debye-Scherrer equation:

$$D = K\lambda / \beta \cos\theta$$

Where D is the crystallite size of the nanoparticles, K is the Scherrer constant, λ is the wavelength of the X-ray source, β is the full width at half maximum (FWHM) of the diffraction peaks, and θ is the Bragg angle.

Four distinct Bragg reflections were observed at the 2θ angles of (38.78°), (44.85°), (64.81°), and (77.07°) corresponding to the (111), (200), (220), and (311) planes, respectively. The average particle size calculated using the Debye-Scherrer equation was 7.7 nm.

These results indicate that the gold nanoparticles exhibit a small nanocrystal size and a regular crystalline structure (FCC), reflecting the efficiency of the bacterial strain in producing high-quality nanoparticles. These results are in strong agreement with those reported by Aliwi (2023), where biosynthesized gold nanoparticles produced using the fungal filtrate of Aspergillus tubingensis strain HRb exhibited similar diffraction peaks at 2θ values of 38.2°, 44.2°, 64.5°, and 77.3°, corresponding to the same crystallographic planes and matching the standard JCPDS card No. 04-0784 for crystalline gold. Furthermore, the average

crystallite size calculated using the Debye–Scherrer equation was approximately 7.4 nm, indicating the formation of highly crystalline gold nanoparticles within the nanoscale range via biological synthesis methods.

The slight variation in peak positions or crystallite size may be attributed to differences in biological reducing agents, synthesis conditions, or strain-specific metabolites involved in nanoparticle formation.

4.7.4 Transmission Electron Microscopy (TEM) of gold nanoparticles

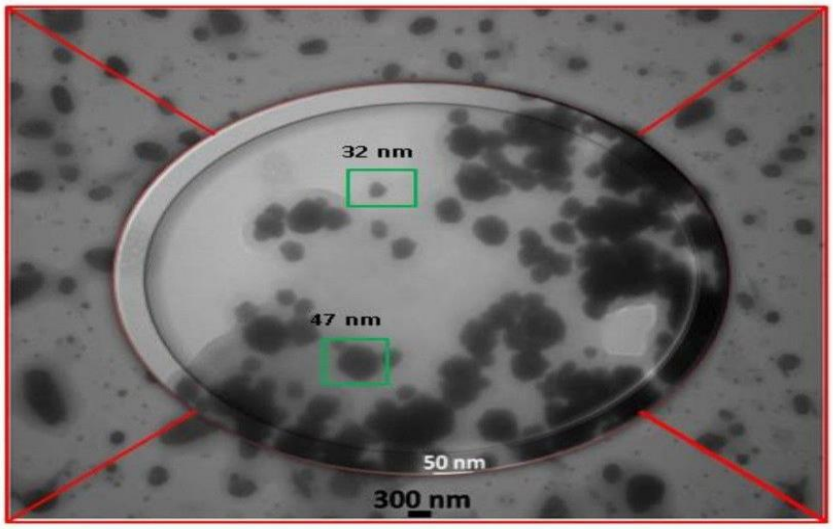

Figure (4.24) . Transmission Electron Microscope analysis of gold nanoparticles

Two nanoparticle sizes were identified: 32 nm and 47 nm. The scale bar shown at the bottom of the image represents 300 nm. Such magnification is sufficient to reveal gold nanoparticles in fine detail at the nanoscale. These values indicate a relatively homogeneous size distribution. It was observed that some particles were slightly aggregated; however, their overall size remained within the nanoscale range (5–50 nm).

The results also confirmed that most of the nanoparticles were spherical or quasi-spherical in shape, with a few exhibiting irregular geometries or sharp angles. These morphological abnormalities were minor and did not significantly affect the overall morphology. This finding is consistent with the study by Ali & Mutlak (2024), where TEM images also showed that the gold nanoparticles were spherical and polycrystalline, with a small proportion (~10%) displaying asymmetric shapes such as triangular and hexagonal forms. Despite slight differences in the proportion of non-spherical shapes, both studies confirm that spherical morphology is predominant in biologically synthesized gold nanoparticles. The minor variation in additional shapes may be attributed to differences in preparation methods or the physicochemical conditions employed in each study.

Furthermore, TEM analysis revealed a uniform distribution of the nanoparticles with slight aggregation. This aggregation is most likely attributed to the low zeta potential value (−8.7 mV), which provides weak electrostatic repulsion between particles. Consequently, attractive van der Waals forces become dominant, leading to particle aggregation and reduced colloidal stability, as explained by Bhattacharjee (2016).

The nanoparticles appeared vertically oriented in the TEM images, suggesting the possibility of self-assembly as a result of the preparation method. Despite a certain degree of aggregation, the vast majority of the particles retained their individual and discrete morphology upon TEM analysis.

Additionally, the examination showed that the gold nanoparticles were highly crystalline, with distinct lattice fringes observed in high-resolution TEM (HRTEM) images, revealing a face-centered cubic (FCC) structure, which is characteristic of gold. These findings are consistent with those reported by

Zabetakis et al. (2012). TEM analysis also indicated that the nanoparticles were largely uniformly distributed, reflecting the quality and consistency of the synthesis process, which is crucial for applications requiring stability, including biomedical applications (Kwon et al., 2018).

4.7.5 Field emission Scanning Electron Microscope (FESEM)

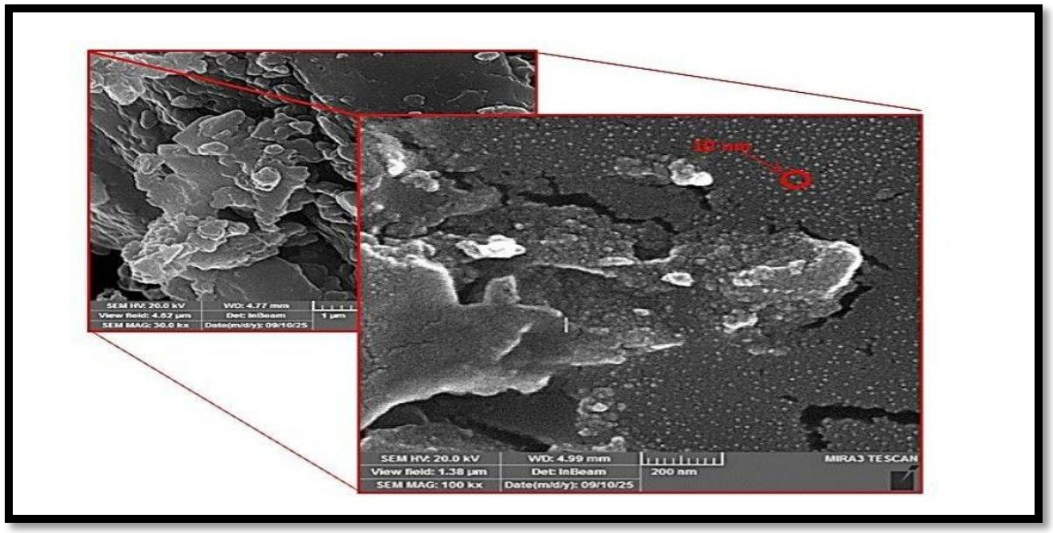

Figure (4.25). SEM images of the morphologies of the gold scale 100 Kx

The surface morphology, structure, size, and shape of the biologically synthesized gold nanoparticles prepared using the bacterial filtrate were studied using Scanning Electron Microscopy (SEM). The SEM image showed that the surface of the gold nanoparticles deposited on the glass surface using the drop-casting technique exhibited both two-dimensional and three-dimensional features. Upon magnifying areas of aggregation, clusters were observed due to the effect of the zeta potential (−8.7 mV). The sizes of these aggregates ranged from 5 nm to 50 nm, with most of the particles falling between 10 and 20 nm. The scale bar in the image represents 200 nm, and the particles were found to be spherical or quasi-spherical, as indicated by the TEM results. These findings are

consistent with the results of Krpetic et al. (2009), who obtained nanoparticles in the 5–50 nm range with a homogeneous distribution.

These results also agree with those reported by Eugenio et al. (2023), where SEM images of gold nanoparticles synthesized using a plant extract showed a homogeneous distribution with most particles being spherical or quasi-spherical and exhibiting slight aggregation, despite a different average particle size of 41 nm. This consistency indicates the effectiveness of biological synthesis in producing stable nanoparticles with uniform shapes.

Furthermore, the findings are in strong agreement with Bibi et al. (2026), where SEM analysis of gold nanoparticles synthesized using Boerhavia diffusa showed well-dispersed, spherical or quasi-spherical nanoparticles with slight aggregation and a narrow size distribution, having an average diameter of approximately 53 nm. This again confirms that biological synthesis can produce gold nanoparticles with similar properties.

The SEM results also correspond well with X-ray diffraction (XRD) analysis, which confirmed that these nanoparticles exhibit a high degree of crystallinity. The crystalline peaks were identified at angles corresponding to specific crystallographic planes, such as the (111) peak, which is a characteristic feature of pure gold in its face-centered cubic (FCC) structure.

4.7.6 Atomic Force Microscope (AFM) of gold nanoparticles

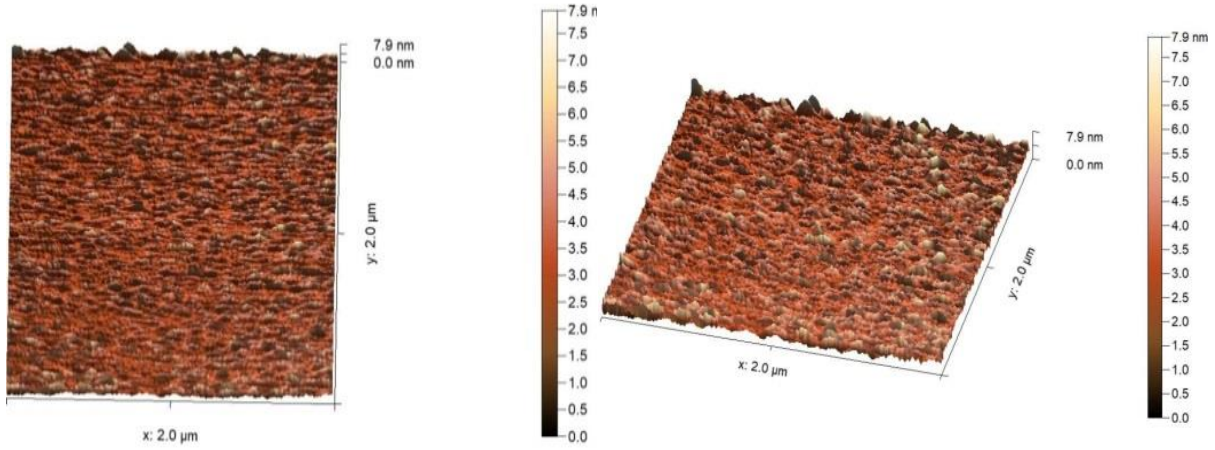

(A) (B)

Figure (4.26). Atomic force Microscope analysis of gold nanoparticles A : two-dimensional image of gold nanoparticles, B : three-dimensional image of gold nanoparticles .

The Atomic Force Microscopy (AFM) technique is used to study and understand the shapes, topography, roughness, and protrusions of surfaces at atomic and molecular levels. Through this examination, many particles and molecules are represented as elevations and surface structures, which facilitates quantitative measurements of surface properties and allows the generation of two-dimensional and three-dimensional images that can be analyzed from various perspectives (Salman & Abd, 2021).

AFM images of biosynthesized gold nanoparticles prepared using the bacterial filtrate of Schallia naturae provide both two-dimensional and three-dimensional representations with sizes below 100 nm. The nanoparticles are spherical or quasi-spherical, well-organized, homogeneous, and exhibit vertical alignment,

supporting the results obtained from TEM and SEM analyses. The average particle size of the gold nanoparticles ranges from 4 to 14 nm. The surface appears very smooth. Three-dimensional images confirm that the particles are evenly distributed within the scan area (500 × 500 nm), with individual particles extending vertically.

These results are in agreement with the study by Adamczyk et al. (2023), which showed that the nanoparticles were spherical, homogeneous, and regularly distributed. The study also confirmed that three-dimensional imaging revealed uniform particle distribution with a relatively smooth surface.

The three-dimensional images of the gold nanoparticle surfaces show surface elevations ranging from 5.278 nm to 18.00 nm, with regions having diameters between 17.3 nm and 618.6 nm. Root mean square (RMS) values for average surface roughness and particle size were calculated.

These findings are consistent with recent studies on thin films, such as Bîrleanu et al. (2021), which demonstrated that AFM analysis can reveal particle distribution, surface roughness, and three-dimensional variation of nanoparticles at the nanoscale, as well as allow precise measurements of surface heights and averages. This study systematically supports the use of AFM to interpret uniform particle distribution, the presence of slight aggregation, and surface roughness (RMS), enhancing our understanding of how surface properties affect the mechanical interactions of nanoparticles.

Table (4.9): Surface parameters of gold nanoparticles observed under atomic force microscopy, including average roughness, average root square roughness, and particle size.

Average grain size (nm)	Roughness average(nm)	Root mean square (nm)
5	7.9	7.0

Our results show that the surface is relatively smooth and uniformly distributed, indicating good stability of the nanocomposite, making it suitable for applications requiring precise and clean surfaces, such as medical or biological applications. Surface roughness contributes to an increased interaction area between atoms and living organisms, enhancing targeted adhesion to organisms and infected regions. It also contributes to increased mechanical stress on bacteria and cancer cells, leading to cell wall disruption and subsequent cell death. Surface amplification enhances chemical interactions and therapeutic effects, allowing atoms to interact with a larger number of molecules and cellular structures, thereby enhancing their ability to achieve the desired therapeutic effect (Ono & Roldan Cuenya, 2008; Rutherford et al., 2015).

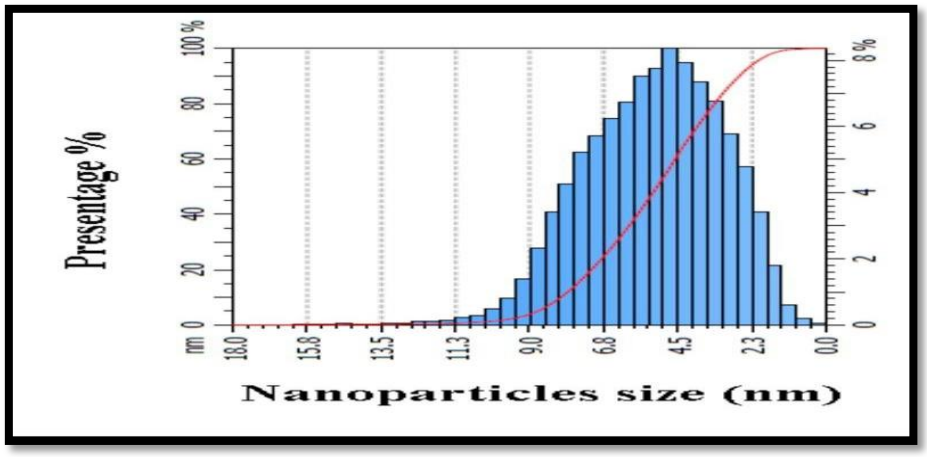

Figure (4.27). Granularity accumulation distribution chart of Gold nanoparticles

4.7.7 Zeta Potential Analysis of gold nanoparticles.

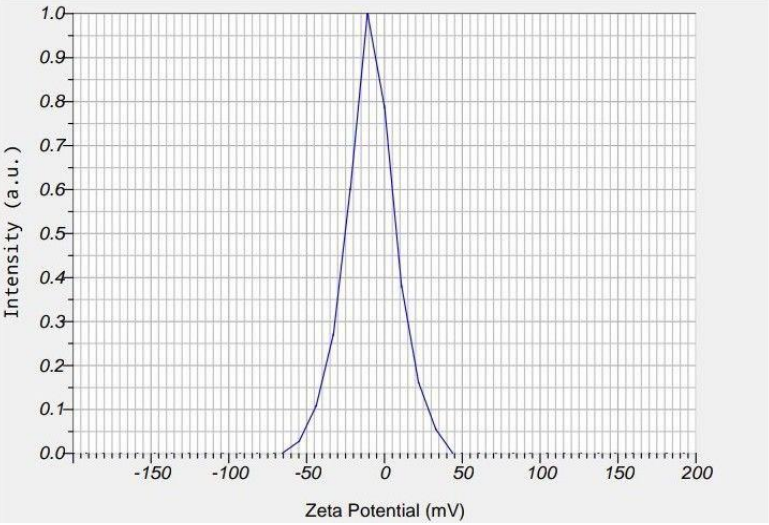

Figure (4.28). the result of zeta potential analysis of the gold nanoparticle

The zeta potential value for the prepared gold nanoparticles was recorded at –8.7 mV. This relatively low negative value indicates that the nanoparticles exhibit weak electrostatic repulsive forces, leading to poor colloidal stability and a tendency to aggregate over time. Zeta potential values ranging between -30 mV and +30 mV typically reflect low to moderate stability in the solution. The stability of nanoparticles depends on the strength of the repulsive forces between the particles. This suggests that the prepared gold nanoparticles are not well-stabilized in suspension. These data are in agreement with the Aarti et al. (2022) result (which gave the value of zeta potential equal to -8 mV) and the findings of Hsieh et al. (2012) on polyphenol-coated gold nanoparticles. Partial coverage of EGCG on the particle surface in their study gave a slight negative charge, which contributed a weak amount of stability, even though the surface potential value was low (-8 mV). The findings are also approximately parallel to the findings of Pertiwi et al. (2025), where the value of the zeta potential was -12.2 mV.

It can be explained by the following factors: the decrease in the value of zeta potential:

1 _The existence of multifunctional organic groups (–OH, -NH, -COOH, -CH), which can be seen through the FTIR spectrum, is linked to the reduction of the zeta potential of the nanoparticles. These functional groups are capable of communicating with water or other molecules within the solution, and the distribution of the surface charge and structural change of the electrical double layer.

The effects of such changes are reduced effective surface charge and an increase in the local ion density over the particle surface, leading toa decrease in the electrostatic repulsive forces between the particles. This then results in increased aggregation of the particles and reduces the zeta potential (Gorohovs & Dekhtyar ,2025).

2 -Viscosity: 0.895 mPa•s

This characterizes a low viscosity, resulting in the possibility of the particles traveling more freely through the medium, thus increasing mechanical contacts among the particles. The resulting effect of these interactions could be the aggregation of the particles instead of keeping them separated, which causes stability to decrease. (Rawat et al., 2023).

4.8 Effects of gold nanoparticles

4.8.1 Antifungal activity

The results of the evaluation of the antifungal activity of gold nanoparticles against Candida spp. showed a variation in the effect of gold nanoparticles at different concentrations on the two fungal isolates. Both isolates showed

sensitivity to gold nanoparticles at concentrations of 500, 250, and 125 µg/ml, while resistance was observed at a concentration of 62.5 µg/ml. The largest diameter of the growth inhibition zone, 24 mm, was recorded for *Candida albicans* at a concentration of 500 µg/ml, while the smallest diameter of the inhibition zone, 10 mm, was recorded for *Candida krusei* at a concentration of 125 µg/ml, as shown in Table (4.11).

Table (4.10) Effect of gold nanoparticles on candida spp . isolates uses different concentrations

Concentration	***Candida albicans***	***Candida krusei***
500	24 mm	15 mm
250	15 mm	13 mm
125	11 mm	10 mm
62.5	R	R

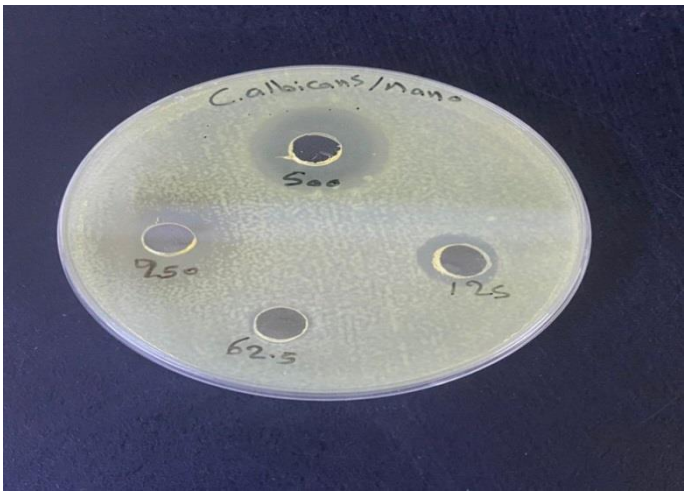

Figure (4.29) Effect of gold nanoparticles on C. albicans

Figure (4.30) Effect of gold nanoparticles on C. krusei

The results showed that the fungal isolate *Candida albicans* was more sensitive to the gold nanoparticles than the isolate *Candida krusei*.

The results of this study were consistent with those of Torabi & Doudi (2016). The inhibition zone diameter against C. albicans isolate reached 22 mm when gold nanoparticles were used at a concentration of 50 µg/mL. It is assumed that the high diameter of the inhibition zone at this low amount is due to the small size of the gold nanoparticles (10 nm).

Lavaee et al. (2021) established a close relationship between the antimicrobial effect of gold nanoparticles and their size. A size reduction is in direct proportion to an increased antimicrobial property.

The size of the nanoparticles is noteworthy in improving the antimicrobial effect because the smaller the size of the nanoparticles, the higher the surface contact with the microorganisms, hence the better inhibitory ability is exercised by the nanoparticles than by the larger ones.

This research was similar to Kareem et al. (2021) in which the gold nanoparticles were effective against Candida albicans with an inhibition zone diameter of

between 10 and 20 mm, with the minimum effective concentration of 40.7 µg/mL. They are nanoparticles that measure between 10 and 50 nm in size, thus providing a high surface area, thus increasing their effectiveness in interacting with the C. albicans cells.

The results of this research favor the application of AuNPs as an alternative or a beneficial supplement to conventional therapy of C. albicans infections, specifically in skin or topical infections.

The antifungal effect of gold nanoparticles was reported by Lotfali et al. (2021) against Candida krusei. Nevertheless, AuNPs were less inhibitory of C. krusei than other organisms (C. albicans) as judged by a weaker response and smaller inhibition zones at the same concentrations. This decreased efficacy of gold nanoparticles against C. krusei is due to the innate resistance property of this species, besides the structural composition of its cell wall, which is highly rich in chitin and mannoproteins, thus reducing the penetration of nanoparticles into the fungal cell.

The findings of Gholami-Shabani et al. (2022) showed that Candida species showed a level of insensitivity or functional resistance to gold nanoparticles (AuNPs), which were green-synthesized in the experimental conditions and concentrations studied. The same reduction of the cytotoxicity or cellular resistance to AuNPs at low concentrations can be explained by the fact that these low concentrations cannot result in the minimum inhibitory level, which can prevent the growth of fungi, as well as the fact that the low concentrations cannot cause the full production of oxidative stress because of the insufficient accumulation of nanoparticles on the surface of the fungi. Moreover, this resistance can also be related to the ability of fungal cells to implement

compensatory and repair responses that alleviate the damage caused by nanoparticles.

4.8.2 Anticancer Activity of gold Nanoparticles

The cytotoxicity of gold nanoparticles (AuNPs) was evaluated on thyroid cancer cells (FTC_133) and normal human dermal fibroblast cells (HdFn) by exposing them to varying concentrations of gold nanoparticles (25, 50, 100, 200, 400 µg/ml) with triplicate for each concentration. for 24 hours at 37°C.

According to the results, the gold nanoparticles demonstrated inhibitory effects on the growth of thyroid cancer cells (FTC_133) starting at a concentration of 25 µg/ml, with an inhibition rate of 13.51%. This rate gradually increased to 59.46% at 400 µg/ml.

Table (4.11) Statistical analysis results of survival (viability) rates in the FTC_133 cancer cell line under the influence of different concentrations of gold nanoparticles .

Concentration	Mean
400	40.54 +- 3.96
200	51.35 +- 1.52
100	62.46 +- 2.28
50	75.96 +- 2.02
25	86.49 +- 2.52

In contrast, normal human dermal fibroblast cells (HdFn) exhibited lower cytotoxicity compared to the cancer cells when exposed to gold nanoparticles. At 25 µg/ml, the inhibition rate for HdFn cells was 3.935%, increasing to 27.62% at 400 µg/ml.

Table (4.12) Statistical analysis results of survival (viability) rates in the HdFn cell line under the influence of different concentrations of gold nanoparticles .

Concentration	Mean
400	72.37 +- 0.59
200	81.25 +- 2.51
100	89.42 +- 1.38
50	94.59 +- 0.54
25	96.06 +- 0.20

The results indicated that the cytotoxicity of the gold nanoparticles increased with higher concentrations in both cell types.

The Lethal Concentration for 50% of the test population (LC50) was: HdFn: IC50 = 208.7 µg/ml

FTC-133: IC50 = 88.25 µg/ml

IC50 refers to the concentration that results in a 50% reduction in cell viability. These findings suggest that gold nanoparticles are more toxic to thyroid cancer cells (FTC-133) compared to normal dermal fibroblasts (HdFn). FTC-133 (cancer cells) are also more susceptible to the lower concentration of gold nanoparticles than the dermal fibroblasts (HdFn).

These findings are consistent with the analysis of Ascar et al. (2019), where the inhibition rate was the highest at 400 µg/ml of the solution.

The values on the HillSlope are as follows:

HdFn: -1.665

FTC-133: -0.8001

In the case of HdFn, the value of HillSlope is -1.665, suggesting that the response to a change in concentration is moderate.

In the case of FTC-133, the -1 HillSlope is - 0.8001, indicating that the cancerous cells are less sensitive to the change in the concentration of the nanogold than the normal HdFn cells.

It is implied by the HillSlope results that HdFn cells are more sensitive to nanogold concentration change than FTC-133 cells, which can mean that nanogold, in comparison, produces a more powerful and faster effect on normal than on cancerous cells.

Moreover, the research article by Khalaf et al. (2023) showed that the treatment of FTC-133 cancer cells with nanoparticles led to a high decrease in cell viability, which depends on the concentration. The greatest inhibition had a record of 400 µg/ml.

Nilubol et al. (2018) have found that the nanoparticle extract induces apoptosis by several different pathways that involve the cell membrane, mitochondria, and nuclear components hence the greater the concentration of the nanoparticle the better the effect will be. In the investigation of the impact of gold nanoparticles on FTC-133 thyroid cancer cells, it was discovered that such nanoparticles can

act on these cells through various means, the most important one being the decrease of the tumour size and proliferation, and the induction of the apoptosis process through the increased levels of cleaved caspase-3 protein in the tumor tissues, which is a primary marker of activation of Apoptosis cell death pathways in FTC-133 cells.

This study findings are in line with the findings of Mahmoud et al. (2024) with respect to the cytotoxicity of gold nanoparticles on HdFn cells. The experiment revealed that these cells retained a high rate of cell viability which was estimated at 95% when subjected to the nanoparticles at a concentration of 30 elongated to mL. It indicates that the cytotoxicity is not very high and the nanoparticles are not fatal to the cells even at the highest levels.

Also, the article by Asker and Al Haidar (2024) established that the gold nanoparticles produced with the help of the green synthesis using *Pelargonium graveolens* extract were not toxic to HdFn cells. The cells were highly viable in low and medium concentrations, but cytotoxicity was not noticed at low and medium concentrations (500 and 1000 µg/mL). Besides, the toxicity was much less than that induced by the plant extract itself, and this was due to the fact that gold nanoparticles were biocompatible with normal cells.

Compared to normal cells, cancer cells have a 600 times higher chance of getting the nanoparticles since they have unique protein repertoires on their surface, including seprase protein and Her2 protein, which have antibodies that attach to the nanoparticles. (Hussein, 2016).

The limited response of gold nanoparticles on normal cells as opposed to cancer cells may be attributed to the capacity of the normal cells to repair themselves and not the failure of the normal cells to respond to nanomaterials. This is

attained by the protection of different defense systems, and one of these is autophagy, which serves as a shield against the period of toxicity caused by nanoparticles. Conversely, cancer cells are more influenced because of their cell dysfunctions. This reaction is one of the survival strategies of normal cells and they assist to sustain cell health and functioning in stressful conditions. (Florance et al., 2024).

The research conducted by AL-Hasnawi (2015) showed that only 7% of the normal cells were affected by gold nanoparticles. It is explained by the fact that autophagy is stimulated as a protective response to the toxicity of oxidative stress, and lipid hydroperoxides are produced as a positive indicator of lipid oxidation. Gold nanoparticles activate these mechanisms.

The contact between the gold nanoparticles and the cancer cells increases the quantity of ROS as compared to non-cancerous cells. This could be the reason why there is a decreased action of gold nanoparticles on normal cells relative to cancer cells (Lee & Hwang, 2022).

The increased cytotoxicity of nanoparticles toward cancer cells, compared with normal cells, is attributed to the higher uptake of these particles by malignant cells. Cancer cells exhibit abnormal metabolism and rapid proliferation, which renders them more susceptible to nanoparticle-induced damage (Khorrami et al.,2018; Pucelik et al., 2022) .

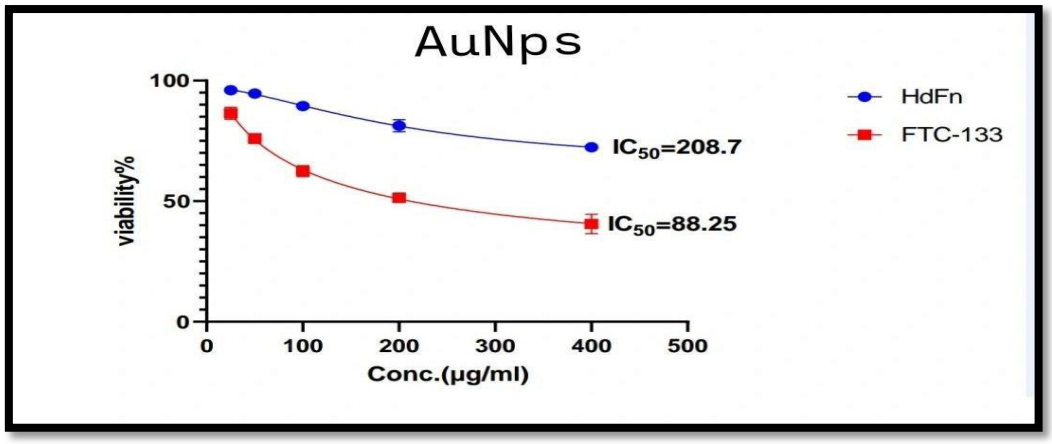

Figure (4.31) Curves IC50 of AuNPs for FTC_133 and HdFn cells

Chapter Five
Conclusion and Recommendations

5.1 Conclusion

1. Riverbank soils provide a rich environment for microorganisms and represent a promising source for discovering microorganisms with unique biological properties.
2. Molecular identification showed that the bacterial isolate belongs to the genus Schaalia; it was registered as a new isolate in the GenBank database and received accession number PV945972.
3. The bacterial strain demonstrated the ability to synthesize a biopolymer and gold nanoparticles.
4. Bacterial products synthesized from the cell-free supernatant of bacterial strain at high concentrations showed a significant inhibitory effect on the growth of antibiotic-resistant Candida fungi.
5. These bacterial products demonstrated the ability to reduce the viability of both cancer cells and normal cells in a concentration-related manner.
6. The cytotoxicity of the bacterial products against cancer cells was higher than that observed against normal cells.
7. This study provides an effective and environmentally friendly approach to synthesizing bacterial products that have demonstrated antifungal and anticancer activities, indicating their potential as safer alternatives to commercial chemical treatments associated with adverse effects on human health.

5.2 Recommendations

1. The exploratory research needs to be extended to riverbank soils since this is an encouraging ecosystem with a large concentration of microorganisms and can be used to identify new microorganisms with distinct biochemical properties.
2. The study suggests that in-depth ecological and taxonomic research of the *Schaalia naturae* is necessary, particularly due to its traditional use as part of the oral cavity of the human and animal body. This research will help in the wider knowledge of its ecological distribution and its presence beyond its host ecosystem.
3. To determine the efficiency of *Schaalia naturae* as a producer of bacterial products and explore the possibility of maximizing production factors, further studies are suggested to enable the exploitation of this microorganism in biotechnological and medical practices.
4. The toxicity of the biopolymer and gold nanoparticles to the red blood cells ought to be assessed.
5. Application of other organisms like fungi, algae, and other related systems is advisable in the production of biopolymers.
6. The anti-tumor activity of the biopolymer and the gold nanoparticles in general should be determined using other types of cancer cell lines, including breast cancer and skin cancer cell lines.

References

References :

Aarti, C., Khusro, A., Agastian, P., Kuppusamy, P., & Al Farraj, D. A. (2022). Synthesis of gold nanoparticles using bacterial cellulase and its role in saccharification and bioethanol production from aquatic weeds. *Journal of King Saud University-Science*, 34(4), 101974.

Abbood, H. K. (2025). Biosynthesis of some nanoparticles from pathogenic bacteria and evaluation their antibacterial and antitumor activities.M.sc thesis . College of Science, University of Misan, Iraq.

Abdalla, A. K., Ayyash, M. M., Olaimat, A. N., Osaili, T. M., Al-Nabulsi, A. A., Shah, N. P., & Holley, R. (2021). Exopolysaccharides as antimicrobial agents: Mechanism and spectrum of activity. *Frontiers in Microbiology*, 12, 664395.

Abd-Elsalam, K. A. (2024). Microbial Nanotechnology. Microorganisms, 12(2), 352.

Abiodun-Solanke, I. M. F., Ajayi, D. M., & Arigbede, A. O. (2014). Nanotechnology and its application in dentistry. *Annals of medical and health sciences research*, *4*(3), 171-177.

Abu Tawila, Z. M., Ismail, S., Dadrasnia, A., and Usman, M. M. (2018). Production and characterization of a bioflocculant produced by Bacillus salmalaya 139SI-7 and its applications in wastewater treatment. *Molecules*, 23(10), 2689.http://dx.doi.org/10.3390/molecules23102689

Acemi, A., Çobanoğlu, Ö., & Türker-Kaya, S. (2019). FTIR-based comparative analysis of glucomannan contents in some tuberous orchids, and effects of

pre-processing on glucomannan measurement. *Journal of the Science of Food and Agriculture*, 99(7), 3681–3686.

Adamczyk, Z., Sadowska, M., & Nattich-Rak, M. (2023). Quantifying nanoparticle layer topography: Theoretical modeling and atomic force microscopy investigations. Langmuir, 39(42), 15067-15077.

Adimule, V. M., Nandi, S. S., Kerur, S. S., Khadapure, S. A., & Chinnam, S. (2022). Recent advances in the one-pot synthesis of coumarin derivatives from different starting materials using nanoparticles: A review**.** *Topics in Catalysis*. Published on January 27, 2022.

Ahmad, M., Gani, A., Hassan, I., Huang, Q., & Shabbir, H. (2020). Production and characterization of starch nanoparticles by mild alkali hydrolysis and ultra-sonication process. Scientific Reports, 10(1), 3533.

Ahmad, T., Wani, I. A., Lone, I. H., Ganguly, A., Manzoor, N., Ahmad, A., … Al-Shihri, A. S. (2013). Antifungal activity of gold nanoparticles prepared by solvothermal method. Materials Research Bulletin, 48(1), 12–20.

Ahmad, T., Wani, I. A., Lone, I. H., Ganguly, A., Manzoor, N., Ahmad, A., ... & Al-Shihri, A. S. (2013). Antifungal activity of gold nanoparticles prepared by solvothermal method. Materials Research Bulletin, 48(1), 12-20.

Ahmed, S., & Ikram, S. (2016). Biosynthesis of gold nanoparticles: a green approach. Journal of Photochemistry and Photobiology B: Biology, 161, 141-153

Ait Assou, S., Anissi, J., Sendide, K., & El Hassouni, M. (2023). Diversity and antimicrobial activities of actinobacteria isolated from mining soils in Midelt Region, Morocco. The Scientific World Journal, 2023(1), 6106673.

Al Jabri, H., Saleem, M. H., Rizwan, M., Hussain, I., Usman, K., & Alsafran, M. (2022). Zinc oxide nanoparticles and their biosynthesis: overview. *Life*, *12*(4), 594.

Al-assdy, H. Q., Al-Tamimi, W. H., & Almansoory, A. F. (2025). Molecular detection of bacteria isolated from polluted environment and screening their ability to produce extracellular biopolymer flocculants. Beni-Suef University Journal of Basic and Applied Sciences, 14(1), 29.

Alawi, A. M. (2023). Biosynthesis of Gold Nanoparticles By Some Endophytic Fungi and Determination Of Their Biological Activities As Anti-Oxidant And Anti-Cancer .M.sc thesis, College of Science, University of Misan, Iraq .

AL-Hasnawi, I. M. (2015). Synthesis and evalution of nanogold bioconjugated with trastuzumab as a drug for human breast cancer cell line. Ph.D thesis, College of Science, AL-Mustansiriyah University, Iraq.

Ali, H. I., & Mutlak, B. H. (2024). Synthesis and Characterization of Gold Nanoparticles and Gold Nanoparticles Loaded with Bromelain. Iraqi Journal of Physics, 22(3), 37-49.

Aljuhani, A., Riyadh, S. M., & Khalil, K. D. (2021). Chitosan/CuO nanocomposite films mediated regioselective synthesis of 1, 3, 4-trisubstituted pyrazoles under microwave irradiation. Journal of Saudi Chemical Society, 25(8), 101276.

Altammar, K. A. (2023). A review on nanoparticles: characteristics, synthesis, applications, and challenges. Frontiers in microbiology, 14, 1155622.

References

Al-Zaidi, M. H. H. (2023). Production and partial purification of biopolymer from Pseudomonas aeruginosa with some medical applications. M.sc thesis, College of Science, University of Basrah,Iraq .

Al-Zaidi, M. H. H., Al-Tamimi, W. H., & Saleh, A. A. (2023). Characterization and antibacterial activity of the natural biopolymer extracted from Pseudomonas aeruginosa. Sci. J. Med. Res., 7(27), 1-8. https://doi.org/10.37623/sjomr.v07i27.01

Amaral, M., Charmier, A. J., Afonso, R. A., Catarino, J., Faísca, P., Carvalho, L., ... & Reis, C. P. (2021). Gold-based nanoplataform for the treatment of anaplastic thyroid carcinoma: A step forward. Cancers, 13(6), 1242.

Amendola, V., Pilot, R., Frasconi, M., Maragò, O. M., & Iatì, M. A. (2017). Surface plasmon resonance in gold nanoparticles: a review. Journal of Physics: Condensed Matter, 29(20), 203002..

Angelin, J., & Kavitha, M. (2020). Exopolysaccharides from probiotic bacteria and their health potential. Int. J. Biol. Macromol., 162, 853–865. Arumugam, G., Muthuselvam, M., de Lima, P. M. N., Rajendran, R., & Junqueira, J. C. (2024). Current perspectives of antifungal therapy: A special focus on Candida auris. Journal of Fungi, 10(6), 408. https://doi.org/10.3390/jof10060408

Ascar, I. F., Al-A'Araji, S. B., & Alshanon, A. F. (2019). Cytotoxicity and antioxidant effect of ginger gold nanoparticles on thyroid carcinoma cells. Journal of Pharmaceutical Sciences and Research, 11(3), 1044-1051.

Asgher, M., Arshad, S., Qamar, S. A., & Khalid, N. (2020). Improved biosurfactant production from Aspergillus niger through chemical mutagenesis:
characterization and RSM optimization. SN Appl. Sci., 2, 1-11.

Asha, A. B., & Narain, R. (2020). Nanomaterials properties. In *Polymer science and nanotechnology* (pp. 343-359). Elsevier.

Asker, A. Y., & Al Haidar, A. H. (2024). Cytotoxic properties of Pelargonium graveolens leaf extract and its green-synthesized gold nanoparticles (in vitro study). Journal of Taibah University Medical Sciences, 19(4), 901-909.

Avram, A. M., Giovanella, L., Greenspan, B., Lawson, S. A., Luster, M., Van Nostrand, D., ... & Vrachimis, A. (2022). SNMMI procedure standard/EANM practice guideline for nuclear medicine evaluation and therapy of differentiated thyroid cancer: abbreviated version. Journal of nuclear medicine, 63(6), 15N-35N.

BacDive — The Bacterial Diversity Metadatabase. (2018). Schaalia naturae BL-79 (Type strain / BacDive ID: 195). DSMZ / BacDive. Retrieved October 9, 2025, from https://bacdive.dsmz.de/strain/195

Baidurah, S. (2022). Methods of analyses for biodegradable polymers: a review. Polymers, 14(22), 4928.

Balagurunathan, R., Radhakrishnan, M., Babu Rajendran, R., & Velmurugan, D. (2011). Biosynthesis of gold nanoparticles by actinomycete Streptomyces viridogens strain HM10. Indian Journal of Biochemistry and Biophysics, 48(5), 331.

Baranwal, J., Barse, B., Fais, A., Delogu, G. L., & Kumar, A. (2022). Biopolymer: A sustainable material for food and medical applications. *Polymers*, *14*(5), 983.

Ben-Ami, R., & Kontoyiannis, D. P. (2021). Resistance to antifungal drugs. Infectious Disease Clinics, 35(2), 279-311.

Berkow, E. L., Lockhart, S. R., & Ostrosky-Zeichner, L. (2020). Antifungal susceptibility testing: Current approaches. Clinical Microbiology Reviews, 33(3), e00069-19. https://doi.org/10.1128/CMR.00069-19

Bharadwaj, K. K., Rabha, B., Pati, S., Sarkar, T., Choudhury, B. K., Barman, A., ... & Mohd Noor, N. H. (2021). Green synthesis of gold nanoparticles using plant extracts as beneficial prospect for cancer theranostics. Molecules, 26(21), 6389.

Bhatia, S. K. (2023). Microbial Biopolymers: Trends in Synthesis, Modification, and Applications. Polymers, 15(6), 1364.

Bhatia, S. K. (2023). Microbial biopolymers: trends in synthesis, modification, and applications. Polymers, 15(6), 1364.

Bhattacharjee, S. (2016). DLS and zeta potential–what they are and what they are not?. Journal of controlled release, 235, 337-351.

Bhatti, A. A., Haq, S., & Bhat, R. A. (2017). Actinomycetes benefaction role in soil and plant health. Microbial pathogenesis, 111, 458-467.

Bibi, Y., Nasreen, Z., Gul, H., Assad, N., Khan, M. N., Kifle, D., ... & Ercişli, S. (2026). Phytosynthesis of gold nanoparticles from Boerhavia diffusa L. and

their antibacterial, antifungal, antioxidant, and anticancer activities. Discover Nano, 21(1), 7.

Bîrleanu, C., Pustan, M., Șerdean, F., & Merie, V. (2021). AFM nanotribomechanical characterization of thin films for MEMS applications. Micromachines, 13(1), 23.

Bitew, A., Molalign, T., & Chanie, M. (2017). Species distribution and antibiotic susceptibility profile of bacterial uropathogens among patients complaining urinary tract infections. BMC infectious diseases, 17(1), 654.

Blanco, I., & Siracusa, V. (2021). The use of thermal techniques in the characterization of bio-sourced polymers. Materials, 14(7), 1686.

Boholm, M. (2016). The use and meaning of nano in American English: Towards a systematic description. Ampersand, 3, 163-173.

Budiman, A., Ivana, H., Huang, K. A., Huang, S. A., Nadhira, M. S., Rusdin, A., & Aulifa, D. L. (2025). Biocompatible natural polymer-based amorphous solid dispersion system improving drug physicochemical properties, stability, and efficacy. Polymers, 17(15), 2059.

Calderón-Jiménez, B., Sarmanho, G. F., Murphy, K. E., Bustos, A. R. M., & Vega-Baudrit, J. R. (2017). NanoUV-VIS: an interactive visualization tool for monitoring the evolution of optical properties of nanoparticles throughout synthesis reactions. Journal of Research of the National Institute of Standards and Technology, 122, 1.

Capes-Davis, A., & Freshney, R. I. (2021). Freshney's culture of animal cells: A manual of basic technique and specialized applications (8th ed.). John Wiley & Sons.

Carmo, P. H. F., Costa, M. F. S. F. D., Lage, A. C. P., Terra Garcia, M., & Junqueira, J. C. (2025). Gold nanorods non-functionalised and associated with gallic acid exhibit activity against non-albicans Candida species. Biofouling, 41(5), 523-535.

Casillo, A., D'Angelo, C., Parrilli, E., Tutino, M. L., & Corsaro, M. M. (2022). Membrane and extracellular matrix glycopolymers of Colwellia psychrerythraea 34H: Structural changes at different growth temperatures. Front. Microbiol., 13, 820714. https://doi.org/10.3389/fmicb.2022.820714

Centers for Disease Control and Prevention (CDC). (2008). Etymologia: Candida. Emerging Infectious Diseases, 14(2), 326. https://doi.org/10.3201/eid1402.ET1402

Chandwad, C., Chandwad, S., & Gutte, S. (2020). Isolation of actinomycetes from rhizosphere soil: a complete approach. Plant Cell Biotechnology and Molecular Biology, 21(65-66), 144-149.

Cheng, C., Nie, S., Li, S., Peng, H., Yang, H., Ma, L., & Zhao, C. (2013). Biopolymer functionalized reduced graphene oxide with enhanced biocompatibility via mussel inspired coatings/anchors. Mater. Chem. Phys B, 1(3), 265-275

Ciurea, C. N., Kosovski, I. B., Mare, A. D., Toma, F., Pintea-Simon, I. A., & Man, A. (2020). Candida and candidiasis opportunism versus pathogenicity: a review of the virulence traits. Microorganisms, 8(6), 857.

Clerici, T., Kolb, W., Beutner, U., Bareck, E., Dotzenrath, C., Kull, C., & Niederle, B. (2010). Diagnosis and treatment of small follicular thyroid carcinomas. Journal of British Surgery, 97(6), 839-844.

Corazzari, V., Nisticò, R., Turci, F., Zanetti, M., Faga, M. G., & Gorrasi, G. (2015). Advanced physico-chemical characterization of chitosan by means of TGA coupled on-line with FTIR and GCMS: Thermal degradation and water adsorption capacity. Polymer Degradation and Stability, 112, 1–9.

De Moraes, D. C., & Ferreira-Pereira, A. (2024). Multidrug-Resistant Fungi. Journal of Fungi, 10(10), 686.

De Sousa Victor, R., Marcelo da Cunha Santos, A., Viana de Sousa, B., de Araújo Neves, G., Navarro de Lima Santana, L., & Rodrigues Menezes, R. (2020). A review on Chitosan's uses as biomaterial: Tissue engineering, drug delivery systems and cancer treatment. Materials, 13(21), 4995.

Derdak, R., Sakoui, S., Pop, O. L., Vodnar, D. C., Addoum, B., Elmakssoudi, A., … El Khalfi, B. (2022). Screening, optimization and characterization of exopolysaccharides produced by novel strains isolated from Moroccan raw donkey milk. Food Chemistry: X, 14, Article 100305. https://doi.org/10.1016/j.fochx.2022.100305

Devillanova, F. A., & Du Mont, W.-W. (2013). Handbook of chalcogen chemistry: new perspectives in sulfur, selenium and tellurium (Vol. 1). Royal Society of Chemistry.

Devillanova, F. A., & DuMont, W.-W. (2013). Handbook of chalcogen chemistry: New perspectives in sulfur, selenium, and tellurium (Vol. 1). Royal Society of Chemistry.

Ding, L., Zhou, J., Li, Q., Tang, J., & Chen, X. (2021). Effects of land-use type and flooding on the soil microbial community and functional genes in reservoir riparian zones. Microbial ecology, 83(2), 393-407.

Dlamini, N. G., Basson, A. K., and Pullabhotla, R. V. (2020). Wastewater treatment by a polymeric bioflocculant and iron nanoparticles synthesized from a bioflocculant. Polymers, 12(7), 1618.https://doi.org/10.3390/polym12071618

DuBois, M., Gilles, K. A., Hamilton, J. K., Rebers, P. T., & Smith, F. (1956). Colorimetric method for determination of sugars and related substances. Anal.
Chem., 28(3), 350–356. https://doi.org/10.1021/ac60111a017

Ebewele, R. O. (2000). Polymer science and technology. CRC press.

Etman, S. M., Elnaggar, Y. S., & Abdallah, O. Y. (2020). Fucoidan, a natural biopolymer in cancer combating: From edible algae to nanocarrier tailoring. International journal of biological macromolecules, 147, 799-808.

Etxabide, A., Kilmartin, P. A., Guerrero, P., de la Caba, K., Hooks, D. O., West, M., & Singh, T. (2022). Polyhydroxybutyrate (PHB) produced from red grape pomace: Effect of purification processes on structural, thermal and antioxidant properties. International Journal of Biological Macromolecules, 217, 449-456.

Eugenio, P. J. G., De Guzman, A. J., Sanidad, E. L., Asuncion, S. C., Dela Cruz, R. G., Patricio, P. B., ... & Monserate, J. J. (2024). Green synthesis of gold nanoparticles using aqueous extract of Allium tuberosum leaves. Journal of Biomimetics, Biomaterials and Biomedical Engineering, 64, 1-10.

Farda, B., Djebaili, R., Vaccarelli, I., Del Gallo, M., & Pellegrini, M. (2022). Actinomycetes from caves: an overview of their diversity, biotechnological

properties, and insights for their use in soil environments. Microorganisms, 10(2), 453.

Farrar, W. E., & Reboli, A. C. (2006). The genus Bacillus—medical. In Theyotes (pp. 609–630). Springer, New York, NY.

Feldman, D. (2008). Polymer history. Designed Monomers and Polymers, 11(1), 1–15. https://doi.org/10.1163/156855508X293853

Ferreira, A. C., Bomfim, M. R. Q., da Costa Sobrinho, C. H. D. B., Boaz, D. T. L., Da Silva Lira, R., Fontes, V. C., ... & Penha, R. S. (2022). Characterization, antimicrobial and cytotoxic activity of polymer blends based on chitosan and fish collagen. AMB Express, 12(1), 102.

Ferreira, A. R., Alves, V. D., and Coelhoso, I. M. (2016). Polysaccharide-based membranes in food packaging applications. Membranes, 6(2), 22.

Florance, I., Cordani, M., Pashootan, P., Moosavi, M. A., Zarrabi, A., & Chandrasekaran, N. (2024). The impact of nanomaterials on autophagy across health and disease conditions. Cellular and Molecular Life Sciences, 81(1), 184.

Fouda, A., Hassan, S. E., Eid, A. M., Awad, M. A., Althumayri, K., Badr, N. F., and Hamza, M. F. (2022). Endophytic bacterial strain, Brevibacillus brevis - mediated green synthesis of copper oxide nanoparticles, characterization, antifungal, in vitro cytotoxicity, and larvicidal activity. Green Processing and Synthesis, 11(1), 931–950.

Gahlawat, G., & Choudhury, A. R. (2019). A review on the biosynthesis of metal and metal salt nanoparticles by microbes. *RSC advances*, *9*(23), 12944-12967.

Gao, Q., Zhu, X. H., Mu, J., Zhang, Y., and Dong, X. W. (2009). Using Ruditapes philippinarum conglutination mud to produce bioflocculant and its applications in wastewater treatment. Bioresource Technology, 100(21), 4996-5001. https://doi.org/10.1016/j.biortech.2009.05.035.

Gathuru, E. M. (2017). Methods of isolating actinomycetes from the soils of Menengai crater in Kenya. Arch Clin Microbiol, 8(3), 45.

Geitel, K., Koschella, A., Lenges, C., & Heinze, T. (2020). Meltable fatty acid esters of α-1, 3-glucan as potential thermoplastics. Advanced Industrial and Engineering Polymer Research, 3(3), 111-119.

Ghirmai, S., Krona, A., Wu, H., Whalin, J., Axelsson, M., and Undeland, I. (2024). Relationship between hemolysis and lipid oxidation in red blood cell-spiked fish muscle; dependance on pH and blood plasma. Scientific Reports, 14(1), 1943

Gholami-Shabani, M., Sotoodehnejadnematalahi, F., Shams-Ghahfarokhi, M., Eslamifar, A., & Razzaghi-Abyaneh, M. (2022). Physicochemical properties, anticancer and antimicrobial activities of metallic nanoparticles green synthesized by Aspergillus kambarensis. IET Nanobiotechnology, 16(1), 1–13.

Ghosh, S., Lahiri, D., Nag, M., Dey, A., Sarkar, T., Pathak, S. K., ... & Ray, R. R. (2021). Bacterial biopolymer: Its role in pathogenesis to effective biomaterials. Polymers, 13(8), 1242.

Giri, S. S., Harshiny, M., Sen, S. S., Sukumaran, V., & Park, S. C. (2015). Production and characterization of a thermostable bioflocculant from

Bacillus subtilis F9, isolated from wastewater sludge. Ecotoxicology and environmental safety, 121, 45-50.

Gola, A., Knysak, T., Mucha, I., & Musiał, W. (2023). Synthesis, Thermogravimetric Analysis, and Kinetic Study of Poly-N-Isopropylacrylamide with Varied Initiator Content. Polymers 2023, 15, 2427.

Goldstein, J. I., Newbury, D. E., Michael, J. R., Ritchie, N. W. M., Scott, J. H. J., & Joy, D. C. (2017). Scanning electron microscopy and X-ray microanalysis (4th ed.). Springer, New York, NY.

Gomes, R. F., García, G. J. Y., Dutra, J. d. C. F., Cardoso, M. S., Costa, E. A., de Abreu Waldow, V., … Góes-Neto, A. (2023). Metabolically active microbial communities in oil fields: A systematic review and synthesis of RNA preservation, extraction, and sequencing methods. Applied Microbiology, 3(4), 1144–1163.

Gómez-Gaviria, M., & Mora-Montes, H. M. (2020). Current aspects in the biology, pathogeny, and treatment of Candida krusei, a neglected fungal pathogen. Infection and Drug Resistance, 13, 1673-1689. https://doi.org/10.2147/IDR.S247944

Gong, X. C., Wang, S. S., & Qu, H. B. (2011). Solid-liquid equilibria of D-glucose, D-fructose, ethanol, and water from 273.2 K to 293.2 K. Chinese Journal of Chemical Engineering, 19(2), 217–222.

Gorohovs, M., & Dekhtyar, Y. (2025). Surface functionalization of nanoparticles for enhanced electrostatic adsorption of biomolecules. Molecules, 30(15), 3206.

Gow, N. A., & Yadav, B. (2017). Microbe Profile: Candida albicans: a shape-changing, opportunistic pathogenic fungus of humans. Microbiology, 163(8), 1145-1147.

Guerra, J. D., Mariscal-Nava, D., Avalos-Borja, M., & Sandoval, G. (2025). Screening Method for the Selection of Oleaginous Yeast-Producing Gold Nanoparticles. International Journal of Molecular Sciences, 26(15), 7534.

Gulwani, D., Upadhyay, P., Goel, R., Sarangthem, V., & Singh, T. D. (2024). Nanomedicine mediated thyroid cancer diagnosis and treatment: an approach from generalized to personalized medicine. Discover Oncology, 15(1), 789.

Gupta, S., & Tripathi, M. (2012). A review on the synthesis of TiO2 nanoparticles by solution route. *Open Chemistry*, *10*(2), 279-294.

Hamed, M. M., & S Abdelftah, L. (2019). Biosynthesis of gold nanoparticles using marine Streptomyces griseus isolate (M8) and evaluating its antimicrobial and anticancer activity. Egyptian journal of aquatic biology and fisheries, 23(1), 173-184.

Hamel, A. H. (2025). Study the ability of some bacteria isolates to synthesize of Silver Nanoparticles and the Production of Exopolysaccharides to improve the growth of Maize (Zea mays L.) and Tomato (Solanum lycopersicum L.). Ph.D thesis,College of Education for Pure Sciences, University of Basrah, Iraq.

Hammami, I., & Alabdallah, N. M. (2021). Gold nanoparticles: Synthesis properties and applications. Journal of king Saud university-science, 33(7), 101560.

Hasan, M. N., Shahriar, S. M. S., Rabbi, S. L., & Jahan, D. (2018). Nanoparticles and their utilization in cancer detection and treatment. Scholars Journal of Applied Sciences Research, 1, 65–75.

Hassan, N. A., Darwesh, O. M., Smuda, S. S., Altemimi, A. B., Hu, A., Cacciola, F., ... & Abedelmaksoud, T. G. (2022). Recent trends in the preparation of nano-starch particles. Molecules, 27(17), 5497.

Hassanein, T. F., Mohammed, A. S., Mohamed, W., Sobh, R. A., & Zahran, M. K. (2021). Optimized synthesis of biopolymer-based zinc oxide Nanoparticles and evaluation of their antibacterial activity. Egyptian Journal of Chemistry, 64(7), 3767-3790.

He, S., Guo, Z., Zhang, Y., Zhang, S., Wang, J., & Gu, N. (2007). Biosynthesis of gold nanoparticles using the bacteria *Rhodopseudomonas capsulata*. *Materials Letters, 61*(18), 3984–3987.

Hong, S., Kim, S. K., Chung, C. H., Yun, C. H., Lee, J., Cho, C. S., & Huh, W. K. (2024). Pullulan nanoparticles inhibit the pathogenicity of Candida albicans by regulating hypha-related gene expression. Microbiology Spectrum, 12(12), e01048-24.

Hsieh, D. S., Lu, H. C., Chen, C. C., Wu, C. J., & Yeh, M. K. (2012). The preparation and characterization of gold-conjugated polyphenol nanoparticles as a novel delivery system. International journal of nanomedicine, 1623-1633.

Hu, Z., Yang, B., Li, T., & Li, J. (2018). Thyroid Cancer Detection by Ultrasound Molecular Imaging with SHP2-Targeted Perfluorocarbon Nanoparticles. Contrast Media & Molecular Imaging, 2018(1), 8710862.

Hussain, I., Singh, N. B., Singh, A., Singh, H., & Singh, S. C. (2016). Green synthesis of nanoparticles and its potential application. Biotechnology letters, 38, 545-560.

Hussein, S. I. (2016). Study the effect of gold nanoparticles on cancer and normal cells (in vitro study). Iraqi Journal of Cancer and Medical Genetics, 9(2).

Husseiny, M. I., Abd El-Aziz, M., Badr, Y., & Mahmoud, M. A. (2007). Biosynthesis of gold nanoparticles using Pseudomonas aeruginosa. Spectrochimica Acta Part A: Molecular and Biomolecular Spectroscopy, 67(3–4), 1003–1006.

Ibrahim, M. I., Ibrahim, H. A., Haga, T., Ishida, A., Nehira, T., Matsuo, K., & Gad, A. M. (2024). Potential bioactivities, chemical composition, and conformation studies of exopolysaccharide-derived Aspergillus sp. strain GAD7. Journal of Fungi, 10(9), 659.

Imre, B., & Pukánszky, B. (2013). Compatibilization in bio-based and biodegradable polymer blends. Journal of Polymer Research, 20(6), 1215–1233.

Iravani, S., & Zolfaghari, B. (2022). Plant viruses and bacteriophages for eco-friendly synthesis of nanoparticles: recent trends and important challenges. *Comments on Inorganic Chemistry*, 42(4), 226-248.

Jadoun, S., Arif, R., Jangid, N. K., & Meena, R. K. (2021). Green synthesis of nanoparticles using plant extracts: A review. *Environmental Chemistry Letters*, *19*(1), 355-374.

Janda, J. M., & Abbott, S. L. (2007). 16S rRNA gene sequencing for bacterial identification in the diagnostic laboratory: pluses, perils, and pitfalls. Journal of clinical microbiology, 45(9), 2761-2764.

Jang, G. G., Jacobs, C. B., Gresback, R. G., Ivanov, I. N., Meyer III, H. M., Kidder, M., ... & Moon, J. W. (2015). Size tunable elemental copper nanoparticles: extracellular synthesis by thermoanaerobic bacteria and capping molecules. Journal of Materials Chemistry C, 3(3), 644-650.

Jangong, O. S., Gareso, P. L., Mutmainna, I., & Tahir, D. (2019). Fabrication and characterization of starch/chitosan reinforced polypropylene as biodegradable. Journal of Physics: Conference Series, 1341, 082022. https://doi.org/10.1088/1742-6596/1341/8/082022

Jayawardena, H. S. N., Liyanage, S. H., Rathnayake, K., Patel, U., & Yan, M. (2021). Analytical methods for characterization of nanomaterial surfaces. Analytical chemistry, 93(4), 1889-1911.

Jeong, H., Hwang, J., Lee, H., Hammond, P. T., Choi, J., & Hong, J. (2017b). In vitro blood cell viability profiling of polymers used in molecular assembly. Scientific Reports, 7(1), 9481.

Jimenez-Sandoval, R., Pedireddy, S., Katuri, K. P., & Saikaly, P. E. (2023). Facile biological-based synthesis of size-controlled palladium nanoclusters anchored on the surface of Geobacter sulfurreducens and their application in electrocatalysis. ACS Sustainable Chemistry & Engineering, 11(3), 1100–1109. https://doi.org/10.1021/acssuschemeng.2c07082

Jurášková, D., Ribeiro, S. C., & Silva, C. C. G. (2022). Exopolysaccharides produced by lactic acid bacteria: From biosynthesis to healthpromoting properties. Foods, 11(2), 156. https://doi.org/10.3390/foods11020156

Kadariswantiningsih, I. N., Empitu, M. A., Santosa, T. I., & Alimu, Y. (2025). Antifungal resistance: Emerging mechanisms and implications. Molecular medicine reports, 32(3), 247.

Kalina, M., Michalicová, P., Sedláček, P., Kratochvíl, Z., Smílek, J., Klučáková, M., & Pekář, M. (2015, October 14–16). Research on stability of biopolymers by means of light scattering techniques. In Proceedings of NANOCON 2015 Conference. Brno, Czech Republic

Karczewska-Golec, J., Sadowska, K., Golec, P., Karczewski, J., & Węgrzyn, G. (2024). Engineered M13-Derived Bacteriophages Capable of Gold Nanoparticle Synthesis and Nanogold Manipulations. *International Journal of Molecular Sciences*, *25*(20), 11222.

Kareem, H. A., Samaka, H. M., & Abdulridha, W. A. M. (2021). Evaluation of the effect of the gold nanoparticles prepared by green chemistry on the treatment of cutaneous candidiasis. Current Medical Mycology, 7(1), 1.

Kaur, N., & Dey, P. (2023). Bacterial exopolysaccharides as emerging bioactive macromolecules: from fundamentals to applications. Res. Microbiol., 174(4), 104024. https://doi.org/10.1016/j.resmic.2022.104024

Kavitake, D., Veerabhadrappa, B., Sudharshan, S. J., Kandasamy, S., Devi, P. B., Dyavaiah, M., & Shetty, P. H. (2022). Oxidative stress alleviating

potential of galactan exopolysaccharide from Weissella confusa KR780676 in yeast model system. Scientific Reports, 12(1), 1089.

Kaya, D. (2011). Polymerase Chain Reaction (PCR) Technique in Detection of Actinomyces SPP by Using Cervico-Vaginal Fluid Samples. Gynecology Obstetrics & Reproductive Medicine, 17(2), 98-102.

Kelsall, R. W., Hamley, I. W., & Geoghegan, M. (2005). Nanoscale science and technology (1st ed.). John Wiley & Sons, Ltd, Chichester, UK.

Khalaf, M. S., Hassan, M. A. M., & Mohammed, A. H. (2023). Exploring the role of phytochemicals: Effect of [6]-gingerol combined with colloidal gold nanoparticles on thyroid carcinoma cells. Nano Biomedicine and Engineering. https://doi.org/10.26599/nbe

Khan, S., Gul, A., Jehan, S., Khan, Z., Saeed, J., Shirazi, R. R., ... & Ullah, H. (2023). Biodiversity of actinomycetes and their secondary metabolites: a comprehensive review. Journal of advanced Biomedical and Pharmaceutical Sciences, 6(1), 36-48.

Khorrami, S., Zarrabi, A., Khaleghi, M., Danaei, M., & Mozafari, M. (2018). Selective cytotoxicity of green synthesized silver nanoparticles against the MCF-7 tumor cell line and their enhanced antioxidant and antimicrobial properties. International Journal of Nanomedicine, 13, 8013–8024. https://doi.org/10.2147/IJN.S178378

Koch, T., Fathi, A., & Addo, M. M. (2021). The COVID-19 vaccine landscape. Coronavirus Disease-COVID-19, 549-573.

Krohn, S., Zeller, K., Böhm, S., Chatzinotas, A., Harms, H., Hartmann, J., ... & Engelmann, C. (2018). Molecular quantification and differentiation of

Candida species in biological specimens of patients with liver cirrhosis. PloS one, 13(6), e0197319.

Krpetic, Z., Scari, G., Caneva, E., Speranza, G., & Porta, F. (2009). Gold nanoparticles prepared using cape aloe active components. Langmuir, 25(13), 7217-7221.

Ku Y, Jansen O, Oles CJ, Lazar EZ, Rader JI. Precipitation of inulins and oligoglucoses by ethanol and other solvents. Food Chem. 2003;81(1):125–32.

Kumar, B., Smita, K., Cumbal, L., & Debut, A. (2017). Green synthesis of silver nanoparticles using Andean blackberry fruit extract. Saudi J. Biol. Sci., 24(1), 45–50.

Kumari, J., Kumawat, R., Prasanna, R., Jothieswari, D., Debnath, R., Ikbal, A. M. A., … Tiwari, O. N. (2025). Microbial exopolysaccharides: Classification, biosynthetic pathway, industrial extraction and commercial production to unveil its bioprospection: A comprehensive review. International Journal of Biological Macromolecules, 297, 139917. https://doi.org/10.1016/j.ijbiomac.2025.139917

Kwon, H. J., Shin, K., Soh, M., Chang, H., Kim, J., Lee, J., ... & Hyeon, T. (2018). Large-scale synthesis and medical applications of uniform-sized metal oxide nanoparticles. Advanced Materials, 30(42), 1704290.

Lavaee, F., Ranjbar, Z., Modaresi, F., & Keshavarz, F. (2021). The effect of gold nano particles with different sizes on Streptococcus species. Journal of Dentistry, 22(4), 235.

Lee, J., & Hwang, B. H. (2022). Evaluation of the effects, causes, and risks of gold nanorods promoting cell proliferation. Biotechnology and Bioprocess Engineering, 27(2), 213-220.

Lee, P. Y., Costumbrado, J., Hsu, C. Y., & Kim, Y. H. (2012). Agarose gel electrophoresis for the separation of DNA fragments. Journal of Visualized Experiments, 62, e3923. https://doi.org/10.3791/3923

Li, Y. M., Wang, Y. Y., & Cheng, B. N. (2017). In-vitro cytotoxicity of biosynthesized gold nanoparticles against thyroid cancer cell lines. Tropical Journal of Pharmaceutical Research, 16(7), 1523-1528.

Li, Y., Zhang, Z., Shen, J., & Ye, M. (2015). Hierarchical nanospheres based on Pd nanoparticles dispersed on carbon coated magnetite cores with a mesoporous ceria shell: a highly integrated multifunctional catalyst. *Dalton Transactions*, *44*(37), 16592-16601.

Liu, S. W., Jadambaa, N., Nikandrova, A. A., Osterman, I. A., & Sun, C. H. (2022). Exploring the diversity and antibacterial potentiality of cultivable actinobacteria from the soil of the saxaul forest in southern Gobi desert in Mongolia. Microorganisms, 10(5), 989.

Liu, Y., Chen, J., Cheng, Y., Li, Y., Li, X., Zhang, Z., … Li, Z. (2022). A simple and rapid technique of template preparation for PCR. Frontiers in Microbiology. https://doi.org/10.3389/fmicb.2022.1024827

Liyaskina, E. V., Rakova, N. A., Kitykina, A. A., Rusyaeva, V. V., Toukach, P. V., Fomenkov, A. A., … Revin, V. V. (2021). Production and characterization of the exopolysaccharide from strain Paenibacillus

polymyxa 2020. PLoS ONE, 16(7), e0253482. https://doi.org/10.1371/journal.pone.0253482

Loeve, S. (2010). About a definition of nano: how to articulate nano and technology. HYLE–International Journal for Philosophy of Chemistry, 16(1), 3-18.

Loganathan, S., Valapa, R. B., Mishra, R. K., Pugazhenthi, G., & Thomas, S. (2017). Thermogravimetric analysis for characterization of nanomaterials. In Thermal and rheological measurement techniques for nanomaterials characterization (pp. 67-108). Elsevier.

Lotfali, E., Toreyhi, H., Sharabiani, K. M., Fattahi, A., Soheili, A., Ghasemi, R., ... & Iranpanah, S. (2021). Comparison of antifungal properties of gold, silver, and selenium nanoparticles against amphotericin B-resistant Candida glabrata clinical isolates. Avicenna journal of medical biotechnology, 13(1), 47.

Madkour, L. H. (2019). Introduction to nanotechnology (NT) and nanomaterials (NMs). In Nanoelectronic materials: fundamentals and applications (pp. 1-47). Cham: Springer International Publishing.

Mahmoud, A. A., Osman, O., Eid, K., Al Ashkar, E., Okasha, A., Atta, D., … Fakhry, A. (2014). FTIR spectroscopy of natural biopolymers blends. Middle East Journal of Applied Sciences, 4(4), 816–824.

Mahmoud, N. N., Hammad, A. S., Al Kaabi, A. S., Alawi, H. H., Khatoon, S., & Al-Asmakh, M. (2024). Evaluating the Effects of BSA-Coated Gold Nanorods on Cell Migration Potential and Inflammatory Mediators in

Human Dermal Fibroblasts. Journal of Functional Biomaterials, 15(10), 284.

Majem, B., Li, F., Sun, J., & Wong, D. T. (2016). RNA sequencing analysis of salivary extracellular RNA. In Oral Biology: Molecular Techniques and Applications (pp. 17–36). New York, NY: Springer New York.

Maji, B. (2019). Introduction to natural polysaccharides. In Functional Polysaccharides for Biomedical Applications (pp. 1–31). Elsevier: Amsterdam, the Netherlands.

Makary, M. A., Kaczmarski, K., & Nachman, K. (2018). A call for doctors to recommend antibiotic-free foods: Agricultural antibiotics and the public health crisis of antimicrobial resistance. The Journal of Antibiotics, 71(8), 685–687.

Manzoor, S., Bashir, D. J., Imtiyaz, K., Rizvi, M. M. A., Ahamad, I., Fatma, T., ... & Samim, M. (2021). Biofabricated platinum nanoparticles: therapeutic evaluation as a potential nanodrug against breast cancer cells and drug-resistant bacteria. RSC advances, 11(40), 24900-24916.

Matsubara, V. H., Wang, Y., Bandara, H. M. H. N., Mayer, M. P. A., & Samaranayake, L. P. (2016). Probiotic lactobacilli inhibit early stages of Candida albicans biofilm development by reducing their growth, cell adhesion, and filamentation. Appl. Microbiol. Biotechnol. 100, 6415-6426.

Mawazi, S. M., Kumar, M., Ahmad, N., Ge, Y., & Mahmood, S. (2024). Recent applications of chitosan and its derivatives in antibacterial, anticancer, wound healing, and tissue engineering fields. Polymers, 16(10), 1351.

Mazuki, N. F., Saadiah, M. A., Fuzlin, A. F., Khan, N. M., & Samsudin, A. S. (2023). Basic aspects and properties of biopolymers. In S. Gopi, P. Balakrishnan, & M. Bračič (Eds.), Biopolymers in nutraceuticals and functional foods (Polymer Chemistry Series No. 36). Cambridge, UK: Royal Society of Chemistry.

McHugh, J. (1988). Concentration of gold in natural waters. Journal of Geochemical Exploration, 30(1-3), 85-94.

Merck. (2020). IR spectrum table and chart. URL: https://www. Sigma-Aldrich. com/technicaldocuments/articles/biology/ir-spectrum-table. html.

Meredith, T. A., & Ulrich, J. N. (2013). Infectious endophthalmitis. In Retina (pp. 2019-2039). WB Saunders.

Moghannem, S. A. M., Farag, M. M. S., Shehab, A. M., & Azab, M. S. (2018). Exopolysaccharide production from Bacillus velezensis KY471306 using statistical experimental design. Braz. J. Microbiol, 49(3), 452–462.

Mohamed, S. S., Amer, S. K., Selim, M. S., & Rifaat, H. M. (2018). Characterization and applications of exopolysaccharide produced by marine Bacillus altitudinis MSH2014 from Ras Mohamed, Sinai, Egypt. Egypt. J. Basic Appl. Sci, 5(3), 204-209.

Mohammadi, F. M., & Ghasemi, N. (2018). Influence of temperature and concentration on biosynthesis and characterization of zinc oxide nanoparticles using cherry extract. *Journal of Nanostructure in Chemistry*, *8*, 93-102.

Mohanraj, V. J., & Chen, Y. J. (2006). Nanoparticles-a review. Tropical journal of pharmaceutical research, 5(1), 561-573.

Mohsin, G. F., Al-Kaabi, W. J., & Alzubaidi, A. K. (2022). Describing Polymers Synthesized from Reducing Sugars and Ammonia Employing FTIR Spectroscopy. Baghdad Science Journal, 19(6), 18.

Muangsawat, S., Chaiyosang, P., Sinkanarak, P., Sukted, J., Thanyasrisung, P., & Matangkasombut, O. (2024). Effects of efflux pumps on antifungal activity of chitosan against Candida albicans. Journal of Oral Microbiology, 16(1), 2357976.

Muddapur, U. M., Alshehri, S., Ghoneim, M. M., Mahnashi, M. H., Alshahrani, M. A., Khan, A. A., ... & Ahmad, M. Z. (2022). Plant-Based Synthesis of Gold Nanoparticles and Theranostic Applications: A Review. Molecules, 27(4), 1391.

Muteeb, G., Rehman, M. T., Shahwan, M., & Aatif, M. (2023). Origin of antibiotics and antibiotic resistance, and their impacts on drug development: A narrative review. Pharmaceuticals, 16(11), 1615.

Németh, Z., Csóka, I., Semnani Jazani, R., Sipos, B., Haspel, H., Kozma, G., ... & Dobó, D. G. (2022). Quality by design-driven zeta potential optimisation study of liposomes with charge imparting membrane additives. Pharmaceutics, 14(9), 1798.

Nguyen, H. C., Ngo, K. N., Tran, H. K., & Barrow, C. J. (2024). Enzyme-assisted coextraction of phenolics and polysaccharides from Padina gymnospora. Marine Drugs, 22(1), 42.

Nguyen, H. T., Pham, T. T., Nguyen, P. T., Le-Buanec, H., Rabetafika, H. N., & Razafindralambo, H. L. (2024). Advances in microbial exopolysaccharides: present and future applications. Biomolecules, 14(9), 1162.

Nikolić, V. D., Ilić, D. P., Nikolić, L. B., Stanojević, L. P., Cakić, M. D., Tačić, A. D., & Ilić-Stojanović, S. S. (2014). The synthesis and characterization of iron (II): Gluconate. Savremene tehnologije, 3(2), 16-24.

Nilubol, N., Yuan, Z., Paciotti, G. F., Tamarkin, L., Sanchez, C., Gaskins, K., ... & Kebebew, E. (2018). Novel dual-action targeted nanomedicine in mice with metastatic thyroid cancer and pancreatic neuroendocrine tumors. JNCI: Journal of the National Cancer Institute, 110(9), 1019-1029.

Nisha, S., Sachan, R. S. K., Singh, A., Karnwal, A., Shidiki, A., & Kumar, G. (2024). Plant-mediated gold nanoparticles in cancer therapy: Exploring anti-cancer mechanisms, drug delivery applications, and future prospects. Frontiers in Nanotechnology, 6, 1490980

Nouioui, I., Carro, L., García-López, M., Meier-Kolthoff, J. P., Woyke, T., Kyrpides, N. C., … & Göker, M. (2018). Genome-based taxonomic classification of the phylum Actinobacteria. Frontiers in Microbiology, 9, 355158**.**

Obeid, H. Q. (2025). Using Fe2O3 nanoparticles and bioflocculant produced by environmental bacteria for industrial wastewater treatment .Ph.D thesis, College of Science, University of Basrah, Iraq.

Ono, L. K., & Roldan Cuenya, B. (2008). Formation and thermal stability of Au2O3 on gold nanoparticles: size and support effects. The Journal of Physical Chemistry C, 112(12), 4676-4686.

Osemwegie, O. O., Adetunji, C. O., Ayeni, E. A., Adejobi, O. I., Arise, R. O., Nwonuma, C. O., & Oghenekaro, A. O. (2020). Exopolysaccharides from bacteria and fungi: current status and perspectives in Africa. Heliyon, 6(6).

Oztekin, S., Dikmetas, D. N., & Karbancıoglu Guler, F. (2025). A novel exopolysaccharide from cold adapted yeast Rhodotorula glutinis, along with structural, rheological, antioxidant, and antibiofilm properties. Biomass Conv. Biorefinery, 15, 1507–1523. https://doi.org/10.1007/s13399-023-05208-3

Pal, S. L., Jana, U., Manna, P. K., Mohanta, G. P., & Manavalan, R. (2011). Nanoparticle: An overview of preparation and characterization. Journal of Applied Pharmaceutical Science, 1, 228–234.

Park, S. B., Lih, E., Park, K. S., Joung, Y. K., & Han, D. K. (2017). Biopolymer-based functional composites for medical applications. Progrin Poly Scie, 68, 77-105.

Parveen, K., Banse, V., & Ledwani, L. (2016, April). Green synthesis of nanoparticles: Their advantages and disadvantages. In AIP Conference Proceedings (Vol. 1724, No. 1). AIP Publishing.

Pasieczna-Patkowska, S., Cichy, M., & Flieger, J. (2025). Application of Fourier transform infrared (FTIR) spectroscopy in characterization of green synthesized nanoparticles. Molecules, 30(3), 684.

Patel, A. M., Upadhayay, D., Andhare, P., & Prajapati, P. (2021). *A review on actinomycetes*. International Journal of Biology, Pharmacy and Allied Sciences, 10(4), 389–395.

Patel, A. M., Upadhayay, D., Andhare, P., & Prajapati, P. (2021). *A review on actinomycetes*. International Journal of Biology, Pharmacy and Allied Sciences, 10(4), 389–395.

Patil, M. P., Bayaraa, E., Subedi, P., Piad, L. L. A., Tarte, N. H., & Kim, G. D. (2019). Biogenic synthesis, characterization of gold nanoparticles using Lonicera japonica and their anticancer activity on HeLa cells. Journal of Drug Delivery Science and Technology, 51, 83-90.

Patil, S. P., & Shirsath, L. P. (2015). Production of exopolysaccharide by an osmotolerant, thermostable and metal resistant Bacillus subtilis. International Journal of Current Microbiology and Applied Sciences, 4(2), 965–971.

Peña, A., Sánchez, N. S., & Calahorra, M. (2013). Effects of chitosan on Candida albicans: conditions for its antifungal activity. BioMed research international, 2013(1), 527549.

Penman, R., Kariuki, R., Shaw, Z. L., Dekiwadia, C., Christofferson, A. J., Bryant, G., ... & Elbourne, A. (2024). Gold nanoparticle adsorption alters the cell stiffness and cell wall bio-chemical landscape of Candida albicans fungal cells. Journal of Colloid and Interface Science, 654, 390-404.

Pérez-Burgos, M., & Søgaard-Andersen, L. (2020). Biosynthesis and function of cell-surface polysaccharides in the social bacterium Myxococcus xanthus. Biological Chemistry, 401(12), 1375-1387.

Pertiwi, R. D., Fitria, P. A., Utami, T. P., Pamungkas, R. A., Pradana, R., & Chamroonsawasdi, K. (2025). Gold Nanoparticle Synthesis Using Quercetin: Innovation in Biopreneur. Aptisi Transactions on Technopreneurship (ATT), 7(1), 294-305.

Pires, P. C., Mascarenhas-Melo, F., Pedrosa, K., Lopes, D., Lopes, J., Macário-Soares, A., ... & Paiva-Santos, A. C. (2023). Polymer-based biomaterials

for pharmaceutical and biomedical applications: A focus on topical drug administration. European Polymer Journal, 187, 111868.

POURJAFAR, D. T., Ahmadi, Z., & AFSHARI, T. F. (2017). Investigation on crystallinity behavior of the polylactic acid and poly-3-hydroxybutyrate bio-based polymers in the presence of the pyromellitic anhydride.

Prashanthi, R., Shreevatsa, G. K., Krupalini, S., & Manoj, L. (2021). Isolation, characterization, and molecular identification of soil bacteria showing antibacterial activity against human pathogenic bacteria. Journal of Genetic Engineering and Biotechnology, 19(1), 120.

Puceli , B., Su e , A., Bor ows i, M., Barzows a, A., Kobielusz, M., & D brows i, J. M. (2022). Synthesis and characterization of size-and charge-tunable silver nanoparticles for selective anticancer and antibacterial treatment. ACS Applied Materials & Interfaces, 14(13), 14981-14996.

Punjabi, K., Choudhary, P., Samant, L., Mukherjee, S., Vaidya, S., & Chowdhary, A. (2015). Biosynthesis of nanoparticles: a review. *Int. J. Pharm. Sci. Rev. Res*, *30*(1), 219-26.

Puoci, F., Iemma, F., Spizzirri, U. G., Cirillo, G., Curcio, M., & Picci, N. (2008). Polymer in agriculture: A review. American Journal of Agricultural and Biological Sciences, 3(1), 299–314. https://doi.org/10.3844/ajabssp.2008.299.314

Purohit, J., Chattopadhyay, A., & Singh, N. K. (2019). Green synthesis of microbial nanoparticle: approaches to application. In Microbial Nanobionics (pp. 35-60). Springer, Cham.

Qais, F. A., Shafiq, A., Khan, H. M., Husain, F. M., Khan, R. A., Alenazi, B., … & Ahmad, I. (2019). Antibacterial effect of silver nanoparticles synthesized using Murraya koenigii (L.) against multidrug-resistant pathogens. Bioinorganic Chemistry and Applications, 2019, 1–11. https://doi.org/10.1155/2019/4649506

Rahbari, R., Zhang, L., & Kebebew, E. (2010). Thyroid cancer gender disparity. Future oncology, 6(11), 1771-1779

Rajasekar, T., Karthika, K., Muralitharan, G., Maryshamya, A., Sabarika, S., Anbarasu, S., ... & Kumaran, S. (2020). Green synthesis of gold nanoparticles using extracellular metabolites of fish gut microbes and their antimicrobial properties. Brazilian journal of microbiology, 51(3), 957-967.

Rajasree, S. R., & Suman, T. Y. (2012). Extracellular biosynthesis of gold nanoparticles using a gram-negative bacterium Pseudomonas fluorescens. Asian Pacific Journal of Tropical Disease, 2(Suppl), S796–S799.

Ramakrishna, M., Rajesh Babu, D., Gengan, R. M., Chandra, S., & Nageswara Rao, G. (2016). Green synthesis of gold nanoparticles using marine algae and evaluation of their catalytic activity. Journal of Nanostructure in Chemistry, 6(1), 1-13.

Ramezani, N., Ehsanfar, Z., Shamsa, F., Amin, G., Shahverdi, H. R., Esfahani, H. R. M., … Shahverdi, A. R. (2008). Screening of medicinal plant methanol extracts for the synthesis of gold nanoparticles by their reducing potential. Zeitschrift für Naturforschung B, 63, 903–908.

Rane, A. V., Kanny, K., Abitha, V. K., & Thomas, S. (2018). Methods for synthesis of nanoparticles and fabrication of nanocomposites. In Synthesis

of Inorganic Nanomaterials (pp. 121–139). Cambridge, UK: Woodhead Publishing.

Rao, J. U., Rash, B. A., Nobre, M. F., Da Costa, M. S., Rainey, F. A., & Moe, W. M. (2012). Actinomyces naturae sp. nov., the first Actinomyces sp. isolated from a non-human or animal source. Antonie Van Leeuwenhoek, 101(1), 155-168.

Rashid, H., & Umamaheswari, G. (2017). Evaluation of the cytotoxic effect of ginger extract against prostate cancer model using in vitro study. World Journal of Pharmacy and Pharmaceutical Sciences, 6(12), 1044–1053.

Rasulov, B. A., Li, L., Liu, Y. H., Mohamad, O. A., Xiao, M., Ma, J. B., & Li, W. J. (2017). Production, characterization and structural modification of exopolysaccharide-based bioflocculant by Rhizobium radiobacter SZ4S7S14 and media optimization. 3 Biotech, 7(3), 179.

Rawat, S. K., Yaseen, M., Khan, U., Kumar, M., Abdulrahman, A., Eldin, S. M., ... & Galal, A. M. (2023). Insight into the significance of nanoparticle aggregation and non-uniform heat source/sink on titania–ethylene glycol nanofluid flow over a wedge. Arabian Journal of Chemistry, 16(7), 104809.

Rehm, B. H. (2010). Bacterial polymers: biosynthesis, modifications and applications. Nature Reviews Microbiology, 8(8), 578-592.

Rehm, B. H. (2015). Synthetic biology towards the synthesis of custom- made polysaccharides. Microbial Biotechnol, 8(1), 19–20.

Reibold, M., Paufler, P., Levin, A. A., Kochmann, W., Pätzke, N., & Meyer, D. C. (2006). Carbon nanotubes in an ancient Damascus sabre. Nature, 444(7117), 286-286.

Rodriguez-R, L. M., Jain, C., Conrad, R. E., Aluru, S., & Konstantinidis, K. T. (2021). Reply to "Re-evaluating the evidence for a universal genetic boundary among microbial species." Nature Communications, 12(1), 4060.

Rosati, D., Bruno, M., Jaeger, M., ten Oever, J., & Netea, M. G. (2020). Recurrent vulvovaginal candidiasis: An immunological perspective. Microorganisms, 8, 144. https://doi.org/10.3390/microorganisms8020144

Roy, A., Bulut, O., Some, S., Mandal, A. K., & Yilmaz, M. D. (2019). Green synthesis of silver nanoparticles: biomolecule-nanoparticle organizations targeting antimicrobial activity. RSC Advances, 9(5), 2673–2702.

Roy, S., Das, T. K., Maiti, G. P., & Basu, U. (2016). Microbial biosynthesis of nontoxic gold nanoparticles. Materials Science and Engineering: B, 203, 41-51

Rui, S., Fengrui, G., Yining, Z., Hong, S., Xuewen, Y., Changping, W., & Chunjia, Y. (2025). Biological activity of secondary metabolites of actinomycetes and their potential sources as antineoplastic drugs: a review. Frontiers in Microbiology, 16, 1550516**.**

Rutherford, G., Xiao, B., Carvajal, C., Farrell, M., Santiago, K., Cashwell, I., & Pradhan, A. (2015). Photochemical growth of highly densely packed gold nanoparticle films for biomedical diagnostics. ECS Journal of Solid State Science and Technology, 4(10), S3071

Saharan, B. S., Kamal, N., Badoni, P., Kumar, R., Saini, M., Kumar, D., … Mandal, N. K. (2024). Biopolymer and polymer precursor production by

microorganisms: Applications and future prospects. Journal of Chemical Technology & Biotechnology, 99(1), 17–30.

Salman, Y. M. & Abd Atae, F. G. (2021). Antibacterial and immunological effects of biosynthesized magnesium oxide (MgO) nanoparticles produced by bacteria. M.Sc. thesis. college of Science, Department of Biology, Babylon. University Babylon.Iraq.

Santos-Beneit, F. (2024). What is the role of microbial biotechnology and genetic engineering in medicine?. Microbiologyopen, 13(2), e1406.

Saravanan, S., & Dubey, R. S. (2020). Synthesis of SiO2 nanoparticles by sol-gel method and their optical and structural properties. Rom. J. Inf. Sci. Technol, 23(1), 105-112.

Sasikumar, K., Kozhummal Vaikkath, D., Devendra, L., & Nampoothiri, K. M. (2017). An exopolysaccharide (EPS) from a Lactobacillus plantarum BR2 with potential benefits for making functional foods. Bioresource Technol., 241, 1152–1156.

Satalkar, P., Elger, B. S., & Shaw, D. M. (2016). Defining nano, nanotechnology and nanomedicine: why should it matter?. Science and engineering ethics, 22, 1255-1276.

Schmid, J., Sieber, V., & Rehm, B. (2015). Bacterial exopolysaccharides: Biosynthesis pathways and engineering strategies. Frontiers in Microbiology, 6, 496.

Selim, M. S. M., Abdelhamid, S. A., & Mohamed, S. S. (2021). Secondary metabolites and biodiversity of actinomycetes. Journal of Genetic Engineering and biotechnology, 19(1), 72.

Seyfarth, F., Schliemann, S., Elsner, P., & Hipler, U. C. (2008). Antifungal effect of high-and low-molecular-weight chitosan hydrochloride, carboxymethyl chitosan, chitosan oligosaccharide and N-acetyl-D-glucosamine against Candida albicans, Candida krusei and Candida glabrata. International journal of pharmaceutics, 353(1-2), 139-148.

Shaba, E. Y., Jacob, J. O., Tijani, J. O., & Suleiman, M. A. T. (2021). A critical review of synthesis parameters affecting the properties of zinc oxide nanoparticle and its application in wastewater treatment. *Applied Water Science*, *11*(2), 48.

Shaker, A. H., & Aadim, K. A. (2024). Synthesis and characterization of aluminum oxide nanoparticles prepared by two different cold plasma jet methods. Iraqi Journal of Physics, 22(1), 20-30.

Shariatinia, Z. (2019). Pharmaceutical applications of natural polysaccharides. In Applications of polysaccharides in drug delivery (pp. 15–57). Cambridge, MA: Academic Press.

Sharma, M., Dangi, P., & Choudhary, M. (2014). Actinomycetes: source, identification, and their applications. International Journal of Current Microbiology and Applied Sciences, 3(2), 801-832.

Shih, P. Y., Liao, Y. T., Tseng, Y. K., Deng, F. S., & Lin, C. H. (2019). A potential antifungal effect of chitosan against Candida albicans is mediated via the inhibition of SAGA complex component expression and the

subsequent alteration of cell surface integrity. Frontiers in Microbiology, 10, 602.

Shinde, N. C. (2012). Nanoparticles: Advances in drug delivery systems. Research Journal of Pharmaceutical, Biological and Chemical Sciences, 3(1), 922–929.

Shrestha, B., Nath, D. K., Maharjan, A., Poudel, A., Pradhan, R. N., & Aryal, S. (2021). Isolation and characterization of potential antibiotic-producing actinomycetes from water and soil sediments of different regions of Nepal. International Journal of Microbiology, 2021, Article ID 6671417.

Shukla, A. K., & Iravani, S. (Eds.). (2018). Green synthesis, characterization and applications of nanoparticles. Amsterdam, The Netherlands: Elsevier.

Siddiqi, K. S., & Husen, A. (2016). Fabrication of metal and metal oxide nanoparticles by algae and their toxic effects. Nanoscale Research Letters, 11, 276.

Sidhu, P. K., & Nehra, K. (2020). Bacteriocin-capped silver nanoparticles for enhanced antimicrobial efficacy against food pathogens. IET Nanobiotechnology, 14(3), 245–252.

Silva, G. D. C., Kitano, I. T., Ribeiro, I. A. D. F., & Lacava, P. T. (2022). The potential use of actinomycetes as microbial inoculants and biopesticides in agriculture. Frontiers in Soil Science, 2, 833181.

Singaravelu, G., Arockiamary, J. S., Kumar, V. G., & Govindaraju, K. (2007). A novel extracellular synthesis of monodisperse gold nanoparticles using marine alga, Sargassum wightii Greville. Colloids and surfaces B: Biointerfaces, 57(1), 97-101.

Skalickova, S., Baron, M., & Sochor, J. (2017). Nanoparticles biosynthesized by yeast: a review of their application. Kvasny Prumysl, 63(6), 290-292.

Slocik, J. M., Naik, R. R., Stone, M. O., & Wright, D. W. (2005). Viral templates for gold nanoparticle synthesis. Journal of Materials Chemistry, 15(7), 749-753.

Song, J. Y., Jang, H.-K., & Kim, B. S. (2009). Biological synthesis of gold nanoparticles using Magnolia kobus and Diospyros kaki leaf extracts. Process Biochemistry, 44(10), 1133–1138.

Soni, N., & Prakash, S. (2012). Synthesis of gold nanoparticles by the fungus Aspergillus niger and its efficacy against mosquito larvae. Reports in Parasitology, 1-7.

Srinath, B. S., & Rai, R. V. (2015). Biosynthesis of gold nanoparticles using extracellular molecules produced by Enterobacter aerogenes and their catalytic study. Journal of Cluster Science, 26(5), 1483-1494

Sun, W., Karmakar, B., Ibrahium, H. A., Awwad, N. S., & El-kott, A. F. (2022). Design and synthesis of nano Cu/chitosan-starch bio-composite for the treatment of human thyroid carcinoma. Arabian Journal of Chemistry, 15(1), 103465.

Tai, Y., Shen, J., Luo, Y., Qu, H., & Gong, X. (2020). Research progress on the ethanol precipitation process of traditional Chinese medicine. Chinese medicine, 15(1), 84.

Tamo, S. B. (2020). Candida Infections: clinical features, diagnosis and treatment. Infect Dis Clin Microbiol, 2(2), 91-102.

Tarek, A., Tartor, Y. H., Hassan, M. N., Pet, I., Ahmadi, M., & Abdelkhalek, A. (2024). Fighting Emerging Caspofungin-Resistant Candida Species: Mitigating Fks 1-Mediated Resistance and Enhancing Caspofungin Efficacy by Chitosan. Antibiotics, 13(7), 578.

Thielbeer, F., Donaldson, K., & Bradley, M. (2011). Zeta potential mediated reaction monitoring on nano and microparticles. Bioconjugate chemistry, 22(2), 144-150.

Tian, X., Teo, W. F. A., Wee, W. Y., Yang, Y., Ahmed, H., Jakubovics, N. S., … Tan, G. Y. A. (2023). Genome characterization and taxonomy of Actinomyces acetigenes sp. nov. and Actinomyces stomatis sp. nov., previously isolated from the human oral cavity. BMC Genomics, 24, 98. https://doi.org/10.1186/s12864-023-09831-2

Torabi, L. R., & Doudi, M. (2016). The effect of gold nano particles compared to dioxide titanium nano particles on vital factors of isolated Candida albicans in patients with oral candidiasis in vitro. Zahedan Journal of Research in Medical Sciences, 18(12), e5666. https://doi.org/10.17795/zjrms-5666

Trabelsi, L., M'sakni, N. H., Ben Ouada, H., Bacha, H., & Roudesli, S. (2009). Partial characterization of extracellular polysaccharides produced by cyanobacterium Arthrospira platensis. Biotechnology and Bioprocess Engineering, 14(1), 27-31.

Tripathi, G. K. (2019). Engineered nanomaterials and their properties: A review. Bioscience Biotechnology Research Communications, 12, 764–771

UK Standards for Microbiology Investigations. (2025). Identification of Actinomyces species. Royal College of Pathologists / UK Health Security Agency.

Upadhye, M., Kuchekar, M., Pujari, R., & Sable, N. (2022). Biopolymers: A comprehensive review. Open Access Research Journal of Science and Technology, 4(01), 13-18.

Van der Meij, A., Worsley, S. F., Hutchings, M. I., & van Wezel, G. P. (2017). Chemical ecology of antibiotic production by actinomycetes. *FEMS microbiology reviews*, *41*(3), 392-416.

Venkatesan, J., Manivasagan, P., Kim, S. K., Kirthi, A. V., Marimuthu, S., & Rahuman, A. A. (2014). Marine algae-mediated synthesis of gold nanoparticles using a novel Ecklonia cava. Bioprocess and biosystems engineering, 37(8), 1591-1597.

Ventura, M., Canchaya, C., Tauch, A., Chandra, G., Fitzgerald, G. F., Chater, K. F., & Van Sinderen, D. (2007). Genomics of Actinobacteria: tracing the evolutionary history of an ancient phylum. Microbiology and molecular biology reviews, 71(3), 495-548.

Verma, P., & Maheshwari, S. K. (2018). Preparation of sliver and selenium nanoparticles and its characterization by dynamic light scattering and scanning electron microscopy. Journal of microscopy and ultrastructure, 6(4), 182-187.

Vitiello, A., Ferrara, F., Boccellino, M., Ponzo, A., Cimmino, C., Comberiati, E., … Sabbatucci, M. (2023). Antifungal drug resistance: An emergent health threat. Biomedicines, 11(4), 1063.

Vivier, E., Rebuffet, L., Narni-Mancinelli, E., Cornen, S., Igarashi, R. Y., & Fantin, V. R. (2024). Natural killer cell therapies. Nature, 626(8000), 727–736.

Wadhwa, R., Aggarwal, T., Thapliyal, N., Kumar, A., Priya, Yadav, P., ... and Maurya, P. K. (2019). Red blood cells as an efficient in vitro model for evaluating the efficacy of metallic nanoparticles. 3 Biotech, 9, 1-15.

Wang, J., Zhao, X., Tian, Z., Yang, Y., & Yang, Z. (2015). Characterization of an exopolysaccharide produced by Lactobacillus plantarum YW11 isolated from Tibet Kefir. Carbohydr. Polym., 125, 16–25. https://doi.org/10.1016/j.carbpol.2015.03.003

Wang, R., Billone, P. S., & Mullett, W. M. (2013). Nanomedicine in action: An overview of cancer nanomedicine on the market and in clinical trials. Journal of Nanomaterials, 2013, Article ID 629405. https://doi.org/10.1155/2013/629405

Wang, X., Yang, Y., Zhao, S., Wu, D., Li, L., & Zhao, Z. (2024). Chitosan-based biomaterial delivery strategies for hepatocellular carcinoma. Frontiers in Pharmacology, 15, 1446030.

Wu, Q., Cen, F., Xie, Y., Ning, X., Wang, J., Lin, Z., & Huang, J. (2025). Nanoparticle-based antifungal therapies innovations mechanisms and future prospects. PeerJ, 13, e19199.

Xiangqian, L., Huizhong, X., Chen, Z., & Chen, G. (2011). Biosynthesis of nanoparticles by microorganisms and their applications. Journal of Nanomaterials, 2011, 1–16.

Xin, J., Song, M., Liu, X., Zou, H., Wang, J., Xiao, L., ... & Jiang, Y. (2024). A new strategy of using low-dose caffeic acid carbon nanodots for high resistance to poorly differentiated human papillary thyroid cancer. Journal of Nanobiotechnology, 22(1), 571.

Yadav, M. K., Song, J. H., Vasquez, R., Lee, J. S., Kim, I. H., & Kang, D. K. (2024). Methods for detection, extraction, purification, and characterization of exopolysaccharides of lactic acid bacteria—a systematic review. Foods, 13(22), 3687.

Yamazaki, H., Sugino, K., Katoh, R., Matsuzu, K., Kitagawa, W., Nagahama, M., ... & Ito, K. (2024). Management of follicular thyroid carcinoma. European Thyroid Journal, 13(5).

Yang, X., Yang, M., Pang, B., Vara, M., & Xia, Y. (2015). Gold nanomaterials at work in biomedicine. Chemical reviews, 115(19), 10410-10488

Yu, T., Hou, J., Hafeez, F., Ge, P., Zou, A., Fu, Y., ... & Xianyu, Y. (2024). Fungus-mediated biosynthesis of gold nanoparticles with synergistic antifungal activity against multidrug-resistant Candida albicans. Nano Today, 59, 102486.

Yuan, H., Ji, W., Chu, S., Liu, Q., Qian, S., Guang, J., … Peng, W. (2019). Mercaptopyridine-functionalized gold nanoparticles for fiber-optic surface plasmon resonance Hg^{2+} sensing. ACS Sensors, 4(3), 704–710.

Yue, F., Zhang, J., Xu, J., Niu, T., Lü, X., & Liu, M. (2022). Effects of monosaccharide composition on quantitative analysis of total sugar content

by phenol–sulfuric acid method. Frontiers in Nutrition, 9, 963318. https://doi.org/10.3389/fnut.2022.963318

Zabetakis, K., Ghann, W. E., Kumar, S., & Daniel, M. C. (2012). Effect of high gold salt concentrations on the size and polydispersity of gold nanoparticles prepared by an extended Turkevich–Frens method. Gold Bulletin, 45(4), 203-211.

Zaboon, M., Saleh, A., & Al-Lami, H. (2019). Comparative cytotoxicity and genotoxicity assessments of chitosan amino acid derivative nanoparticles toward human breast cancer cell lines. Egyptian Journal of Chemistry, 62(11), 2061-2075.

Zaghloul, E. H., & Ibrahim, M. I. A. (2022). Production and characterization of exopolysaccharide from newly isolated marine probiotic Lactiplantibacillus plantarum EI6 with in vitro wound healing activity. Front. Microbiol., 13, 903363.
https://doi.org/10.3389/fmicb.2022.903363

Zaghloul, E., Ibrahim, M., & Zaghloul, H. (2023). Antibacterial activity of exopolysaccharide produced by bee gut-resident Enterococcus sp. BE11 against marine fish pathogens. BMC Microbiology, 23, 231. https://doi.org/10.1186/s12866-023-02977-9

Zhang, Q., Ma, Y., Yang, S., Xu, B., & Fei, X. (2015). Small-sized gold nanoparticles inhibit the proliferation and invasion of SW579 cells. Molecular Medicine Reports, 12(6), 8313–8319.

Zhang, X., He, X., Wang, K., & Yang, X. (2011). Different active biomolecules involved in biosynthesis of gold nanoparticles by three fungus species. Journal of biomedical nanotechnology, 7(2), 245-254.

Zhang, X., Qu, Y., Shen, W., Wang, J., Li, H., Zhang, Z., ... & Zhou, J. (2016). Biogenic synthesis of gold nanoparticles by yeast Magnusiomyces ingens LH-F1 for catalytic reduction of nitrophenols. Colloids and Surfaces A: Physicochemical and Engineering Aspects, 497, 280-285.

Zhou, H., Li, X., Lemoff, A., Zhang, B., & Yan, B. (2010). Structural confirmation and quantification of individual ligands from the surface of multi-functionalized gold nanoparticles. Analyst, 135(6), 1210-1213.

الخلاصة :

في هذه الدراسة، تم جمع عشر عينات تربة من مناطق ضفاف نهر دجلة في محافظة ميسان خلال الفترة من 1 نوفمبر 2024 إلى 1 يونيو 2025، نظرًا لكون هذه البيئات غير مستكشفة بيولوجيًا بشكل كافٍ. تم عزل البكتيريا تحت ظروف لا هوائية، وخضعت للتعريف الأولي استنادًا إلى الخصائص المورفولوجية باستخدام المجهر الضوئي، تلاه التعريف الجزيئي باستخدام جين 16 .S rRNAأظهرت التحليلات الجزيئية أن البكتيريا المعزولة تمثل سلالة بكتيرية جديدة، وقد تم تسجيلها في قاعدة بيانات NCBI تحت رقم الوصول PV945972 وسُمّيت.*Schaalia natura* strain RFAT2
تمت دراسة قدرة هذه السلالة على إنتاج البوليمر الحيوي والتخليق الحيوي لجسيمات الذهب النانوية باستخدام راشح البكتيريا الخالي من الخلايا. وتم توصيف البوليمر الحيوي باستخدام مجموعة من التقنيات التحليلية شملت UV–Vis و FTIRو XRDو FESEMو AFMوتحليل جهد زيتا والتحليل الحراري الوزني(TGA) ، بالإضافة إلى قياس الذوبانية وتحديد محتوى الكربوهيدرات. في المقابل، تم تأكيد تكوين جسيمات الذهب النانوية وتوصيفها باستخدام تقنيات UV–Vis و FTIRو XRDو FESEMو TEM و AFMوتحليل جهد زيتا. تم تقييم النشاط المضاد للفطريات للبوليمر الحيوي والجسيمات النانوية الذهبية ضد الفطرين *Candida albicans* و *Candida krusei* باستخدام تراكيز مختلفة (500، 250، 125، و62.5 ميكروغرام/مل). أظهرت النتائج أن التركيز 62.5 ميكروغرام/مل لم يُظهر أي تأثير مثبط على نمو الفطريات، في حين أظهرت التراكيز الأعلى تأثيرًا تثبيطيًا واضحًا مع وجود علاقة طردية بين زيادة التركيز وازدياد قطر مناطق التثبيط. كما تم تقييم السمية الخلوية للبوليمر الحيوي والجسيمات النانوية الذهبية ضد خلايا سرطان الغدة الدرقية (FTC–133) وخلايا الأورمات الليفية الجلدية البشرية الطبيعية (HdFn)باستخدام تراكيز مختلفة (25، 50، 100، 200، و400 ميكروغرام/مل). أظهرت النتائج أن التأثير السام كان معتمدًا على التركيز، حيث سجلت الجسيمات النانوية الذهبية أعلى نسبة تثبيط للخلايا السرطانية بلغت 60.46% عند تركيز 400 ميكروغرام/مل، مع تأثير أقل على الخلايا الطبيعية. وأكد التحليل الإحصائي باستخدام برنامج GraphPad Prism وجود فروق معنوية عند مستوى دلالة ($p\leq 00.05$)

تشير هذه النتائج إلى إمكانية استخدام هذه السلالة البكتيرية كمصدر حيوي واعد لإنتاج البوليمرات الحيوية والجسيمات النانوية الذهبية ذات التطبيقات الطبية الواعدة في مجال مضادات الفطريات ومكافحة السرطان .

وزارة التعليم العالي والبحث العلمي
جامعة ميسان
كلية العلوم
قسم علوم الحياة

انتاج وتنقية جزئية للبوليمر الحيوي و التخليق الحيوي لجسيمات الذهب النانوية من بكتيريا *Actinomycetes* وتحديد فعاليتهما البايولوجية

رسالة مقدمة الى
كلية العلوم / جامعة ميسان جزء من متطلبات نيل شهادة الماجستير في علوم الحياة

من الطالبة
رقية طالب حسن

بكالوريوس علوم الحياة (2021)

بإشراف
الاستاذ الدكتور رشيد رحيم حتيت

1447 هـ **2026م**